
[All ETDs from UAB](#)

[UAB Theses & Dissertations](#)

1993

Characterization Of Nuclear-Mitotic Apparatus Protein During The Cell Cycle.

Changqing Zeng
University of Alabama at Birmingham

Follow this and additional works at: <https://digitalcommons.library.uab.edu/etd-collection>

Recommended Citation

Zeng, Changqing, "Characterization Of Nuclear-Mitotic Apparatus Protein During The Cell Cycle." (1993).
All ETDs from UAB. 4655.
<https://digitalcommons.library.uab.edu/etd-collection/4655>

This content has been accepted for inclusion by an authorized administrator of the UAB Digital Commons, and is provided as a free open access item. All inquiries regarding this item or the UAB Digital Commons should be directed to the [UAB Libraries Office of Scholarly Communication](#).

INFORMATION TO USERS

This manuscript has been reproduced from the microfilm master. UMI films the text directly from the original or copy submitted. Thus, some thesis and dissertation copies are in typewriter face, while others may be from any type of computer printer.

The quality of this reproduction is dependent upon the quality of the copy submitted. Broken or indistinct print, colored or poor quality illustrations and photographs, print bleedthrough, substandard margins, and improper alignment can adversely affect reproduction.

In the unlikely event that the author did not send UMI a complete manuscript and there are missing pages, these will be noted. Also, if unauthorized copyright material had to be removed, a note will indicate the deletion.

Oversize materials (e.g., maps, drawings, charts) are reproduced by sectioning the original, beginning at the upper left-hand corner and continuing from left to right in equal sections with small overlaps. Each original is also photographed in one exposure and is included in reduced form at the back of the book.

Photographs included in the original manuscript have been reproduced xerographically in this copy. Higher quality 6" x 9" black and white photographic prints are available for any photographs or illustrations appearing in this copy for an additional charge. Contact UMI directly to order.

U·M·I

University Microfilms International
A Bell & Howell Information Company
300 North Zeeb Road, Ann Arbor, MI 48106-1346 USA
313/761-4700 800/521-0600

Order Number 9419305

**Characterization of nuclear-mitotic apparatus protein during the
cell cycle**

Zeng, Changqing, Ph.D.

University of Alabama at Birmingham, 1993

U·M·I
300 N. Zeeb Rd.
Ann Arbor, MI 48106

**CHARACTERIZATION OF NUCLEAR-MITOTIC APPARATUS
PROTEIN DURING THE CELL CYCLE**

by

CHANGQING ZENG

A DISSERTATION

**Submitted in partial fulfillment of the requirements for
the degree of Doctor of Philosophy in the Department of
Cell Biology in the Graduate School,
The University of Alabama at Birmingham**

BIRMINGHAM, ALABAMA

1993

ABSTRACT OF DISSERTATION
GRADUATE SCHOOL, UNIVERSITY OF ALABAMA AT BIRMINGHAM

Degree Ph.D. Major Subject Cell Biology
Name of Candidate Changqing Zeng
Title CHARACTERIZATION OF NUCLEAR-MITOTIC APPARATUS
PROTEIN (NuMA) DURING THE CELL CYCLE

Using a monoclonal antibody 2D3, a 220 KD protein was identified with a distinct cell-cycle-dependent pattern of distribution. Initially termed centrophilin, this protein resides in the interphase nucleus and translocates to the spindle poles during mitosis as shown by immunofluorescence. A 1.9 kb cDNA fragment was cloned by screening a λ gt11 expression library with 2D3. Comparison of partial cDNA sequence of centrophilin with the full length sequence of the nuclear mitotic apparatus protein (NuMA) indicated that NuMA and centrophilin were the same protein. A variety of biochemical, immunochemical, and microscopic approaches were performed to characterize the properties and functions of NuMA. Two probes, mAb 8.22 and pAb P9, were produced against the fusion protein from the positive λ -recombinant. In immunoblots P9 resolved NuMA as a doublet ≥ 200 KD, which represents isoforms of NuMA produced by alternative RNA splicing as demonstrated by peptide mapping. Throughout mitosis the formation and breakdown of the spindle correlates in time and space with the aggregation and disaggregation of NuMA. During recovery from microtubule inhibition, NuMA foci act as nucleation sites for the assembly of nascent spindle microtubules. Sequential fractionation along with EM immunogold labeling and immunoblotting revealed that in interphase NuMA isoforms are components of nuclear core filaments. Moreover, mAb 8.22 reveals an unexpected nuclear speckle pattern which appears to represent a newly discovered structural/functional state

of NuMA in interphase. These nuclear speckles are colocalized with spliceosomes as detected by double label immunofluorescence with 8.22 and an anti-snRNP autoantibody. Immunoprecipitation with snRNP antibodies indicated that NuMA is associated with snRNPs in a complex from HeLa extract. Moreover, NuMA appears to associate with the active spliceosomes that are reconstituted *in vitro* using wild type pre-mRNA, but not with nonspecific RNA. Cumulatively, NuMA, consistent with its dynamic translocation, appears to have dual functions during the cell cycle. In interphase, NuMA likely plays a structural role in core filaments as a long coiled-coil protein and serves as the structural interface between the nucleoskeleton and RNA processing. In mitosis NuMA is a MTOC component at the minus end of MTs involved in spindle organization.

Abstract Approved by: Committee Chairman B. R. Brinkley
Program Director J. K. Concha
Date 1/14/94 Dean of Graduate School Joan Hodson

DEDICATION

This dissertation is dedicated to my parents,

Yinqing Liu and Yanwei Zeng (the late).

ACKNOWLEDGEMENTS

A deep interest in microtubules led me to the decision to become one of Dr. Bill Brinkley's students when I was on the other side of the ocean. During these memorable years of working with him, I have learned not only how to do science, but also how to be a scientist. Dr. Brinkley's invaluable guidance and encouragement are heartily appreciated.

Sincere appreciation is extended also to the other members of my graduate committee including: Dr. Lester Binder, Dr. Gerald Fuller, Dr. Thomas Rado, and Dr. Thomas Howard. Their advice and guidance have helped considerably in my research and facilitated my pursuit of a Ph.D. degree. I am deeply grateful for their interest and support. I would like especially to thank Dr. Gerald Fuller and Dr. Richard Marchase, as the former directors of Graduate Studies, and Dr. John Couchman, the current Director of Graduate Studies, for their valuable assistance in my educational goals.

I would like also to extend special thanks to three scientists and their groups at other institutions, whose advice and support are deeply appreciated. Dr. Lan Bo Chen and his colleagues Qi An and Shideng Bao, at the Dana Farber Cancer Institute, Harvard Medical School, patiently taught me DNA screening and sequencing technology, and they provided experimental material and technical procedures during my brief tenure there. Dr. Shelden Penman and his colleague Dr. Katherine Wan in MIT unselfishly provided material and support while I worked in their lab. Dr. Susan Berget, Baylor College of Medicine, led me to consider the exciting field of RNA splicing, and she provided technical support and instruction in splicing reactions and immunoprecipitation approaches in my research.

I would like also to extend my appreciation to Dr. Mary Ann Accavitti and Fran Allen in the Hybridoma Core Facility at UAB, who contributed significantly in the generation of monoclonal antibodies in this research.

I also thank several present and former members of Dr. Brinkley's lab: Dr. Ron Balczon, Dr. Paula Gregory, Dr. Ray Zinkowski, Dr. Ilia Ouspensky, Albert Tousson, Becky Scott, Donna Turner, Michael Wise, Ric Villani, Jennifer Kidd, and Ed Philips. All of these individuals provided helpful discussions and technical support during various phases of my study. Thanks also is extended to Ann Harrell, Sherry Crittenden, and Betty Ledlie for their help and understanding in administrative and educational pursuits.

Last, I would like to acknowledge greatly Dr. Dacheng He for his earnest support and help during these years.

TABLE OF CONTENTS

	<u>Page</u>
ABSTRACT	ii
DEDICATION	iv
ACKNOWLEDGEMENTS	v
LIST OF TABLES	viii
LIST OF FIGURES	ix
LIST OF ABBREVIATIONS	xi
INTRODUCTION	1
CENTROPHILIN: A NOVEL MITOTIC SPINDLE PROTEIN INVOLVED IN MICROTUBULE NUCLEATION	24
LOCALIZATION OF NuMA PROTEIN ISOFORMS IN THE NUCLEAR MATRIX OF MAMMALIAN CELLS	70
NuMA: A STRUCTURAL PROTEIN INTERFACE BETWEEN THE NUCLEOSKELETON AND RNA SPLICING	100
SUMMARY AND GENERAL CONCLUSIONS	121
GENERAL LIST OF REFERENCES	128

LIST OF TABLES

<u>Table</u>		<u>Page</u>
	INTRODUCTION	
1	NuMA and NuMA-like proteins	19

LIST OF FIGURES

<u>Figure</u>		<u>Page</u>
INTRODUCTION		
1	The predicted secondary structure of NuMA protein	20
2	A schematic representation of pre-mRNA splicing	22
CENTROPHILIN: A NOVEL MITOTIC SPINDLE PROTEIN INVOLVED IN MICROTUBULE NUCLEATION		
1	Immunoblot of whole HeLa cell extract with 2D3	50
2	Profile of centrophilin localization during the cell cycle	52
3	Immunogold electron microscopic localization of centrophilin at the mitotic poles in HeLa cells	54
4	Centrophilin foci nucleate spindle tubule growth	56
5	Single-label immunofluorescence pattern of centrophilin morphogenesis with 2D3 and spindle microtubule reformation with antitubulin antibody after recovery from mitotic block	58
6	Double-label immunofluorescence with 2D3 and CREST antiserum in prometaphase after a 2-h recovery from mitotic block	60
7	A basal level of centrophilin is present at the interphase centrosome	62
8	Profile of centrophilin relocation during the cell cycle in cells which were Triton X-100 permeabilized in 0.1 M Pipes, pH6.9, with 21 mM CaCl ₂ before fixation	64
9	Centrophilin transiently associates with kinetochore in prometaphase	66
10	Model showing how centrophilin, a relocating marker protein for microtubule nucleation, may systematically help to modulate spindle tubule turnover throughout mitosis	68

LIST OF FIGURES (Continued)

<u>Figure</u>		<u>Page</u>
LOCALIZATION OF NuMA PROTEIN ISOFORMS IN THE NUCLEAR MATRIX OF MAMMALIAN CELLS		
1	Immunoblots of NuMA antibodies	88
2	Peptide maps of proteins resolved in immuno-blot by NuMA antibodies	90
3	Detection of NuMA in CasKi cells during each step of extraction for core filament preparation	92
4	Immunoblotting confirms NuMA as a component of core filaments	94
5	NuMA localization is deformed when core filaments are destructed by RNA digestion	96
6	EM immuno-gold labeling of 2D3 on core filaments of CasKi cells	98
NuMA: A STRUCTURAL PROTEIN INTERFACE BETWEEN THE NUCLEOSKELETON AND RNA SPLICING		
1	NuMA antibodies recognize large nuclear proteins	113
2	NuMA antibody 8.22 stains nuclear speckles	115
3	NuMA antigens are associated with snRNPs	117
4	NuMA antibodies immunoprecipitate <i>in vitro</i> reconstituted spliceosomes	119

LIST OF ABBREVIATIONS

3-D	three-dimension
α -Sm	human autoantibody against snRNPs
ATP	adenosine triphosphate
BHK	baby hamster kidney
BSA	bovine serum albumin
cDNA	complementary DNA
CENP	centromere protein
CHO	cultured Chinese hamster ovary cells
CMTC	cytoplasmic microtubule complex
CREST	calcinosis, Raynaud phenomenon, esophageal dismotility, sclerodactyly telangiectasia
DMEM	Dulbecco's modified essential medium
DNA	Deoxyribonucleic acid
EM	electron microscopy
FBS	fetal bovine serum
FITC	fluorescein isothiocyanate
HeLa	cultured human cells derived from carcinoma of the cervix
h, hr	hour(s)
IgG	immunoglobulin G
IgM	immunoglobulin M
kb	kilobases

LIST OF ABBREVIATION (Continued)

KD	kilodaltons
mAb	monoclonal antibody
MAP	microtubule associated proteins
min	minute(s)
mM	millimolar
MT	microtubule
MTOC	microtubule organizing center
NuMA	nuclear mitotic apparatus protein
nm	nanometer
pAb	polyclonal antibody
PAGE	polyacrylamide gel electrophoresis
PBS	phosphate buffered saline
PLAP	PMSF, leupeptin, antipain, pepstatin
PEM	Pipes, EGTA, MgCl₂, buffer
PMSF	phenylmethylsulfonyl fluoride
PtK1, 2	cultured cells from the rat kangaroo
RNA	ribonucleic acid
RNP	ribonucleoprotein
SDS	sodium dodecylsulfate
snRNA	small nuclear RNA
snRNP	small nuclear RNP
WGA	wheat germ agglutinin

INTRODUCTION

This dissertation presents a study of the nuclear mitotic apparatus protein (NuMA), a component of both the nucleus and the mitotic spindle (51). My investigation began with an analysis of a monoclonal antibody 2D3, which was generated against a kinetochore-enriched chromosome fraction from HeLa cells (87). Indirect immunofluorescence studies showed that 2D3 produces a diffuse staining pattern throughout the interphase nucleus and a bright crescent staining at each mitotic spindle pole. Therefore, we initially termed the protein recognized by 2D3, centrophilin, based on its translocation from the nucleus to the mitotic centrosomes. Studies with microtubule (MT) inhibitors suggested that centrophilin was involved in spindle MT assembly.

Comparison of the partial cDNA sequence of centrophilin with the full length sequence of NuMA indicated that centrophilin and NuMA are the same protein (93, 16). Several other proteins, including SPN (40), SP-H (53), and W1 (83) identified in other independent studies, have also been shown to be NuMA. Collectively, these studies have provided considerable information on the mitotic distribution of NuMA protein. Since most investigations concerning NuMA have been limited to the mitotic phase of the cell cycle, relatively little has been learned about the function of this protein during interphase. Therefore, much of the present investigation has been designed to elucidate the role of NuMA in the interphase nucleus. The following section will briefly review the current literature on properties and functions of NuMA in eukaryotic cells. The first chapter (reprint 1) of this thesis will describe the initial discovery of centrophilin which has contributed to our understanding of NuMA's function during mitosis. The second and third chapters

(preprints 1 and 2) will explore the localization and function of NuMA isoforms with particular emphasis on the interphase nucleus and nuclear matrix.

Identification of NuMA

NuMA was initially identified as a high molecular weight protein in an electrophoretic analysis of the nonhistone chromatin proteins by Pettijohn and his colleagues in 1980 (50). They partially purified NuMA protein by gel filtration chromatography in the presence of SDS and used this protein fraction to produce antibodies. NuMA was so named because of its cell cycle specific redistribution from the nucleus to the mitotic apparatus, as revealed by immunofluorescence (51). In fact, two nuclear patterns were identified with different NuMA antibodies despite their identical mitotic polar staining. A mouse antiserum, the first antibody of NuMA, stained the nucleus with a diffuse fluorescence marked by a number of more intense speckles (51), and later a monoclonal antibody, 2E4, produced a mostly diffuse nuclear staining pattern (89, 68).

In these pioneering studies, NuMA was characterized as a phosphorylated protein by affinity purification of ^{32}P labeled cellular NuMA (68). This protein was also found to be an autoantigen in the patients with connective tissue diseases (67). Following these initial reports, research on NuMA essentially ceased for a number of years and resumed independently in several laboratories in early 1990s.

Properties and Distribution of NuMA in Proliferating Cells

NuMA is present in human cells at a concentration of $\sim 2 \times 10^5$ copies of protein per cell (16). The gene for NuMA has been localized to chromosome 11 at band q13 by in situ hybridization (77). NuMA has been identified as a common protein in mammalian cells using a variety of probes (68, 40, 83), however, most of anti-NuMA mAbs are primate specific or react with only a few other mammalian cell lines, suggesting a diversity among species (51, 16, 40, chapter 1). The apparent molecular mass of NuMA is 200–240 KD in

different studies which is consistent with the predicted molecular mass of 236 KD derived from its primary structure (93, 16).

cDNA analysis has indicated that NuMA has an unusually large central α -helical domain of approximately 1480 amino acids long flanked by nonhelical terminal domains (Fig. 1) (93, 16). The α -helical domain contains several segments of heptad periodicity, a protein motif that is folded into a coiled-coil configuration. In addition, the central domain has significant sequence similarities to some structural proteins including myosins, cytokeratins and nuclear lamins, which also have been shown or predicted to be coiled-coils (93). Therefore, the secondary structure of NuMA may be organized into several coiled-coil segments that are separated by short nonhelical linkers.

Predominant amino acids in positions a and d of the heptad in the NuMA helical region are hydrophobic respectively (93, 16). These hydrophobic residues can generate a spine along one side of the helix which is capable of interacting with the hydrophobic spine of a second molecule to form a coiled-coil dimer (14, 15). In this regard, the primary structure of NuMA predicts that it may exist as a coiled-coil rod through the interactions along the hydrophobic faces of two or more NuMA proteins (93).

There appears to be interesting differences in the primary structure of NuMA from the literatures (93, 16). For instance, in the present study, a 1.9 kb cDNA fragment screened from an expression library by NuMA antibody 2D3, was localized in the nucleotide position 1796–3726 as compared with the cDNA sequence reported by Yang et al. (93), or 2058–3992 by Compton et al. (16). An analysis involving a pool of NuMA cDNA clones by Tang et al. has helped to resolve this enigma (83). In human cells, multiple messengers are derived from a single gene of NuMA by alternative splicing of the RNA transcript. Six sequence blocks containing from 42–1012 nucleotides have been identified in human NuMA cDNA clones. Multiple mRNA species can be generated through

alternatively excising one or more of these various blocks. Comparison of cDNA sequence from three human cDNA libraries have revealed several possible splicing products. In immunoblots, a few antibodies have resolved two NuMA isoforms ≥ 200 KD which probably correspond the predicted NuMA isoforms 230 and 194/195 KD (chapter 2, 83, 40).

In addition, post translational modification is also predicted from the sequence study. NuMA appears to be a target of several cell cycle related protein kinases which is consistent with the previous identification of NuMA as a phosphorylated protein (68). The known kinase recognition sequence motifs identified in NuMA cDNA include cAMP-dependent kinase, PKC, CDC2 and Ca^{2+} /calmodulin kinases, dispersed through the rod and carboxyl-terminal domains (93). Such multiple regulations of phosphorylation/dephosphorylation along with the post transcriptional modification indicates the complexity of control mechanism in the redistribution and function of NuMA in dividing cells.

From the literature most NuMA antibodies stain either a diffuse or uniformly punctuate pattern in the interphase nucleus as shown by immunofluorescence (89, 53, 40, 17, 93). Some antibodies, however, including the first anti-NuMA (51), mAb 8.22 in the present study, and mAb W1 (83, Tang, personal communication), have revealed a pattern of dots and speckles plus lighter diffuse staining in the nucleus. In addition, some NuMA antibodies stain the nucleus uniformly as shown by conventional epifluorescence, but display a dot and speckle pattern when visualized by laser scanning confocal microscopy (16). The different nuclear staining patterns produced by various NuMA antibodies are most likely due to the differential availability of NuMA epitopes for each antibody. However, the actual molecular mechanism responsible for the staining pattern is not clear. Possibly, modifications at the RNA and/or protein level, or the association of NuMA with

different components at the discrete nuclear domains may contribute to differential epitope availability.

The translocation of NuMA during mitosis begins with the aggregation of NuMA into the interchromosomal space in early prophase. Progressively, NuMA transfers to the two centrosomes that will become the spindle poles. The process of aggregation and migration of NuMA coincides with chromosome condensation and the disassembly of the nuclear lamina (23, 1). Although pole-derived spindle fibers are occasionally stained with the NuMA antibodies at metaphase (16), the majority of NuMA is localized at the spindle poles as pericentriolar material. Under certain conditions, NuMA has also been detected in the centromere/kinetochore regions by immunofluorescence (17, 16, chapter 1). Since this pattern is most often observed in either isolated chromosomes or in arrested cells treated with mitotic inhibitors, it may represent an artifact caused by experimentally-induced redistribution of pericentriolar component (16).

NuMA gradually diminishes from the mitotic poles in anaphase and begins to reappear in the daughter nuclei regions at late telophase (chapter 1, 16, 93). Possibly, a dramatic conformational change occurs to bring about the disassociation of NuMA in the mitotic apparatus and its relocation in the nucleus. This may explain why most antibodies fail to detect the majority of NuMA at late anaphase through telophase. The carboxyl terminus may be important for the transition of NuMA between the mitotic state and the interphase state. An expression of a mutant NuMA lacking C-terminal by microinjection of truncated NuMA coding sequence has shown failure to either associate with the spindle poles at metaphase or relocate in the daughter nuclei after mitosis (18).

Whether NuMA relocates to the daughter nuclei before or after the nuclear envelope assembly remains disputed. Microinjection of rhodamine-conjugated wheat germ agglutinin (R-WGA) into the prometaphase cell for 2 hr has appeared to block the re-

entry of NuMA into the nuclei (16). Since WGA can impair nuclear pore permeability and block the later steps of nuclear assembly (21, 95, 58, 2), the post-mitotic nuclear import of NuMA may occur via transit through the nuclear pores (16). This conclusion, however, seems inconsistent with the most immunofluorescence results where NuMA commences to locate at the still condensed chromosome regions in telophase without the formation of new nuclei (chapter 1, 93, 68). Double label immunofluorescence with anti-NuMA and anti-lamin antibodies has shown directly that NuMA associates with condensed chromosomes before lamins (93). Moreover, the primary structure of NuMA does not contain a nuclear localization signal consensus sequence (NLS), a signal domain required for active transport through the nuclear pores (26, 38, 46, 47). All of these data support the possibility that the post-mitotic relocation of NuMA probably does not require to the assembly of the nuclear envelope. Regarding the WGA effect on the cell, at least one possibility for the cytoplasmic accumulation of NuMA is due to a 2-hr-long incubation after microinjection in mitosis. Consequently, what is blocked by R-WGA may be the newly synthesized NuMA in the cytoplasm of daughter cells but not the protein from the mother cell. Nevertheless the half-life and metabolism of NuMA remain unclear. Whether or how newly synthesized NuMA enters the nucleus during interphase requires further study.

Mitotic Function of NuMA

Two possible functions of NuMA during mitosis have been proposed for mitotic cells. Due to its localization in the pericentriolar regions, a logical conjecture is that NuMA may be involved in polar MT assembly during mitosis (chapter 1, 40, 53, 41). Alternatively, NuMA may play a role in the nuclear reassembly at the end of mitosis (68, 16, 93).

A) NuMA and Spindle MT Organization

Several studies involving MT inhibition, including experiments represented in the first chapter of this dissertation, have demonstrated an intimate association of NuMA with

the spindle MTs (40, 41, 53, 52). Treatments with inhibitors such as nocodazole, colcemid, and vinblastine, resulted in the dissolution of spindle MTs and the simultaneous disaggregation of NuMA. In all arrested cells, the dispersed MT foci invariably colocalized with the foci of NuMA protein. Furthermore, the process of spindle recovery after the removal of MT inhibitors indicated that foci with positive NuMA staining served as MTOCs. Nascent MTs emanated radially from these centers; and with the gradual consolidation of NuMA from multiple spots to polar crescents, corresponding MT asters elongate and converge to form the bipolar spindle (chapter 1).

A similar pattern of NuMA localization has also been reported in taxol treated PtK1 and PtK2 cells (53, 41). Taxol causes MTs of the mitotic cell to form short bundles and relocate at the cell periphery. It has been shown that NuMA foci dispersed by taxol are always associated with the minus end of MT bundles as detected by the method of tubulin hook decoration (53). Other proteins, including a constituent centrosomal component 5051 and a kinesin-like MT motor protein CHO1, have also been detected in the pericentriolar regions (9, 13, 45). However, 5051 protein is not dispersed from the centrosome by taxol treatment, and CHO1 protein distributes as small cytoplasmic spots which do not colocalize with the MT foci (52). Thus, NuMA appears to be the one of perhaps a few proteins in mitotic cells that invariably localizes at multiple MT nucleation centers during MT regrowth following mitotic arrest.

These observations suggest the possibility that NuMA is a specific MT associated protein in mitosis. An argument against this view is that NuMA does not contain any known MT binding motifs (93, 16), such as those identified in MAP1B (64), MAP2 (48), tau (29), and a 205 KD MAP in *Drosophila* (32). It should be noticed that these MAPs usually bind stoichiometrically to the wall of MTs (7, 4, 74). Perhaps, due to its specific minus end-associating, NuMA binds to MTs through a different mechanism from the conventionally

defined MAPs. Moreover, co-sedimentation of NuMA from extracts of mitotic HeLa cells with the taxol stabilized brain MT assemblies has provided biochemical evidence that NuMA may indeed be a mitosis-specific MT associated protein (51, 41). In the light of its coiled-coil structure and lack of ATP binding site (93, 16), NuMA is unlikely to serve as a MT motor but likely plays a role involved in nucleation or stabilization of spindle MTs.

Microinjections of NuMA antibodies also strongly support the notion that NuMA may serve as a minus-end organizing component of spindle MTs. The effects of antibodies in the injected cells are obviously different among species however. In primate such as African green monkey (CV-1) or human (HeLa), cells injected in prophase and up to 50% of cells injected at interphase displayed a failure to form the mitotic apparatus. The injected cells appeared to be arrested at prometaphase with deformed spindles and many of the non-arrested cells developed micronuclei after 24 hr (40, 94). Furthermore, injection of metaphase cells resulted in the immediate destruction of the spindle within 15–30 min followed by the formation of an abnormal monopolar MT array. In contrast, cells injected during anaphase were able to successfully complete mitosis and the spindle appeared to be unaffected (94). Consequently the effect of antibody microinjected into the cells depends on the mitotic stage; being more effective prior to than after the onset of anaphase. Thus, NuMA appears to be most important in the establishment and stabilization of mitotic spindle.

Microinjection of NuMA antibody into PtK2 cells induced a different pattern from that seen in primates (39). Injection in interphase cells failed to arrest cells in prometaphase but >50% of the injected cells later develop micronuclei. Injections prior to anaphase resulted in formation of micronucleated daughter cells. Unlike the distortion of the spindle as seen in primates, these antibody injections seemed to interfere with the normal function of the mitotic apparatus without disturbing the structure or morphology of

the spindle. However, injection of the same antibody into taxol arrested mitotic PtK2 cells caused disruption of MT bundles and results in a disorganized display of MTs in the cytoplasm (41). Thus, despite the rather different phenotype seen by the injection of antibodies into primate cells, NuMA appears to be generally involved in the MTOC function in PtK2 cells. Similar to the results in HeLa cells, 95% of cells injected after the onset of anaphase yielded daughter cells with the apparently normal nuclei, suggesting that antibodies only interfered with earlier events in mitosis.

The different mitotic defects induced by microinjections of NuMA antibodies into HeLa and PtK2 cells are rather similar to the different responses of mammalian cell lines to MT inhibitors, a phenomenon known for many years (71, 82, 35, 8, 44). For instances, human cell such as HeLa S3 cells, representing the primate type, can remain arrested in mitosis by colcemid throughout the course of treatment up to 72 hr or until cell detachment or death. Whereas Chinese hamster ovary cells, at the other extreme, are only transiently inhibited and consequently resume an interphase morphology (44). The fate of cells that escape mitotic block without chromosome segregation is to become micro-nucleated (44, 71). Indeed a striking difference has been observed between PtK2 and HeLa cells after colcemid and taxol treatment (39). Apparently marsupials are "rodent-like" in the response to MT inhibitors (35, 39).

Comparing the phenotypes between antibody injection and MT inhibition, it is not difficult to find considerable similarity in the outcomes of the two treatments. Both antibody injection and MT inhibition lead to a high ratio of mitotic arrest and a low ratio of micronuclei formation in primate cells, and an alternatively high ratio of micronuclei formation (escape from the mitotic block) in marsupial cells (94, 39). Therefore, perhaps the inability of PtK2 cells to be arrested by anti-NuMA antibody injection relates to a similar mechanism occurring in MT inhibition which permits the cells to escape the mitotic block.

The mechanism responsible for the escape from mitotic arrest, which may be also related to the Ptk2 microinjection phenotype, remains unknown. However, it appears to be a more complicated processes than merely the disassembly of spindle MT alone. It has been shown that the disruption of spindle assembly in HeLa cells is correlated with abnormal maintenance of elevated cyclin B levels and continued activation of p34^{cdc2}, whereas the oscillation of cyclin B level and p34^{cdc2} activity is only transiently inhibited in CHO cells (44). One hypothesis involves a check point serving to couple cell cycle progression to the completion of other cellular events. Such a check point must either exist in some cell lines but not in others, or the stringency of the control mechanism varies among cell species, thereby causing different cellular responses to the mitotic block (56).

A distinct effect in antibody injection is that antibodies interrupt the normal functions of spindle in early mitosis when the mitotic apparatus is being assembled. In addition, a striking staining pattern of NuMA in most mitotic cells is its crescent shape at the spindle poles, suggesting that most of NuMA molecules resides at the minus end of kinetochore MTs, but rarely at the ends of astral MTs. Such a specific distribution supports the notion that NuMA functions specifically in the formation of the chromosome-associated spindle.

Collectively, NuMA closely associates with the minus end of spindle fibers during mitosis as shown by MT inhibition and MT co-sedimentation. Despite the different cellular effects induced by antibody microinjections, NuMA appears to be essential in early mitosis and to contribute to spindle organization in both primates and marsupials. The mechanism responsible for the different phenotypes of antibody injection may be related to species-dependent cell responses to MT inhibition, a process that is yet poorly understood. The actual physiological relationship between NuMA and spindle formation and maintenance

must await further investigation. An experiment involving *in vitro* assembly of MTs of the mitotic apparatus in the presence of purified NuMA protein could be helpful in understanding the mechanism of NuMA's function as a polar MTOC component.

B) NuMA and Post Mitotic Reassembly

In view of its cell cycle dependent localization and identification in the nuclear matrix (51), NuMA has been proposed to function in post-mitotic nuclear assembly (68, 16, 93). Major evidence for this hypothesis comes from *in vivo* over-expression of human wild type and mutant NuMA in interphase hamster cells by transfection or microinjection of constructed plasmids carrying various portions of coding sequence (18). Expressed NuMA lacking an amino terminal head accumulated in the interphase nucleus before and after mitosis and associated with the polar regions of mitotic apparatus as observed in wild type. In contrast, expressed NuMA lacking the C-terminal tail remained diffusely distributed in the cytoplasm without association with the spindle pole or nuclear structure. Regardless of the different localizations of the mutant NuMAs which suggest a potential role of each domain in the redistribution of NuMA, the terminal phenotypes obtained by expression of headless and tailless NuMA were similar. Both resulted in the formation of micronuclei without distortion of mitotic spindles, suggesting that NuMA is required for the proper completion of mitosis.

A temperature sensitive hamster cell line tsBN2 shares certain similarity to the mitotic phenotype as induced by the expression of truncated NuMA (62, 63). Shifting to the restrictive temperature initiates premature entry into mitosis and later formation of micronuclei. A missense mutation in the RCC1 gene that encodes a highly conserved chromatin binding protein is responsible for the temperature sensitive phenotype (37, 86). The endogenous NuMA in tsBN2 associates with spindle poles in abnormal mitosis at the restrictive temperature but fails to re-enter interphase micronuclei. Expression of wild type

human NuMA suppressed the post mitotic micro-nucleation in tsBN2 cells without affecting the RCC1-dependent phenotype of premature entry into mitosis (18).

These data suggest a function of NuMA in a terminal phases of chromosome separation, and/or nuclear reassembly based on two premises. First, the expression of both headless and tailless mutants in normal BHK cells induced micronucleation without disruption of the mitotic apparatus. Secondly, the expression of wild type NuMA can suppresses the abnormal micronucleation in the mutant tsBN2 cells without interfering with the original phenotype of premature mitosis. Since both the normal and mutant host cells are rodent, however, the induction of micronucleation by truncated NuMAs or restrictive temperature may also be a species-specific phenotype unique to rodent cells. This may be in someway related to the escape of rodent cells from mitotic block as mentioned in the previous section. Furthermore, the introduction of wild type or truncated NuMA genes in these experiments all involved interphase cells. Consequently, all exogenous NuMA must be expressed at a certain time in interphase. Therefore, it is not clear at which stage of mitosis (for example, prior to or after the onset of anaphase) that the exogenous NuMA proteins commenced their function. In this regard, the over-expression of wild type or mutant NuMA *in vivo* provides relatively little information on the role of NuMA in spindle organization or nuclear formation.

Perhaps, the strongest evidence for NuMA's function in nuclear formation is that NuMA may interact with the chromatin binding protein, RCC1 or an RCC 1-dependent protein. In RCC-1 mutant cell (tsBN2), the endogenous NuMA has an abnormal relocation in the cytoplasm at the restrictive temperature after mitosis (18), implying NuMA may be involved in the decondensation of chromosome. Collectively, the *in vivo* expression data is relatively inconclusive concerning the precise function of NuMA because it appears to be consistent with both the proposal that NuMA may play a role in post mitotic nuclear

reassembly and the view that NuMA may be involved in a MTOC function in the organization of the mitotic apparatus.

In summary, most experimental data involving mitotic cells argue that NuMA may be a mitosis specific, minus–end MAP involved in the organization and function of spindle. Antibody injection experiments also strongly suggest that NuMA is essential in early stages of mitosis. The limited results from *in vivo* expression experiments suggest that NuMA may play a role in post–mitotic assembly. Therefore, the proposal that NuMA functions in the organization of the spindle is more attractive and more widely supported in the current literature. How NuMA actually interacts with the mitotic components requires much more rigorous experimentation.

Interphase Function of NuMA

Most reports on NuMA protein have been restricted to its function during mitosis which of course represents only a small portion of the total cell cycle. My studies on the localization of NuMA in the nucleoskeleton and associated RNA splicing apparatus argue for a more global role for NuMA in nuclear organization and function. Since these studies will be discussed in detail in chapters 2 and 3, a brief review will be described in the next sections.

A) Localization of NuMA in the Core Filaments

The presence of a non–chromatin matrix in the eukaryotic nucleus has now been well established (reviews see 88, 91, 59, 3). The nuclear matrix is the site of many nuclear processes involved in organization of chromatin loops (72, 25, 22), DNA replication (30, 57), RNA transcription, splicing and transportation (96, 11, 12, 70), and hormone response (24). Therefore, the nuclear matrix has exceedingly complicated biochemical composition including various structural and functional factors involved in numerous nuclear activities.

Generally speaking, the term nuclear matrix refers to the structure that remains as a network after removal of chromatin by nuclease treatment and salt extraction. Electron microscopy has provided excellent morphological evidences for the presence of such a complex scaffold as a ~10 nm filamentous skeleton associated with more or less granules and amorphous materials revealed by different extraction procedures respectively (34, 20). A smooth, highly branched RNA containing nuclear network termed core filaments has recently been identified following a sequential extraction of the nucleus (28). This intermediate filament-like system appears to represent a true nucleoskeleton serving as a scaffold to which other proteins associate to form the complete nuclear matrix. Unlike the cytoskeleton, nuclear core filaments are composed of heterogenous proteins and hnRNAs involved in various nuclear activities (20, 28, 60). A thorough identification and characterization of specific core filament components, however, has lagged due to the lack of specific probes.

NuMA was first identified by an antibody raised against a biochemical fraction of nuclear matrix from HeLa cells (51). Its nuclear staining is resistant to DNA digestion and salt extraction up to 2M as shown by immunofluorescence (chapter 2, 40). Moreover, during the course of this research I identified NuMA protein as a stable component of core filaments. A monoclonal antibody to NuMA, 2D3, specifically decorates a subclass of core filaments as detected by immuno-gold labeled electron microscopy (chapter 2).

The similarities of the primary and secondary structures between NuMA and intermediate filament elements strongly favors NuMA being a component of nuclear core filaments, which also share several common features with intermediate filaments including size, morphology and solubility properties (28, 59). Immunoblots have indicated that ≥ 200 KD NuMA isoforms contribute to the formation of core filaments (chapter 2). Therefore, in the light of its unusually long coiled-coil configuration with hydrophobic heptad repeats,

NuMA may form hetero-dimers or polymers as the subunits of some nucleoskeletal filaments.

B) Association of NuMA with the Spliceosomes

RNA splicing takes place in the spliceosomes which are the macromolecular complexes consisting of pre-mRNA, small nuclear ribonucleoprotein (snRNP) particles, and other splicing factors (76, 5, 55, 43, for reviews). The snRNPs are assembled by various species of U small nuclear RNAs (snRNAs) respectively and the common or unique polypeptides binding to each snRNA (49, 54 for reviews). At the cellular level, the spliceosome components are organized in the interphase nucleus that is specifically recognized by anti-snRNP antibody α Sm as a pattern of dots and speckles (78, 79, 70, 65).

As mentioned earlier, at least three NuMA antibodies have been shown to produce similar nuclear speckle patterns in interphase (51, 83). One of them, mAb 8.22, characterized extensively in the present study, labels nuclear domains that are superimposable with spliceosomes stained by α Sm antibody in double-label immunofluorescence. The colocalization persists even in the nuclear core filament preparation, or after RNase treatment which deformed the speckles to amorphous blobs. An anti-snRNA antibody could immunoprecipitate NuMA isoforms from HeLa extract as shown by immunoblotting, suggesting a relatively strong association between NuMA and snRNPs. More importantly, in an *in vitro* reconstituted splicing reaction (19, 75), two NuMA antibodies (2D3 and 8.22) have precipitated exogenously provided pre-mRNA but not the control RNA lacking consensus sequence recognized by U snRNPs.

Spliceosomes are assembled by the specific recognitions of snRNPs to the consensus sequence elements within RNA precursors (55, 49). First, U1 and U2 snRNPs bind to splice junctions and branch point sequences of pre-mRNA, respectively, to form

macromolecular complex A. Followed by the access of U5 and U4/6 snRNPs, a two-step cleavage and ligation processing occurs to yield spliced exons and excised lariat introns through the formations of complex B and C (55, 49) (Fig. 1). Precipitation of wild type pre-mRNA with anti-NuMA antibodies in reconstituted splicing reaction has indicated that NuMA protein associates with the active spliceosomes, at least those of complex A. In this view, NuMA appears to play a role in mRNA processing at least in initiation stage such as the formation of spliceosomes. It will indeed be interesting to know whether NuMA associates with splicing complexes B and C as indicated by the detection of intermediate and final products in the appropriate immunoprecipitations.

C) NuMA as a Structural Interface between the Nucleoskeleton and RNA Splicing

Compared to the significant achievements in understanding the biochemical reactions of the splicing process (Fig. 1), little is known about how spliceosomes are organized within discrete nuclear domains. However, different studies have noticed a preferential association of splicing with the nuclear matrix (96, 80, 75, 70, 90). Recent microscopic studies have suggested that pre-mRNA are both transcribed and processed in a discrete nuclear "track" that might correspond to nuclear architecture (12, 92, 31, 36). An EM visualization of purified *in vitro* reconstituted splicing complexes has even revealed a fibrous protein extension from the large globular complex that could represent the NuMA and/or NuMA-like nucleoskeletal proteins (69). Therefore the present study contributes to how the spliceosomes are organized within the nuclear matrix. Given its filamentous nature and our knowledge of its primary structure, it is unlikely that NuMA play a catalytic role in splicing. As a coiled-coil component of nuclear core filaments, NuMA appears to form a structural interface between the splicing apparatus and the nucleoskeleton and probably plays a key role in the organization of splicing factors into 3-D nuclear domains. A more detailed analysis of NuMA and its associated components will be very helpful in

understanding how NuMA is involved in the formation and organization of spliceosomes. Perhaps this investigation provides the first step toward the goal of defining the structural integration of the spliceosomes with the nuclear architecture in eukaryotic cells.

Multiple Functions of NuMA and NuMA-like Proteins in the Cell Cycle

NuMA was so named for its striking property of relocating from the interphase nucleus to the mitotic spindle during each cell cycle (51). Since its initial discovery, other proteins with the similar cell cycle dependent redistribution properties have been described in recent years, including mitotin (85), fA12 (27), H1B2 (61), CC-3 (84), 2D5-MAP (33) (table 1), and several less abundant MAPs identified in *Drosophila* embryo (42). In addition, several antibodies raised against brain MAPs, especially MAP1, have also produced similar staining patterns as shown by immunofluorescence (66, 73, 6). All of these proteins are localized in the interphase nucleus either uniformly or as dots or speckles in interphase and then reside in the mitotic apparatus at the poles, spindle, centromeres, etc. (table 1). In this view, the term NuMA, originally selected to describe one specific ≥ 200 KD protein, may be a more appropriate term for a class of proteins that oscillate between the nucleus and mitotic apparatus. If so, then the NuMA isoforms may be more appropriately designated as NuMA1A, NuMA1B, etc.

During mitosis, nonchromosomal nuclear proteins are distributed in two ways: either dispersed throughout the cytoplasm of the mitotic cell, or specifically associated with the mitotic apparatus. Most nonchromosome proteins seem to be dispersed including nuclear lamins (23) and snRNPs (81, 75). However, NuMA is specifically associated with the polar regions of the spindle and represent the second category. In this regard, most studies of NuMA suggest that it is not only passively segregated by spindle but directly involved in the function of mitotic apparatus (chapter 1, 39, 94, 18). Very possibly other members of this class of proteins as mentioned above also play bifunctional roles in the

nucleus and spindle. Interestingly, many of these proteins have been localized in the interphase nucleus as dots and speckles very similar to the pattern of spliceosomes (85, 84, 61), suggesting that they may be also directly or indirectly involved in RNA processing or in some way related to the function of NuMA. Additional cDNA and functional analysis will therefore be most helpful for further elucidation of this class of proteins. It is perhaps worthwhile to note that NuMA can be classified either as a nucleoskeletal or cytoskeletal protein depending on the stage of the cell cycle. Proteins such as NuMA that assume multiple roles in cells would seem to have selective advantage in evolution and may indeed be more common than anticipated. It is likely, therefore, that NuMA is one member of a class of structural proteins that resides in both the nucleus and mitotic apparatus forming a molecular fabric to embrace the genome throughout the cell cycle.

Table 1

NuMA and NuMA-like Proteins

proteins	nuclear pattern	mitotic pattern	KD	reference
NuMA	diffuse & speckle	poles	200-240	51,16,93
mitotin	speckles	poles & midbody	125	85
fA12	diffuse	poles & peri-chromosomes	30-50	27
H1B2	speckles	poles, midbody, & peri-chromosomes	240	61
CC-3	speckles	poles, kinetochore, midbody, & spindle	255	84
2D5-MAP	dots	spindle fibers	200	33

Figure 1. The predicted secondary structure of NuMA protein. Interruptions in the helical domain by pairs of proline (PP) residues are indicated by open spaces. (Modified from Compton et al., 1992).

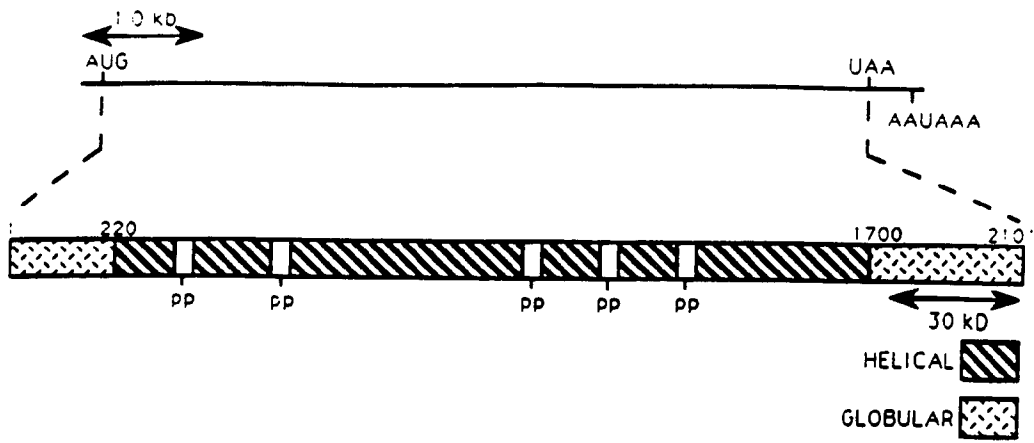
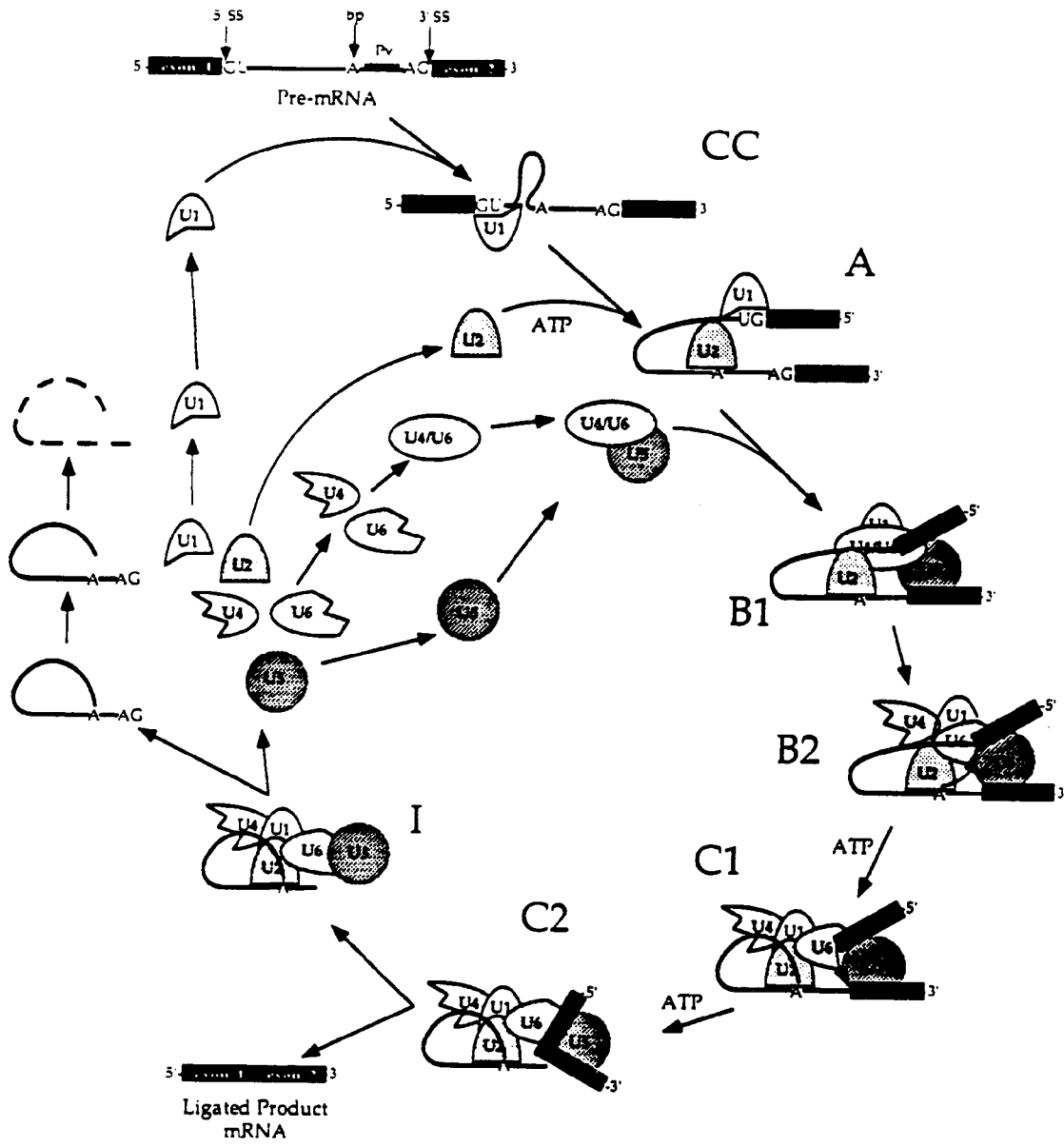


Figure 2. A schematic representation of pre-mRNA splicing (Other required non-snRNP factors are not included for simplicity). CC (commitment complex), A, B1, B2, C1, C2, and I represent macromolecular complexes within the splicing pathway that have been distinguished biochemically and/or genetically. (Copied from Moore, et al., 1993)



**CENTROPHILIN: A NOVEL MITOTIC SPINDLE PROTEIN
INVOLVED IN MICROTUBULE NUCLEATION**

A. TOUSSON, C. ZENG, B.R. BRINKLEY, and M.M. VALDIVIA

**The Journal of Cell Biology, Vol. 112, No. 3, pp. 427–440
February, 1991**

Copyright
1991

The Rockefeller University Press
222 East 70th Street
New York, N.Y. 10021

Used by permission

ABSTRACT

A novel protein has been identified which may serve a key function in nucleating spindle microtubule growth in mitosis. This protein, called centrophilin, is sequentially relocated from the centromeres to the centrosomes to the midbody in a manner dependent on the mitotic phase. Centrophilin was initially detected by immunofluorescence with a monoclonal, primate specific antibody (2D3) raised against kinetochore-enriched chromosome extract from HeLa cells (Valdivia, M.M., and Brinkley, B.R., 1985, *J. Cell Biol.* 101:1124–1134). Centrophilin forms prominent crescents at the poles of the metaphase spindle, gradually diminishes during anaphase, and bands the equatorial ends of midbody microtubules in telophase. The formation and breakdown of the spindle and midbody correlates in time and space with the aggregation and disaggregation of centrophilin foci. Immunogold EM reveals that centrophilin is a major component of pericentriolar material in metaphase. During recovery from microtubule inhibition, centrophilin foci act as nucleation sites for the assembly of spindle tubules. The 2D3 probe recognizes two high molecular mass polypeptides, 180 and 210 kD, on immunoblots of whole HeLa cell extract. Taken together, these data and the available literature on microtubule dynamics point inevitably to a singular model for control of spindle tubule turnover.

INTRODUCTION

Progression of cells into mitosis is characterized by the disassembly of the cytoplasmic microtubule complex (CMTC) and the concomitant assembly of microtubules of the mitotic spindle. The dissolution of the spindle is similarly synchronous with the formation of the midbody. When division is complete, midbody microtubules depolymerize, and a new CMTC is formed in each daughter cell (Brinkley et al., 1975; Brinkley, 1985). The organization of microtubule arrays *in vivo* appears to be regulated by discrete foci

known as microtubule organizing centers (MTOCs) (see Brinkley, 1985). These foci either nucleate or capture microtubules.

The centrosome, the cell's major MTOC, is usually located near the cell center and serves as the nucleation site for the interphase CMTC. Other MTOCs in mammalian cells include kinetochores and midbodies. As cells progress from the G2 phase of the cell cycle into mitosis, the centrosome splits into two identical components (diplosomes) with each functioning to nucleate opposing halves of the microtubule array making up the mitotic apparatus (see McIntosh, 1983). At the same time, there is a prominent increase in protein kinase activity as the centrosome (Verde et al., 1990; Bailly et al., 1989), and a corresponding rise in its capacity to nucleate microtubules (Telzer and Rosenbaum, 1979; McIntosh et al., 1975). These changes in centrosomal activity are accompanied by an increase in the abundance of electron-dense pericentriolar material (Rieder and Borisy, 1982). Aggregation of electron-dense material is also seen during the formation of the midbody in telophase. This material has been shown to nucleate microtubule growth in vitro (Gould and Borisy, 1977). Such major changes in structure and activity suggest that MTOCs and associated proteins play an important role in regulating the assembly and distribution of microtubules during the cell cycle.

Despite an extensive body of literature, the phenomenon of microtubule nucleation in the living cell remains nebulous. Neither is it clear how the shortening of kinetochore microtubules is orchestrated with both the elongation of interpolar microtubules and the formation of the midbody. The mechanism by which MTOCs intervene in microtubule dynamics awaits the clarification of their molecular composition.

Antibodies have provided a seminal approach to defining the molecular composition of centrosomes and related MTOCs. The availability of human and rabbit autoantibodies directed against the centrosome (Gosti-Testu et al., 1986; Sager et al.,

1986; Calarco–Gillam et al., 1983; Connolly and Kalnins, 1978; Brenner et al., 1981) has indicated that common antigenic sites exist among cells of varied origins including those of higher plants (Clayton et al., 1989). A potentially unique type of microtubule–associated protein (MAP) at the centrosome was detected by antibodies raised against brain MAP1A (Sato et al., 1983). This MAP may lower the critical concentration of tubulin required for microtubule assembly, thus, allowing for favored nucleation at the centrosome. Antibodies that are respectively specific for kinesin (Neighbors et al., 1988) and dynein (Pfarr et al., 1990) also recognize mammalian centrosomes. Vandre et al. (1986) initially identified a family of phosphoproteins associated with the centrosome, centromeres, and midbody utilizing an mAb, MPM–2. A 225–kD centrosomal phosphoprotein detected with an mAb, CHO3, appears crucial to the shift from mitosis to interphase (Kuriyama and Sellitto, 1989). The cdc2 protein kinase has been localized in the pericentriolar region using the monoclonal probe, CTR453 (Bailly et al., 1989). Anticalmodulin immunofluorescence reveals a polar pattern (Welsh et al., 1978) and a 165–kD centrosomal protein in mammals aggregates in the presence of Ca^{2+} , as revealed with anticentrin antibody (Salisbury et al., 1986). Centrosomal proteins with molecular masses of 43 kD (Rao et al., 1989), 64 kD (Petzelt, 1979), 110–115 kD (Sager et al., 1986), and a series of proteins characterized by molecular masses of 60–65, 130, and 180–250 kD (Gosti–Testu et al., 1986, 1987) have also been discovered using immunological probes. Although strong similarities exist, these probes recognize antigens with different immunofluorescent and/or electrophoretic patterns from that recognized by a new spindle probe to be described here.

In this report, we describe an mAb 2D3, which was raised against kinetochore–enriched chromosome extract from HeLa cells (Valdivia and Brinkley, 1985). This probe recognizes two polypeptides, 180 and 210 kD, on immunoblots of whole HeLa cell extract. The detected protein, here called centrophillin, is sequentially relocated from the

centromeres to the centrosomes to the midbody in a manner dependent on the mitotic phase. We demonstrate centrophilin to be a novel marker protein for spindle microtubule nucleation which potentially serves to capacitate the MTOCs.

MATERIALS AND METHODS

Preparation of Kinetochore-Enriched Extract for Immunization

HeLa cells were grown in suspension culture in McCoy's 5a medium supplemented with 7% FCS. Cells in exponential growth were synchronized by adding 2.5 mM thymidine (Sigma Chemical Co., St. Louis, MO) to the medium for 18h, and the mitotic cells were accumulated by treatment with Colcemid at 0.06 µg/ml in fresh medium for 16 h. A mitotic index of 98% was commonly obtained as determined by phase-contrast microscopy. The hexylene glycol method for metaphase chromosomes isolation was used, starting with 10⁸ mitotic cells (Valdivia and Brinkley, 1985). These preparations contained centrosomal material which persisted even after glycerol gradient purification.

Kinetochore enrichment involved incubating crude chromosome suspensions with 10 mM Tris-HCl, pH 7.1, 2 mM CaCl₂, 1 mM PMSF containing 200 U/ml micrococcal nuclease (MNase) (Worthington Biochemical Corp., Freehold, NJ) for 1 h at 37°C. Later, the suspension was centrifuged in a Beckman JA-20 rotor at 5,000 rpm for 10 min at 4°C. The pellet was resuspended in 10 mM Tris-HCl, pH 7.1, 1 mM EDTA, 1 mM PMSF (TEP) containing heparin (Sigma Chemical Co.) at 2 mg/ml and incubated at 4°C for 60 min. The suspension was centrifuged as above and the pellet was resuspended in TEP containing 3 M urea and incubated for 1 h at 4°C. The preparation was then centrifuged at 10,000 rpm for 15 min at 4°C. The supernatant was used as the source for immunizations.

MAB Production

BALB/c mice immunized intraperitoneally with crude urea extracts prepared from HeLa metaphase chromosomes as described. Approximately 200–300 µg of total protein

was used per injection emulsified in Freund's adjuvant. The mice were boosted every 4 wk for several months. Blood samples obtained from the tail were screened by immunofluorescence for the presence of antibodies against mitotic spindle antigens. For immunofluorescence screening, HeLa cells were cultured on sterile glass coverslips and fixed with methanol for 10 min at 4°C. Coverslips were then incubated in undiluted mouse serum for 30 min at 37°C, washed in PBS, and incubated with a 1:20 dilution of goat antimouse IgG-FITC for 30 min at 37°C. (For more details, see "Immunofluorescence" in this section). The spleen from the selected mouse was removed, dissociated, and the spleenocytes were fused with mouse myeloma SP 2/0 cells using standard procedures as described by Kohler and Milstein (1975). Supernatants from our hybridoma cultures were again screened by immunofluorescence. Hybridomas found by the assay to secrete the desired antibody were harvested and cloned three times by limiting dilution. The hybridoma clones were then grown up in flasks and used as the source of mAbs for subsequent experiments. To maintain the stability of the mAb, the hybridoma supernatant was concentrated by tangential flow ultra-filtration (Millipore Continental Water Systems, Bedford, MA); 500 ml of supernatant would yield ~50 ml of concentrated filtrate. Antibody filtrate was further dialyzed against a mixture of one part 2X borate-buffered saline, pH 8.2, and one part glycerol. Dialyzed antibody was aliquoted and stored at -80°C.

Cell Culture and Microtubule Disassembly/Reassembly In Vivo

All cell lines (HeLa, W138, human lung carcinoma, African green monkey, CHO, BHK, PtK, 3T3, Chinese Muntjac, and Indian Muntjac) were maintained in cell culture flasks containing suitable growth medium (DME, RPMI, McCoy's, or Ham's F10 [Cellgro]) supplemented with 10% FBS, 2 mM glutamine, 1 mM sodium pyruvate, 100 U/ml penicillin and 100 µg/ml streptomycin. All cell lines were passaged with 0.1% trypsin in HBSS (Sigma Chemical Co.). HeLa cells were used exclusively in all microtubule inhibition

experiments because of their fastidious growth and strong recognition by 2D3. The other cell lines were used only to determine the extent of 2D3 crossreactivity. HeLa were trypsinized from culture flasks and seeded onto sterile glass coverslips in bacteriological grade 60–mm plastic petri dishes (Falcon Labware, Oxnard, CA). When coverslips reached ~75% confluence, they were incubated with 10 µg/ml nocodazole (Amersham Corp., Arlington Heights, IL) or 0.1 µM vinblastine (Fisher Scientific Co., Pittsburgh, PA) diluted from a 10–mg/ml or 10–mM stock in DMSO stored frozen, or 0.1 µg/ml Colcemid diluted from a 100X stock in buffer (Gibco Laboratories, Grand Island, NY). The drugs were added directly to culture medium for 4 h. For cold treatment experiments, HeLa cells were identically cultured and incubated at 0°C for 40 min in fresh medium. Cells were recovered from mitotic inhibitor (0–5 h) or cold treatment (0–1 h) in fresh prewarmed medium (37°C) and processed for immunofluorescence. In Ca²⁺ treatment experiments, HeLa cells were rinsed in PBS or Pipes buffer, permeabilized with nonionic detergent, rinsed in buffer, incubated with CaCl₂, and subsequently fixed (see "Immunofluorescence" for details).

Immunofluorescence

Cells on glass coverslips were rinsed in PBS and processed for single-label 2D3 immunofluorescence in one of five ways: (1) absolute methanol fixation (histological grade, Fisher Scientific Co.) for 7 min at 20°C; (2) 3% formaldehyde fixation (TEM grade, Tousimis) in PBS for 45 min at room temperature, rinsing in PBS, permeabilization with 0.5% Triton X–100 in PBS for 2 min, and rinsing in PBS; (3) permeabilization with 0.5% Triton X–100 in 0.1 M Pipes, 1 mM EGTA, 1 mM MgCl₂, pH 6.9 (PEM), rinsing in PEM, and fixation in 3% formaldehyde in PBS for 45 min; (4) permeabilization with 0.5% Triton X–100 in 0.1 M Pipes, pH 7.4, with various levels of CaCl₂ (0, 1 µM, 10 µM, 1 mM), rinsing in 0.1 M Pipes, incubation with 0.1 M Pipes containing CaCl₂ for 9 min at room temperature, and

fixation in 3% formaldehyde in PBS for 45 min; or (5) permeabilization with 0.5% Triton X-100 in PBS for 2 min, rinsing in 0.1 M Pipes, pH 7.4, incubation with 21 mM CaCl_2 in 0.1 M Pipes for 9 min at room temperature, and fixation in 3% formaldehyde in PBS for 45 min. All coverslips were then incubated with 1:10 dilution of concentrated, dialyzed 2D3 hybridoma supernatant in PBS for 30 min at 37°C in a humidified chamber, washed in PBS (four changes within 10 min), incubated, with a 1:20 dilution of affinity-purified goat anti-mouse IgG FITC (Boehringer Mannheim Biochemicals, Indianapolis, IN) in PBS for 30 min at 37°C, washed in PBS, optionally incubated with a 1:20 dilution of affinity-purified swine anti-goat IgG-FITC (Boehringer Mannheim Biochemicals) in PBS for 30 min at 37°C, washed in PBS, stained with 20 $\mu\text{g/ml}$ Hoechst 33258 (Calbiochem-Behring Corp., La Jolla, CA) in PBS for 2 min, rinsed briefly in PBS, and mounted on slides in 1:9 PBS/glycerol containing 0.1% phenylene diamine (Fisher Scientific Co.). Negative control experiments, which were performed with the omission of primary antibody, revealed only diffuse, low level background staining.

All else unchanged, single-label antitubulin immunofluorescence was performed using a monoclonal IgG antibody specific for β -tubulin (Tu27B; L.I. Binder) diluted 1:40 on formaldehyde/Triton X-100 processed cells in place of 2D3 incubation. This probe preferentially recognizes microtubule polymer and does not require detergent extraction of soluble tubulin. An affinity-purified, monospecific sheep antitubulin antibody was originally used in early experiments.

For double-label 2D3/antitubulin immunofluorescence experiments, cells were rinsed in PEM, permeabilized in 0.5% Triton X-100 in PEM for 2.5 min, rinsed with several changes of PBS, fixed in 3% formaldehyde in PEM for 45 min, rinsed in PBS, blocked with TBS, pH 7.4, for 2 min, post-blocked with 1% BSA in PBS for 10 min, incubated with 2D3 diluted 1:10 in 1% BSA in PBS for 30 min at 37°C, washed in PBS, blocked with 1% BSA

in PBS, incubated with goat anti-mouse IgG-biotin (Boehringer Mannheim Biochemicals), diluted 1:20 in 1% BSA in PBS for 30 min at 37°C, washed in PBS, blocked with 1% BSA, incubated with avidin-Texas Red (Boehringer Mannheim Biochemicals) diluted 1:200 in 1% BSA in PBS for 30 min at 37°C, washed in PBS, blocked with 1% BSA in PBS, incubated with monoclonal antitubulin antibody (5H1, IgM, L.I. Binder) diluted 1:40 in 1% BSA in PBS for 30 min at 37°C, washed in PBS, blocked with 1% BSA in PBS, incubated with affinity-purified μ -chain-specific rabbit anti-mouse IgM (Nordic Immunology, Tilburg, The Netherlands) diluted 1:20 in 1% BSA in PBS for 30 min at 37°C, washed in PBS, blocked with 1% BSA in PBS, incubated with affinity-purified goat anti-rabbit IgG-FITC diluted 1:20 in 1% BSA in PBS for 30 min at 37°C, washed in PBS, stained with Hoechst, and mounted.

In antikinetochore/2D3 double-label immunofluorescence experiments, kinetochore localization was detected by sequential incubation with 1:100 CREST antiserum (Brenner et al., 1981), 1:20 anti-human IgG-biotin (Boehringer Mannheim Biochemicals), and 1:200 avidin-Texas Red. Centrophilin localization was highlighted by sequential incubation with 2D3, goat anti-mouse IgG-FITC, and swine anti-goat IgG-FITC.

Slide specimens were analyzed on a Leitz fluorescence microscope equipped with a Vario Orthomat II camera system. Micrographs were prepared with Kodak T-Max 400 film push processed to 1600 ASA.

Immunoelectron Microscopy

HeLa cells were grown on Thermanox coverslips (Lux Scientific Inc., Newbury Park, CA), rinsed in PBS, permeabilized in 0.5% Triton X-100 in PBS, rinsed with several changes of PBS, fixed in 3% formaldehyde in PBS, rinsed in PBS, blocked with 1% BSA in PBS, incubated with 2D3 diluted with 1% BSA in PBS, washed in PBS, blocked with 1% BSA, incubated with anti-mouse IgG conjugated to colloidal gold, 10 nm (Amersham

Corp.), diluted 1:2 with 1% BSA in TBS for 1 hr at room temperature, washed in PBS, postwashed in 0.1 M Pipes, 1 mM MgCl₂, 1 mM CaCl₂, pH 7.2; fixed in 3% glutaraldehyde (EMS) in Pipes for 1.5 h, washed in Pipes, postfixed in 1% osmium tetroxide in Pipes, washed in Pipes, en block stained with 2% uranyl acetate (Ted Pella, Inc., Irvine, CA) in 30% ethanol, dehydrated in a graded ethanol series, infiltrated with Spurr's low viscosity resin (EMS), embedded overnight at 70°C in flat molds and thin sectioned for electron microscopic analysis. Control experiments were performed by omitting the incubation with first antibody.

Electrophoretic Transfer and Immunoblotting

Electrophoresis was performed on 4–16% polyacrylamide gels using the buffer system of Laemmli (1970). Exponentially growing HeLa cells were trypsinized from two T175 cultures flasks after attaining 80% confluence. The cells were washed in PBS, pelleted in a low-speed table-top centrifuge, resuspended in a small volume (200 µl) of Tris buffer (10 mM Tris, pH 7.5, 150 mM NaCl, 1 mM CLAP) sonicated with 1 ml SDS-PAGE sample buffer, and boiled for 5 min. The boiled samples were pelleted in a microfuge, and the supernatants were collected for electrophoresis. Sample aliquots of 50–100 µl were loaded on minigels or regular gels, and electrophoresed at 100–120 V for 1.5–2 or 5–7 h, respectively. Gels were either stained with Coomassie blue R-250 or electrophoretically transferred to nitrocellulose sheets (0.2 µm pore size) at 100 V for 2 h in SDS-free transfer buffer (Towbin et al., 1979). In a procedure modified from Towbin et al., protein-bound nitrocellulose sheets were then blocked with 5% dry milk in borate-buffered saline (BBS) for 30 min with continuous agitation, incubated in 1:100 in 2D3 in blocking solution overnight at room temperature with agitation, washed in BBS (4X, within 30 min), incubated with 1:100 rabbit anti-mouse IgG in blocking solution for 2 h at room temperature with agitation, washed in BBS, incubated with 1:200 mouse IgG-peroxidase-

antiperoxidase complex (Clono PAP; Sternburger Meyer) in blocking solution for 2 h at room temperature, washed in BBS, and developed with DAB in Tris–imidazole buffer. Occasionally, this procedure was abbreviated by using goat–antimouse IgG directly conjugated to peroxidase (Boehringer Mannheim Biochemicals). Control trials were performed by omitting the incubation with first antibody.

RESULTS

Nature and Specificity of the 2D3 mAb

The production of 2D3 involved the immunization of mice with kinetochore–enriched chromosome extracts from HeLa mitotic cells (prepared according to Valdivia and Brinkley, 1985). The fact that 2D3 recognizes centrosomes as well as centromeres is not surprising considering that the original immunogen in part contains centrosomal material that transiently associates with kinetochores during mitosis.

The 2D3 antibody was classified as an IgG1 by Ouchterlony double immunodiffusion. In this assay, 2D3 hybridoma supernatant was run against specific subclasses of mouse immunoglobulins (data not shown). Our antibody crossreacts with all primate cell lines tested, including HeLa, WI38, human lung carcinoma cells, and African green monkey. Non–primate lines such as CHO, PtK1, Indian muntjac, and Chinese muntjac yield negative results. Although the particular epitope recognized by 2D3 is restricted to primates, the protein is likely to be common to the mitotic spindles of other species. Two polypeptides which respectively migrate at 180 and 210 kD are resolved on electrophoretic transfers of whole HeLa cell extract immunoblotted with 2D3 (Fig. 1).

Corresponding Coomassie–stained gels of HeLa extract showing the full complement of extract proteins and negative control assays in which 2D3 was excluded together confirm the blotting immunospecificity. The two polypeptides might either be subunits of centrophilin, or one of the polypeptides may be a distinct protein that shares

a common epitope with centrophilin. The first possibility is more likely, for no anomalous staining pattern indicative of another localized protein is seen in immunofluorescence assays with 2D3 (see Fig. 2). It is also plausible that the 180-kD polypeptide is a proteolytic fragment of the 210-kD polypeptide, although a "ladder pattern" between the two bands indicative of proteolysis is not observed.

Localization of Centrophilin During the Cell Cycle

Centrophilin forms crescents at the poles of the mitotic spindle and bands the center of the midbody during cell division, as revealed by immunofluorescence with 2D3 (Fig. 2). The formation and breakdown of the spindle and midbody is synchronous with the appearance and disappearance of centrophilin. Formaldehyde/Triton X-100 fixation and permeabilization was employed in our initial immunofluorescence assays. This protocol was ideal for demonstrating the prominent association of centrophilin with the centrosomes and midbody. However, diffuse, punctate staining of chromosomes and kinetochore tubules in prometaphase, and subtle staining of interzonal fibers in anaphase was also observed. This low-level staining was particularly enhanced using other fixation protocols, as will be shown. Fig. 2, A-G provides an abbreviated profile of centrophilin localization throughout the cell cycle; *a-g* show the corresponding microtubule pattern in each respective phase. During interphase, centrophilin is diffusely localized in the nucleus (*A,a*) and excluded from the cytoplasm. In prometaphase, the protein concentrates into a central focus correlating in time and space with the developing monaster (*B,b*). Due to the close proximity of the double centrosomes, the diplosome is not yet clearly visible. Later in prometaphase, the centrophilin focus becomes resolvable as two foci, corresponding with the clear separation of the diplosome (*C,c*). In metaphase, prominent crescents of centrophilin appear at the spindle poles (*D,d*). This pronounced staining correlates with the increasing accumulation of dense pericentriolar material seen by

electron microscopy (Rieder and Borisy, 1982). As the kinetochore microtubules shorten in anaphase, the centrophilin crescents gradually disappear (*E,e; F,f*). In telophase, centrophilin reappears in the center of the forming midbody (*G,g*). Again, this localization corresponds with the aggregation of electron–dense material.

Immunoelectron Microscopic Localization of Centrophilin

Immunogold EM with 2D3 in permeabilized metaphase HeLa cells confirms that centrophilin is part of the electron–dense pericentriolar material, aggregating into crescents (Fig. 3). The protein does not, however, reside on centrioles or a narrow zone surrounding the centriole. These observations correlate with both the polar "doughnut" pattern (*top inset*) and the diffuse crescent localization seen by immunofluorescence (*bottom inset*). The fact that centrophilin plaques variably appear as globular densities or as defined or diffused crescents (Figs. 2 and 3), most likely reflects changes in spindle dynamics during metaphase alignment.

Effect of Microtubule Inhibitory Agents on Centrophilin Localization in Arrested Mitotic Cells

From its cell cycle colocalization with spindle tubules, it is clear that centrophilin is intimately associated with microtubules. Treatment with nocodazole, colcemid, vinblastine, or cold results in the disaggregation of centrophilin and the simultaneous dissolution of spindle tubules (Fig. 4, *A,a*). The cells in Fig. 4 were permeabilized in Triton X–100 before fixation and processing for immunofluorescence. No remaining tubulin foci are observed, except for a tiny double spot characteristic of the centrioles (Fig. 4*a*). Centrophilin foci, however, resist both detergent extraction and dissolution by microtubule inhibitors, as shown in Fig. 4*A*.

Centrophilin Foci are Nucleation Centers for Spindle Reassembly after Removal of Microtubule Inhibition

HeLa cells recover very slowly from mitotic arrest. This sluggish recovery is not a disadvantage because it allows for easy visualization of otherwise fleeting phases of

spindle regrowth (Fig. 4). Within 1 h after removal of microtubule inhibitor, tubulin (Fig. 4b) aggregates onto persistent centrophilin centers (Fig. 4B). Shortly afterward, nascent microtubules (Fig. 4c) emanate from these centers (Fig. 4C). Note that centrophilin centers serve as authentic nucleation sites for microtubule assembly. This is not merely a passive colocalization since tubulin, originally in a soluble diffuse state, is seen to aggregate at insoluble centrophilin sites. With the gradual consolidation of centrophilin from multiple nuclei to polar crescents (Fig. 4, B-F), corresponding microtubule foci interconnect and associate to form the bipolar spindle in absolute spatial and temporary harmony (Fig. 4, b-f). The growth of microtubules off of centrophilin nuclei after recovery from cold treatment occurs similarly (data not shown).

Centrophilin Coats Nascent Microtubules

In double-label immunofluorescence of spindles, reforming after removal of microtubule inhibitor, centrophilin foci often appear indistinguishable from growing microtubule centers (Fig. 4, C-c, E-e). The possibility of image "bleed through" exists, however, resulting from the potential overlap in the wavelengths for fluorochrome excitation selected by the fluorescein and Texas red filters. We consequentially ran corresponding single-label experiments to more accurately document centrophilin morphogenesis during spindle tubule reassembly. After 1–2 h recovery from microtubule inhibitor, centrophilin nuclei become rod-like and progressively more fibrous, resulting in astral formations (Fig. 5, A and B, *arrowheads*). These astral formations develop synchronously with nascent astral microtubule centers (Fig. 5C). Comparable patterns are also seen during recovery from cold treatment. In light of our double-label 2D3/antitubulin experiments, it is clear that centrophilin coats forming microtubules.

Centrophilin Associates with Kinetochores During Prometaphase

The multiple foci of centrophilin seen after cell exposure to microtubule disassembly agents are for the most part, non-randomly arranged. Treatment with

nocodazole, vinblastine, colcemid, or exposure to cold results in a deployment in which most centrophilin foci are intimately associated with kinetochores of chromosomes, as determined by double-label immunofluorescence with 2D3 and antikinetochores antiserum from patients with scleroderma CREST autoimmune disease. After removal of microtubule inhibitor, chromosomes begin to form small clusters with centrophilin foci at the centers of resulting kinetochores rosettes. Considering that spindle microtubules nucleate from centrophilin foci (Fig. 4) and that centrophilin foci associate with kinetochores rosettes (Fig. 6), it follows that microtubule foci are also at the centers of kinetochores rosettes. During later steps of recovery from microtubule inhibition, interkinetochores microtubule foci associate into short-lived multipolar spindles, as centrophilin is transported from the kinetochores and gradually takes on its polar status (Fig. 4, *D-d*, *E-e*, *F-f*).

Centrophilin is Detected at the Interphase Centrosome after Microtubule Inhibition

Centrophilin is not normally detected at the interphase centrosome by routine immunofluorescence. However, in the presence of nocodazole or immediately after recovery, interphase cells exhibit centrosomal staining with 2D3 (Fig. 7). This phenomenon is also observed in permeabilized cells treated with millimolar levels of CaCl_2 . Either the diminished CMTC or the induced disaggregation of other centrosomal proteins appears to allow for greater accessibility of the relevant centrophilin epitope to 2D3. As such, a basal level of centrophilin may persist at the interphase centrosome.

Centrophilin Transiently Associates with Centromeres and is Transported on Kinetochores Microtubules to the Mitotic Poles

Immunofluorescence assays in which normal, undrugged HeLa cells were permeabilized with Triton X-100 before formaldehyde fixation results in enhancement of the transitory diffuse low-level fluorescence patterns seen with the formaldehyde/Triton X-100 protocol. These elusive patterns become progressively most prominent when the cells are treated with increasing levels of CaCl_2 (Fig. 8). It is likely that these

permeabilization conditions help to expose antigenic sites for 2D3 recognition. With the exception of millimolar CaCl_2 addition, these treatments have no visible effect on the structure of the CMTC or mitotic spindle (data not shown, but see Olmsted and Borisy, 1975).

During interphase, centrophilin (Fig. 8A) exhibits a diffuse punctate pattern in the nucleus (Fig. 8a). In prophase, centrophilin condenses down with the compacting chromosomes into discrete foci. These foci assume a characteristic kinetochore pattern (Fig. 8 B-b) and are clearly seen to colocalize with kinetochores in normal prometaphase as determined by double-label immunofluorescence with 2D3 and CREST antiserum (Fig. 9). Later during prometaphase, centrophilin eventually disappears from kinetochores. It subsequently appears along kinetochores fibers and gradually concentrates at the poles (Fig. 8 C-c, D-d, E-e, F-f, Fig. 9). This general pattern is also seen in cells recovering from microtubule inhibition (Figs. 4 and 6) and can be rapidly reversed by cold treatment (data not shown). By late anaphase, centrophilin associates with interpolar and midbody microtubules (Fig. 8 G-g), progressively becoming restricted to their equatorial ends (Fig. 8 H-h). The simplest interpretation of these events is that centrophilin is transported from kinetochores to the poles along kinetochore microtubules in prometaphase, and from the poles to the center of the developing midbody along interpolar microtubules in late anaphase to telophase.

DISCUSSION

We have described a mitotic protein, centrophilin, which sequentially reallocates from the centromeres to the centrosomes, to the midbody, presumably along spindle microtubules. Although the foci stained with 2D3 nucleate spindle microtubules growth, our data do not demonstrate that centrophilin is actually the principal nucleating factor at these sites. It is very possible that other proteins present at these foci in concert with centrophilin nucleate microtubule assembly. It is improbable that centrophilin is passively

associated with these spindle nucleating foci since it undergoes morphogenesis and redistribution in a manner dependent on the mitotic phase. Furthermore, there is a tenet in biology that structure and location implies function. Proteins that are integral components of mitochondria, for example, invariably affect the function of mitochondria, as is true for proteins of the lysosomes, ribosomes, chloroplasts, and the plasma membrane. This is also valid for proteins associated with microtubules. There is no known MAP that does not influence microtubule assembly or function. At the evolutionary level, selective pressures impede the persistence of nonfunctional or passive proteins since the organism's limited resources otherwise become allocated for needless synthesis.

Whatever the exact function of centrophilin, its presence as detected with 2D3 appears to be a reliable marker for spindle microtubule nucleation based on the following data: (a) the formation and breakdown of the spindle in both normal and drug-recovered mitosis corresponds in time and space with the aggregation and disaggregation of centrophilin foci; (b) The regions of the spindle reported to exhibit net incorporation of subunits (Mitchison, 1989; Nicklas, 1989; Wadsworth et al., 1989; Gorbsky and Borisy, 1989; Gorbsky et al., 1987; Masuda and Cande, 1987; Mitchison et al., 1986) correlate ideally with localization of centrophilin throughout mitosis; (c) Centrophilin is a major component of electron-dense pericentriolar material (PCM) in mitosis; (d) PCM has been shown to nucleate microtubule assembly in vitro (Gould and Borisy, 1977); (e) During recovery from microtubule inhibition in vivo, soluble tubulin protein aggregates at centrophilin sites and assembles into microtubules that radiate from these sites; and (f) Centrophilin foci characteristically decondense and coat nascent microtubules during recovery from microtubule inhibition.

Centrophilin as a Marker for End-associated Microtubule Dynamics

The distribution of centrophilin, a protein tightly coupled to sites of nucleation corresponds precisely with observed high-turnover regions of spindle microtubules during the course of mitosis (Fig. 10). Prometaphase congression and alignment of chromosomes at metaphase is accompanied by a net incorporation of tubulin subunits at the kinetochore-associated end of microtubules (Mitchison et al., 1986; Gorbsky and Borisy, 1989; Mitchison, 1989; Wise et al., 1990). This correlates with the transient localization of centrophilin at the centromere during prometaphase. The gradual diminution of centrophilin immunofluorescence at the kinetochore and the concomitant accumulation of staining at the poles throughout metaphase corresponds to a shift in end-associated microtubule dynamics by early anaphase. The poleward movement of chromosomes at anaphase is characterized by a net disassembly of microtubules from their kinetochore-associated ends (Mitchison et al., 1986; Gorbsky et al., 1987; Nicklas, 1989) and de novo assembly from the poles (Wadsworth et al., 1989).

As the polar accumulation of centrophilin gradually diminishes during anaphase chromosome migration, kinetochore microtubules correspondingly cease to turnover (Wadsworth et al., 1989). At this stage, spindle microtubule dynamics shift again to the interzone where overlapping interpolar microtubules incorporate subunits and the midbody begins to form (Masuda and Cande, 1987). This emerging MTOC activity corresponds with the relocation of centrophilin to the plus ends of interpolar microtubules.

Transport of Centrophilin along Microtubules

The concept of a nucleation factor which is relocated in a manner dependent on the mitotic phase can help explain the rather complicated shifts in spindle tubule turnover. It is not clear, however, how such a protein is deployed or how its potential nucleation activity is regulated. From the cell cycle profile of centrophilin localization presented in Fig. 8 in which centrophilin transiently spans across spindle microtubules before concentrating

at the poles or the center of the midbody, it appears that centrophilin is transported along microtubules. This notion is supported by the observation that prevention of HeLa spindle formation with microtubule inhibitors or the complete dissolution of the spindle by cold treatment results in the interruption of centrophilin aggregation or in the dissemination of centrophilin onto kinetochores, respectively. Reaggregation only occurs after recovery from microtubule inhibition (Fig. 4). In late interphase, during the G₂/M transition, the condensation of centrophilin onto kinetochores is probably coupled to chromosome condensation.

The observation that certain mitotic factors shuttle along spindle microtubules is not new. In early reports on mitotic movements, electron dense material and vesicles were seen to translocate to the poles along microtubules in prometaphase, reaching maximum polar concentration at metaphase, and to translocate to the center of the forming midbody along interpolar microtubules in anaphase (Bajer, 1967; Rebhun, 1972). Centrophilin may be a key component of this material.

The association of centrophilin with spindle microtubules (Fig. 8) is not likely to result from the artifactual deposition of the protein on microtubules caused by the permeabilization conditions of our immunofluorescence assays since centrophilin-microtubule association is indicated in mitotic cells that have not been detergent-permeabilized before fixation (i.e., Fig. 5). Furthermore, centrophilin association with microtubules becomes progressively restricted to the poles during mitosis (Fig. 4, E-e and F-f). If this localization was an artifact due to permeabilization, centrophilin would be detected along the entire spindle or CMTC. However, this is never seen. To our knowledge there is no other intracellular mitotic transport system aside from a spindle microtubule complex that can accommodate centrophilin relocation. Centrophilin does not colocalize with either microfilaments or intermediate filaments. It is unlikely that the apparent transport of centrophilin during mitosis is actually the result of timed post-

translational modifications and "counter demodifications" of persistent centrophilin at each site that affect recognition of the antigen by 2D3. If this were true, microtubule inhibition would not be seen to stabilize the association of centrophilin with centromeres, cold treatment would not cause centrophilin at the poles of the metaphase spindle to reassociate with the centromeres, and centrophilin would not transiently span across microtubules before concentrating at each site. Furthermore, we would still have to evoke a transport model to explain how the hypothetical post-translational modifier, itself, can be shuttled, as well as elaborating an explanation for the "counter demodifications" of centrophilin. The sheer clumsiness of this three-part model renders it improbable. The possibility that centrophilin is relocated during mitosis simply by diffusion is also not tenable because centrophilin progressively aggregates at each new location, ever against the concentration gradient. This implies an active, energy-consuming transport.

Considering that the interaction of centrophilin with microtubules appears dynamic, it is probable that some microtubule-associated mechanochemical ATPase such as kenisin (Neighbors et al., 1988) or dynein (Pfarr et al., 1990) impels centrophilin translocation. It is also likely that centrophilin binds to other MAPs such as centrosomal MAP 1A (Bonifacino et al., 1985; Sato et al., 1983) or directly binds to tubulin. The presence of both phosphoproteins (Vandre et al., 1986) and cell cycle-dependent protein kinase activity at the centrosome (Bailly et al., 1989) suggests that phosphorylation may play a part in centrophilin regulation. Of all the reported centrosome-associated proteins that might interact with centrophilin, including POPA (Sager et al., 1986), CHO3 antigen (Kuriyama and Sellitto, 1989), NuMA (Lydersen and Pettijohn, 1980), centrin (Baron and Salisbury, 1988), and MPM 13 antigen (Rao et al., 1988), calmodulin (Welch et al., 1978) seems to be the most likely candidate. Calmodulin appears as polar crescents in the metaphase spindle and is found in midbodies in a pattern which closely resembles centrophilin localization. Calmodulin has also been shown to colocalize with kinetochore

microtubules (Sweet and Welsh, 1988; Sweet et al., 1988) and is found associated with growing microtubule foci during recovery from nocodazole treatment (Sweet et al., 1989). Although the operation and regulation of the mitotic apparatus remains unclear, the 2D3 probe may help add a third dimension to our somewhat two-dimensional understanding of spindle dynamics.

We extend our thanks to Bill Mollon for his assistance in EM and Ray Zinkowski and Tamas Yilling who graciously helped us with image analysis. We are grateful to Gary Martin, Jennifer Kidd, and Ric Villani for maintaining our cell cultures; and Harry Johnson and L. I. Binder for providing guidance in hybridoma cell culture and antibody production. We thank Arnold Rivera and Patty Loomis for helpful tips in electrophoresis and immunoblotting. We are also grateful to Sherry Crittenden for typing and Ann Harrell for proofreading the manuscript.

This work was sponsored by NIH grant CA 41424 to B. R. Brinkley.

REFERENCES

- Bailly, E., M. Doree, P. Nurse, and M. Bornens. 1989. p34^{cdc2} is located in both nucleus and cytoplasm; part is centrosomally associated at G2/M and enters vesicles at anaphase. *EMBO (Eur. Mol. Biol. Organ.) J.* 8:3985–3995.
- Bajer, A. S. 1967. Notes on ultrastructure and some properties of transport within the living mitotic spindle. *J. Cell Biol.* 33:713–720.
- Baron, A. T., and J. L. Salisbury. 1988. Identification and localization of a novel, cytoskeletal, centrosome-associated protein in PtK2 cell. *J. Cell Biol.* 107:2669–2678.
- Bonifacino, J. S., R. D. Klausner, and I. V. Sandoval. 1985. A widely distributed nuclear protein immunologically related to the microtubule-associated protein MAP1 is associated with the mitotic spindle. *Proc. Natl. Acad. Sci. USA.* 82:1146–1150.
- Brenner, S., D. Pepper, M. W. Berns, E. T. Tan, and B. R. Brinkley. 1981. Kinetochores structure, duplication, and distribution in mammalian cell: analysis by human autoantibodies from scleroderma patients. *J. Cell Biol.* 91:95–102.
- Brinkley, B. R. 1985. Microtubule organizing centers. *Annu. Rev. Cell Biol.* 1:145–172.

- Brinkley, B. R., G. M. Fuller, and D. R. Highfield. 1975. Cytoplasmic microtubules in normal and transformed cells in culture: analysis by tubulin antibody immunofluorescence. *Proc. Natl. Acad. Sci. USA.* 72:4981–4985.
- Calarco–Gillam, P. D., M. C. Siebert, R. Hubble, T. Mitchison, and M. Kirschner. 1983. Centrosome development in early mouse embryo as defined by an auto–antibody against pericentriolar material. *Cell* 35:621–629.
- Clayton, L., C. M. Black, and C. W. Lloyd. 1985. Microtubule nucleating sites in higher plant cells identified by an autoantibody against pericentriolar material. *J. Cell Biol.* 101:319–324.
- Connolly, J. A., and V. I. Kalnins. 1978. Visualization of centrioles and basal bodies by fluorescent staining with nonimmune rabbit sera. *J. Cell Biol.* 79:526–532.
- Gorbsky, G. J., P. J. Sammak, and G. G. Borisy. 1987. Chromosomes move poleward in anaphase along stationary microtubules that coordinately disassemble from their kinetochore ends. *J. Cell Biol.* 104:9–18.
- Gosti–Testu, F., M. C. Marty, J. Berges, R. Maunoury, and M. Bornes. 1986. Identification of centrosomal proteins in a human lymphoblastic cell line. *EMBO (Eur. mol. Biol. Organ.). J.* 5:2545–2550.
- Gosti–Testu, F., M. C. Marty, J. C. Courvalin, R. Maunoury, and M. Bornens. 1987. Centrosomal proteins and lactate dehydrogenase possess a common epitope in human cell lines. *Proc. Natl. Acad. Sci. USA.* 84:1000–1004.
- Gould, R. R., and G. G. Borisy. 1977. The pericentriolar material in Chinese hamster ovary cells nucleated microtubule formation. *J. Cell Biol.* 73:601–615.
- Izant, J. G., J. A. Weatherbee, and J. R. McIntosh. 1982. A microtubule–associated protein found in the mitotic spindle and interphase nucleus. *Nature (Lond.).* 295:248–250.
- Kohler, G., and C. Milstein. 1975. Continuous cultures of fused cells secreting antibody of defined specificity. *Nature (Lond.)* 256:495–497.
- Kuriyama, R., and C. Sellitto. 1989. A 225 KD phosphoprotein associated with the mitotic centrosome in sea urchin eggs. *Cell Motil. Cytoskeleton.* 12:90–103.
- Laemmli, U. K. 1970. Cleavage of structural proteins during the assembly of the head of bacteriophage T4. *Nature (Lond.).* 227:680–685.
- Lydersen, B., and D. Pettijohn. 1980. Human–specific nuclear protein that associates with the polar region of the mitotic apparatus: distribution in a human/hamster hybrid cell. *Cell.* 22:489–499.
- Masuda, H., and W. Z. Cande. 1987. The role of tubulin polymerization during spindle elongation in vitro. *Cell* 49:193–202.
- McIntosh, J. R. 1983. The centrosome as an organizer of the cytoskeleton. In: *Modern Cell Biology.* vol 2. Alan R. Liss, Inc., New York. 115–142.

- McIntosh, J. R., Z Cande, J. Snyder, and K. Vanderslice. 1975. Studies on the mechanism of mitosis. *Annu. NY Acad. Sci.* 252:407–427.
- Mitchison, T. 1989. Poleward microtubule flux in the mitotic spindle: evidence from photoactivation of fluorescence. *J. Cell Biol.* 109:637–653.
- Mitchison, T., L. Evans, E. Schulze, and M. Kirschner. 1986. Sites of microtubule assembly and disassembly in the mitotic spindle. *Cell.* 45:515–527.
- Moroi, Y., C. Peebles, M. J. Fritzler, J. Steingerwald, and E. M. Tan. 1980. Autoantibody to centromere (kinetochore) in scleroderma sera. *Proc. Natl. Acad. Sci. USA.* 77:1627–1631.
- Neighbors, B.W., R. C. Williams, Jr., and J. R. McIntosh. 1988. Localization of kinesin in cultured cells. *J. Cell Biol.* 106:1193–1204.
- Nicklas, R.B. 1989. The motor for poleward chromosome movement in anaphase is in or near the kinetochore. *J. Cell Biol.* 109:2245–2255.
- Olmsted, J. B., and G. G. Borisy. 1975. Ionic and nucleotide requirements for microtubule polymerization in vitro. *Biochem.* 14:2996–3005.
- Petzelt, C. 1979. Biochemistry of the mitotic spindle. *Int. Rev. Cytol.* 60:53–92.
- Pfarr, C. M., M. Coue, P. M. Grisson, T. S. Hays, M.E. Porter, and J. R. McIntosh. 1990. Cytoplasmic dynein localizes to kinetochores during mitosis. *Nature (Lond.)* 345:263–265.
- Rao, P. N., J. Zhao, R. K. Ganju, and C. L. Ashorn. 1989. Monoclonal antibody against the centrosome. *J. Cell Sci.* 93:63–69.
- Rebhun, L. I. 1972. Polarized intracellular particle transport: saltatory movements and cytoplasmic streaming. *Int. Rev. Cytol.* 32:92–139.
- Rieder, C. L., and G. G. Borisy. 1982. The centrosome cycle in the PtK2 cells: asymmetric distribution and structural changes in the pericentriolar material. *Biol. Cell.* 44:117–132.
- Sager, P. R., N. L. Rothfield, J. M. Oliver, and R. D. Berlin. 1986. A novel mitotic spindle pole component that originates from the cytoplasm during prophase. *J. Cell Biol.* 103:1863–1872.
- Salisbury, J. L., A. T. Baron, D. E. Colins, V. E. Martindale, and M. A. Sanders. 1986. Calcium-modulated contractile proteins associated with the eukaryotic centrosome. *Cell Motil. Cytoskel.* 6:193–197.
- Sato, C., K. Tanabe, K. Nishizawa, T. Nakayma, T. Kobayashi, and H. Nakamura. 1985. Monoclonal antibody against MAP-1 produces immunofluorescence spots in the nucleus and centrosome of cultured mammalian cells. *Cell Struct. Funct.* 8:245–254.

- Snyder, J. A., and J. R. McIntosh. 1975. Initiation and growth of microtubules from mitotic centers in lysed mammalian cells. *J. Cell Biol.* 67:744–760.
- Stemple, d. L., S. C. Sweet, M. J. Welsh, and J. R. McIntosh. 1988. Dynamics of a fluorescent calmodulin analog in the mammalian mitotic spindle at metaphase. *Cell Motil. Cytoskel.* 9:231–242.
- Sweet, S. C., and M. J. Welsh. 1988. Calmodulin colocalization with cold-stable and nocodazole-stable microtubules in living PtK1 cells. *Eur. J. Cell Biol.* 47:88–93.
- Sweet, S. C., C. M. Rogers, and M. J. Welsh. 1989. Calmodulin stabilization of kinetochore microtubule structure to the effect of nocodazole. *J. Cell Biol.* 107:2243–2251.
- Sweet, S. C., C. M. Rogers, and M. J. Welsh. 1988. Calmodulin is associated with microtubules forming in PtK1 cells upon release from nocodazole treatment. *Cell Motil. cytoskel.* 12:113–122.
- Szollose, D., P. Calarco, and R. P. Donahue. 1972. Absence of centrioles in the first and second meiotic spindles of mouse oocytes. *J. Cell Sci.* 11:521–541.
- Telzer, B.R., and J. L. Rosenbaum. 1979. Cell Cycle-dependent, in vitro assembly of microtubules onto pericentriolar material in HeLa cells. *J. Cell Biol.* 64:146–158.
- Towbin, H., T. Staehelin, and J. Gordon. 1979. Electrophoretic transfer of proteins from polyacrylamide gels to nitrocellulose sheets: procedure and some application. *Proc. Natl. Acad. Sci. USA.* 76:4350–4354.
- Tuffanelli, D. L., F. McKeon, D.A. Kleismith, T. K. Burham, and M. Kirschner. 1983. Anticentrosome and anticentriole antibodies in the scleroderma spectrum *Arch. Dermatol.* 119:560–566.
- Valdivia, M. M. and B. R. Brinkley. 1985. Fractionation and initial characterization of the kinetochore from mammalian metaphase chromosomes. *J. Cell Biol.* 101:1124–1134.
- Vandre, D. D., F. M. Davis, P. N. Rao, and G. G. Borisy. 1986. Distribution of cytoskeletal proteins sharing a conserved phosphorylated epitope. *Eur. J. Cell Biol.* 41:72–81.
- Verde, F., J. Labbe, M. Doree, and E. Karsenti. 1990. Regulation of microtubule dynamics by cdc2 protein kinase in cell-free extract of Xenopus eggs. *Nature (Lond.)* 343:233–237.
- Wadsworth, P., E. Shelden, G. Rupp, and C. L. Rieder. 1989. Biotin-tubulin incorporates into kinetochore fiber microtubules during early but not late anaphase. *J. Cell Biol.* 109:2257–2265.
- Welsh, M. J., J. R. Deman, B. R. Brinkley, and A. R. Means. 1978. Calcium dependent regulator protein: localization in the mitotic apparatus of eukaryotic cells *Proc. Natl. Acad. Sci. USA.* 75:1867–1871.

Wise, D., L. U. Cassimeris, C. I. Rieder, P. Wadsworth, and E. D. Salmon. 1990. Chromosome fiber dynamics and congression oscillations in metaphase of PtK2 cells at 23°C. *Cell Motil. Cytoskel.* In press.

Figure 1. Immunoblot of whole HeLa cell extract with 2D3. (A) PAGE migration pattern of molecular weight standards. (B) Coomassie blue stain of PAGE-separated proteins present in HeLa extract. (C) Two high-molecular mass polypeptides, 180 and 210 KD are revealed upon probing with 2D3 (arrows). (D) Corresponding negative control assay in which 2D3 was omitted.

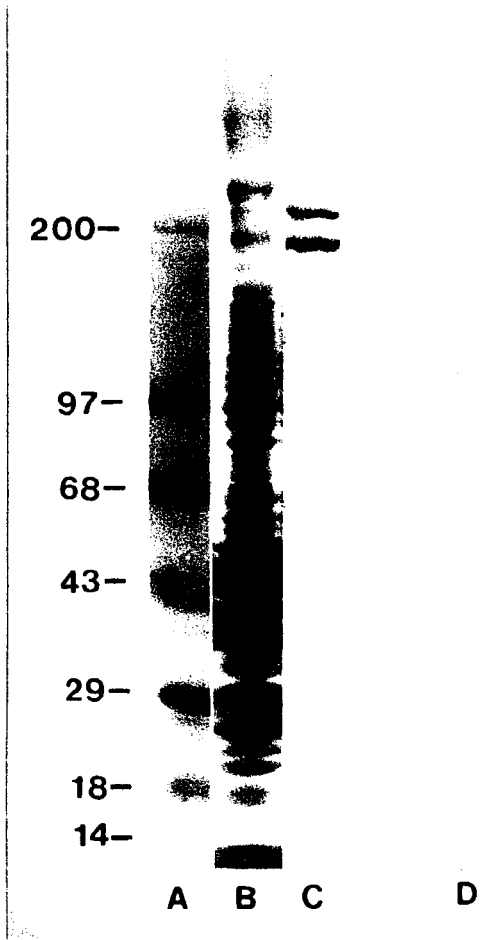


Figure 2. Profile of centrophilin localization during the cell cycle. A–G show immunofluorescence with 2D3. a–g show corresponding immunofluorescence with antitubulin antibody. After its nuclear deposition (A, a), centrophilin associate with the prometaphase centrosomes (B, b; C, c), forms crescents at the poles of the metaphase spindle (D, d), gradually vanishes during anaphase (E, e; F, f), and reappears as a band at the center of the midbody (G, g). Upon reversion to its nuclear localization, the centrophilin cycle is complete. Bar, 10 μm .

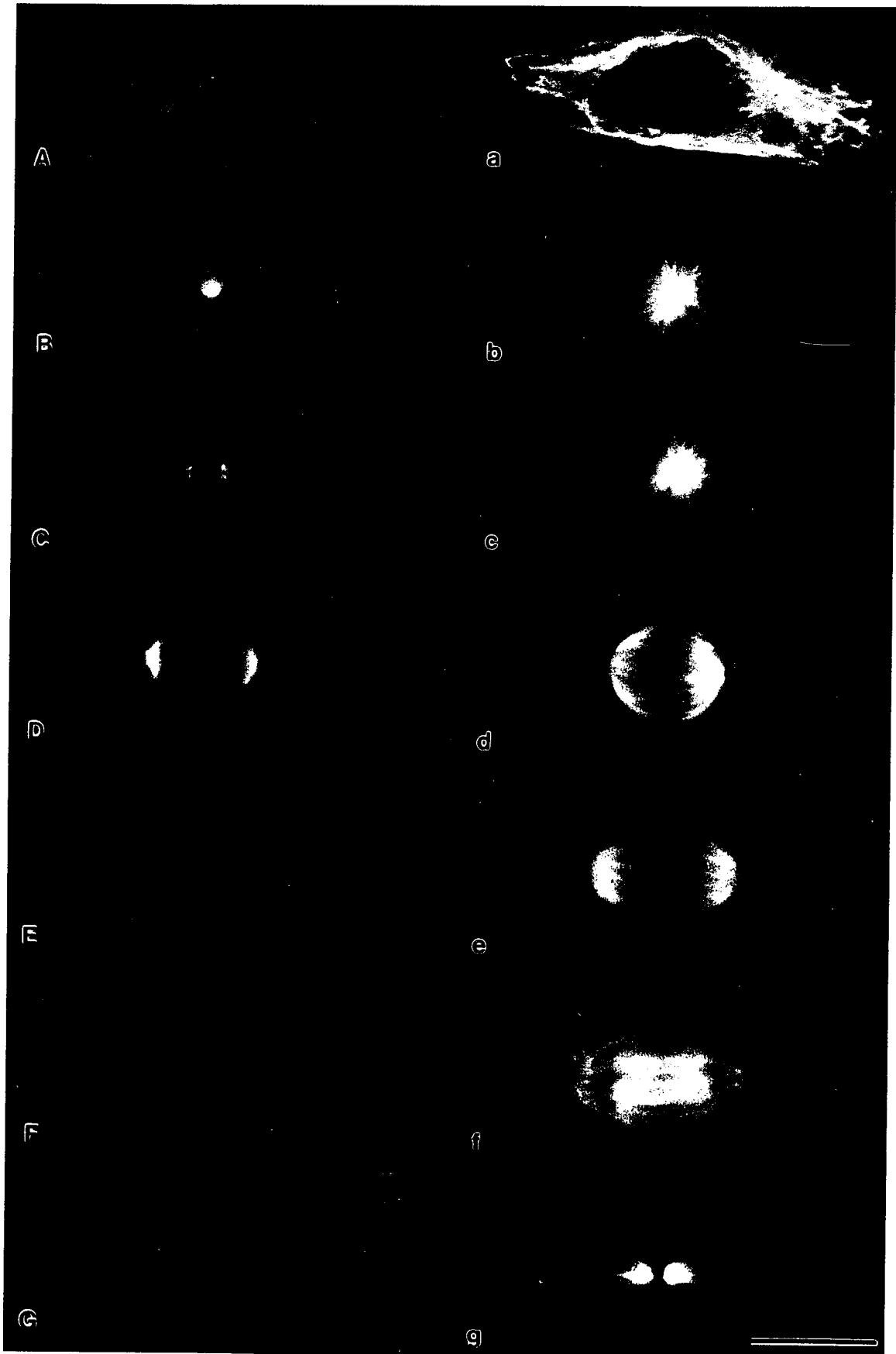


Figure 3. Immunogold electron microscopic localization of centrophilin at the mitotic poles in HeLa cells. Centrophilin is localized in the pericentriolar material as a diffuse electron-dense crescent (arrowheads) but does not bind to the centriole (c) or the immediately surrounding region. Bar, 0.5 μm . This pattern correlates with the immunofluorescence localization of centrophilin (insets). Bars, 5 μm .

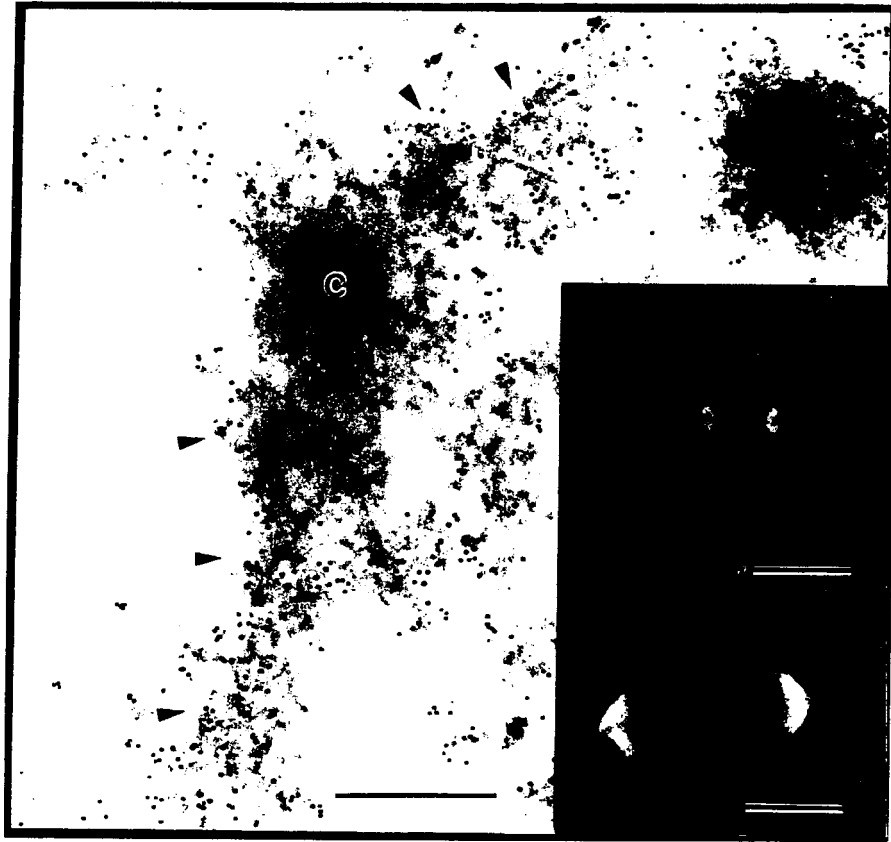


Figure 4. Centrophilin foci nucleate spindle tubule growth. Treatment with 10 $\mu\text{g/ml}$ nocodazole results in the reversible disaggregation of centrophilin into detergent-insoluble foci throughout the cytoplasm (A) and induces the complete breakdown of spindle microtubules into soluble tubulin (a). This tubulin is completely detergent extractable except for the tiny double focus of tubulin characteristic of the centrioles. Within 1 h after removal of nocodazole, tubulin (b) focuses on insoluble centrophilin nuclei (B). Roughly 30 min later, microtubules (c) are seen to extend from these nuclei (C). Centrophilin often appears to coat growing spindle tubules, taking on a fibrous appearance. as centrophilin nuclei gradually aggregate into polar crescents over a 5-h recovery period (D–F), corresponding microtubule centers interconnect and converge to form the bipolar spindle (d–f). Visualization by double label immunofluorescence. Bar, 5 μm .

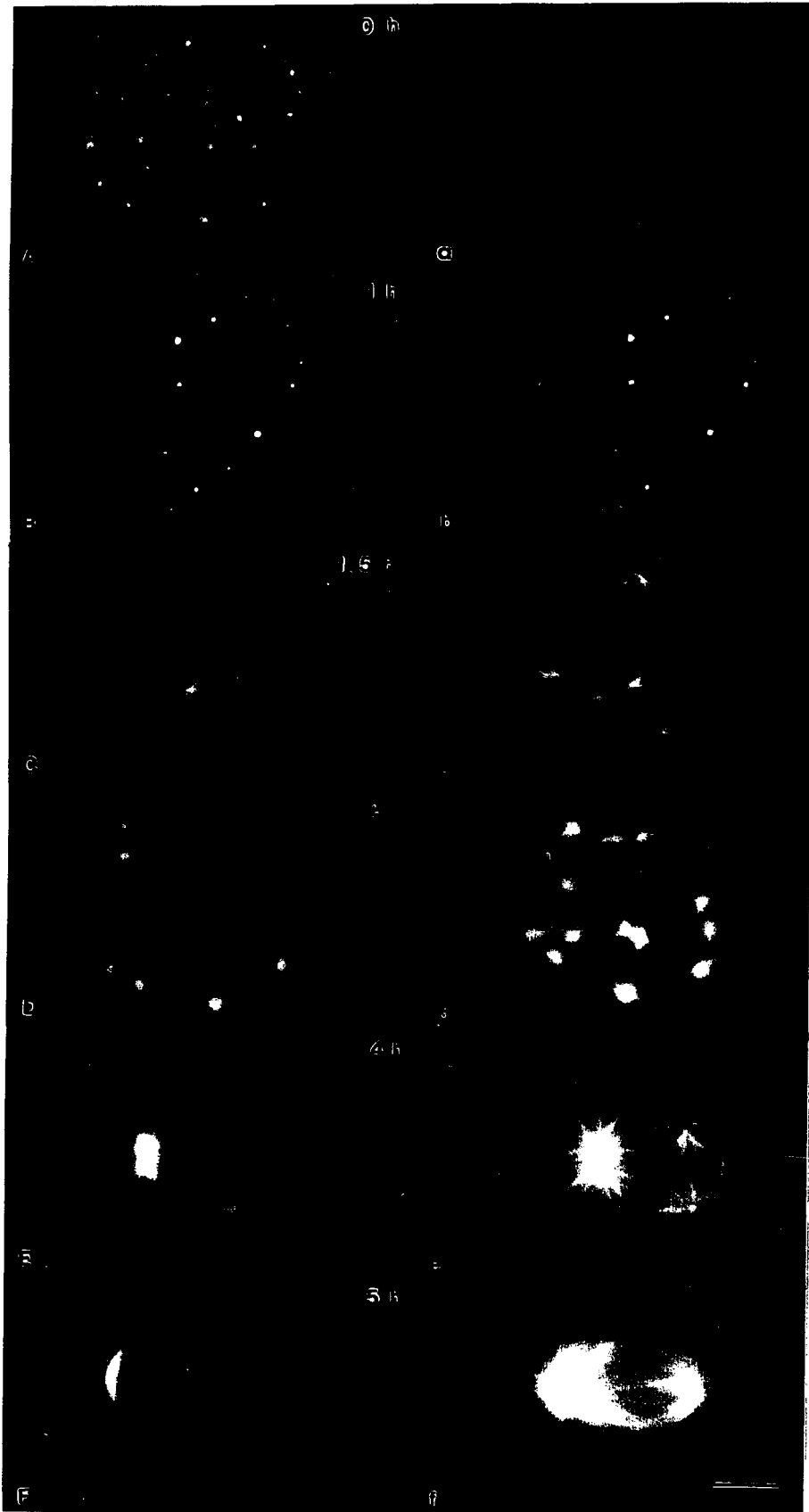


Figure 5. Single-label immunofluorescence pattern of centrophilin morphogenesis with 2D3 and spindle microtubule reformation with antitubulin antibody after recovery from mitotic block. Within 1.5–2 h after recovery, centrophilin foci (arrowheads) become rod-like and progressively more fibrous, resulting in astral arrays (A and B). These astral arrays of centrophilin develop synchronously with forming astral microtubule centers (C), taking on their characteristic appearance. Bars, 5 μm .

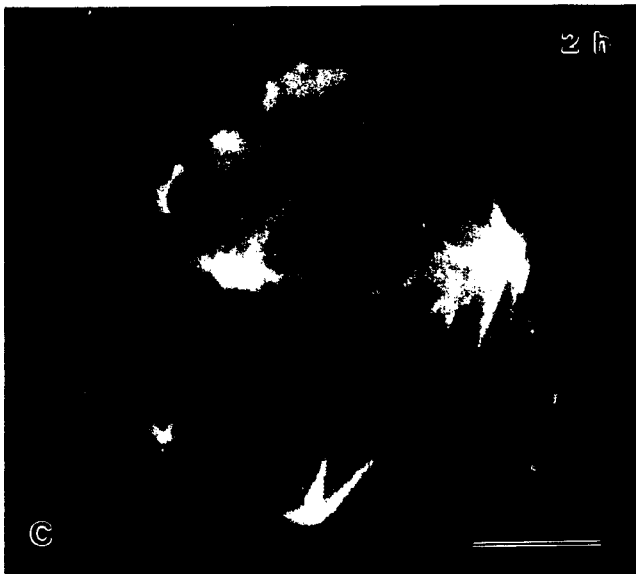
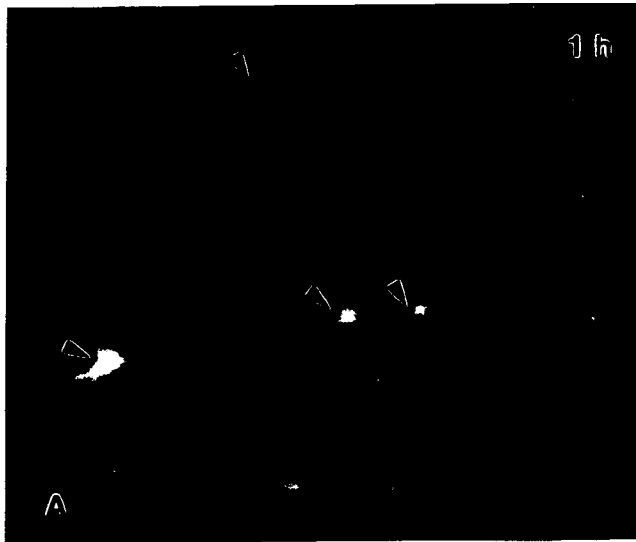


Figure 6. Double-label immunofluorescence with 2D3 and CREST antiserum in prometaphase after a 2-h recovery from mitotic block. centrophilin foci (A) are seen at the centers of kinetochore rosettes (B) as indicated by arrowheads. The two "doughnut-shaped" foci in A which do not colocalize with kinetochores are presumably the centrosomes (c). This stage of recovery corresponds with that in Fig. 4D, d. Chromosomes in the same cell were stained with Hoechst (C). Their clustered appearance corresponds with kinetochore rosettes. Bar, 5 μ m.

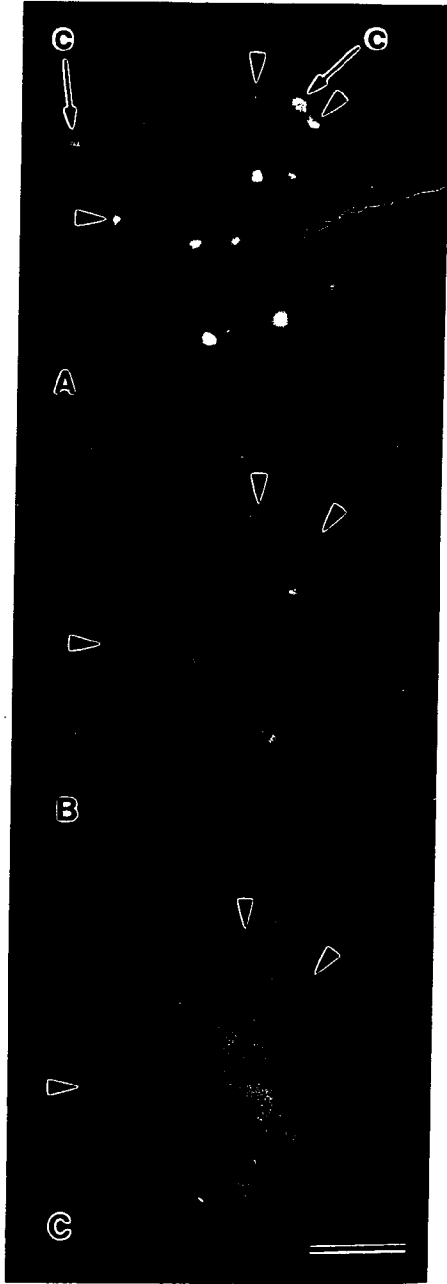


Figure 7. A basal level of centrophilin is present at the interphase centrosome. (A) forming CMTCs after removal of nocodazole, shown here to mark location of MTOCs. (B) Centrophilin localization in same cells. Bar, 5 μ m.

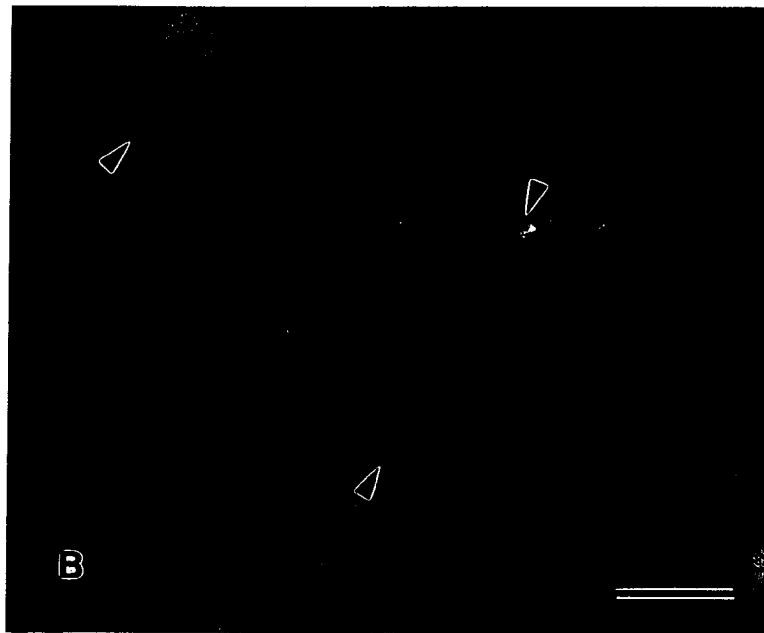


Figure 8. Profile of centrophilin relocation during the cell cycle in cells which were Triton X-100 permeabilized in 0.1 M Pipes, pH 6.9, with 21 mM CaCl_2 before fixation. Comparable images, but with reduced sharpness, are obtained when CaCl_2 is decreased to micromolar levels or when it is omitted from the permeabilization buffer. (A–H) Centrophilin patten. (a–c) Visualization of chromatin and chromosomes by Hoechst staining in the same cells shown in A–C. (d–h) Corresponding shingle-label spindle microtubule patten. Cells shown are deliberately nonidentical to those shown in D–H to discount the possibility of artifactual image "bleed through". Diffuse granules of centrophilin in the interphase nucleus (A, a) condense down progressively to form discrete foci on the prometaphase chromosomes (B, b). From prometaphase to metaphase, centrophilin dissociates from the chromosomes and appears to be transported to the mitotic poles (arrowheads) along kinetochore microtubules (C–c, D–c, E–e, F–f). In late anaphase to telophase, centrophilin (G, H) is apparently transported to the center of the forming midbody along interzonal microtubules (g, h). Bar, 5 μm .



Figure 9. Centrophilin transiently associates with kinetochores in normal prometaphase. cells were Triton X-100 permeabilized in 0.1 M Pipes, pH 6.9, with 1 mM EGTA and 1 mM $MgCl_2$ before fixation. (A-C) Centrophilin localization. (a-c) Respective kinetochore localization in same cells. (a'-c') Chromosome pattern. Arrowheads indicate regions of centrophilin colocalization with kinetochores. Centrophilin-kinetochore association occurs even in the absence of the microtubule inhibitory effects of $CaCl_2$. Comparable patterns are also seen with omission of $MgCl_2$. Later in prometaphase (C-c'), centrophilin relocates to the poles (arrows). Image bleed-through is minimal, thereby authenticating the colocalization of centrophilin with kinetochores in A-a, and B-b.

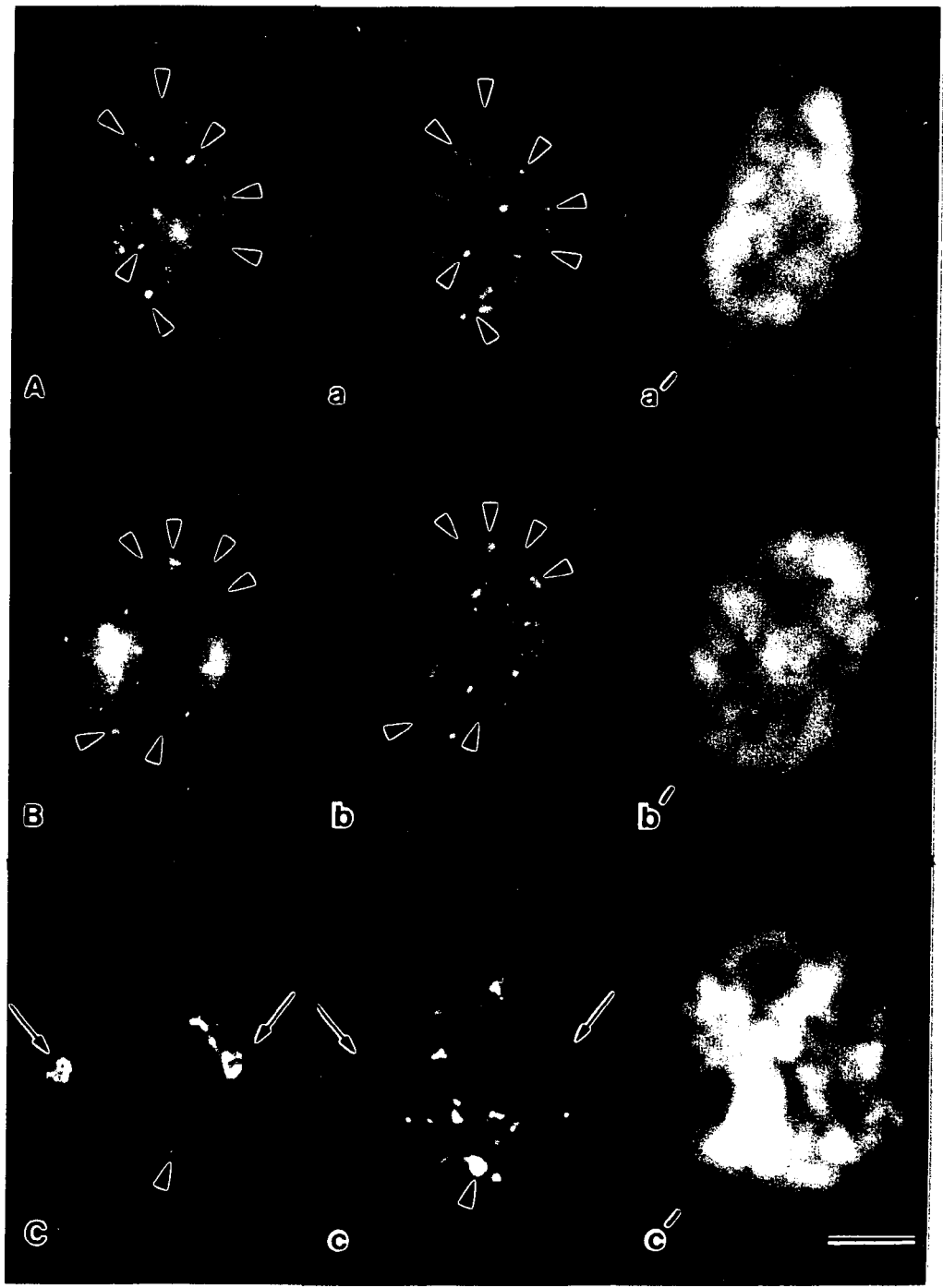
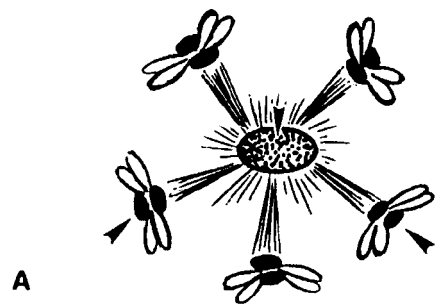
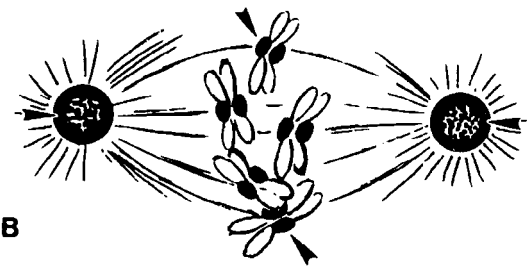


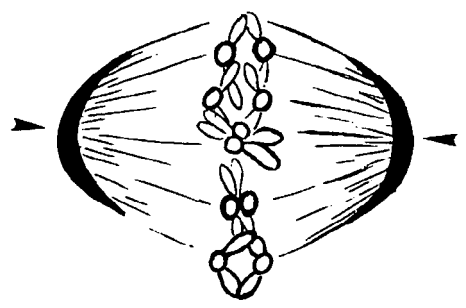
Figure 10. Model showing how centrophilin, a relocating marker protein for microtubule nucleation, may systematically help to modulate spindle tubule turnover throughout mitosis. This model is completely consistent with reported observations of spindle tubule dynamics (see discussion). Shaded or blackened regions (indicated by arrowheads) represent the variable distribution of centrophilin in the mitotic apparatus. Lines represent spindle fibers. Centrophilin distribution indicates regions of net localized subunit incorporation in the spindle. Lightly shaded or white areas respectively signify reduction or absence of centrophilin and consequentially mark zones of lessening assembly or disassembly of spindle tubules. The transient association of centrophilin with the centromeres in prometaphase (A and B) correlates with the net incorporation of tubulin subunits at the kinetochore-associated end of microtubules. The relocation of centrophilin from the centromeres to poles in late metaphase corresponds in turn with the net disassembly of microtubules from their kinetochore-associated ends and with de novo assembly from the poles in early anaphase (C). The developing MTOC activity of the forming midbody corresponds with the relocation of centrophilin from the poles to the equatorial ends of interpolar microtubules in late anaphase (D) and telophase (E).



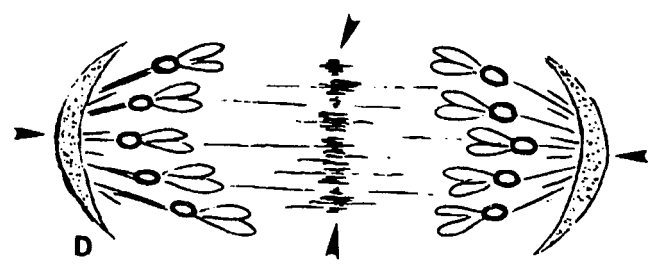
A



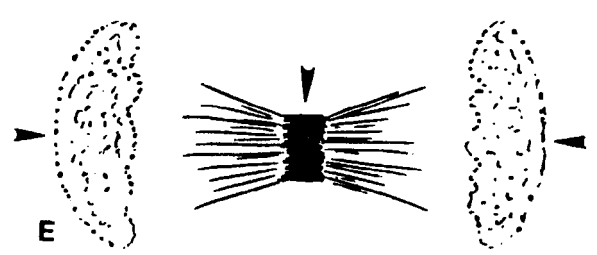
B



C



D



E

**LOCALIZATION OF NuMA PROTEIN ISOFORMS IN
THE NUCLEAR MATRIX OF MAMMALIAN CELLS**

C. ZENG, D. HE, and B. R. BRINKLEY

Submitted to J. Cell Biology

ABSTRACT

Using a monoclonal antibody 2D3 generated against a kinetochore-enriched human chromosome preparation, we identified a high molecular mass protein with nuclear staining in interphase and polar staining of the pericentriolar region in the mitotic spindle. Initially termed centrophilin (Tousson et al., 1991), this protein associates with the minus-ends of spindle microtubules (MT) and appears to be important in MT nucleation. Comparison of a partial cDNA sequence obtained for centrophilin with the full length cDNA sequence of nuclear mitotic apparatus protein (NuMA) strongly indicated that NuMA and centrophilin were the same protein (Compton et al., 1992; Yang et al., 1992). A polyclonal anti-NuMA antibody identified that NuMA exists as isoforms as shown by peptide mapping and immunoblots. Sequential fractionation experiments along with immunofluorescence, immunoblotting and EM immunogold labeling indicated that NuMA isoforms are novel components of nuclear core filaments. Thus, NuMA, a coiled-coil protein with a long α -helical domain, appears to have dual functions in interphase and mitosis during the cell cycle. In interphase, NuMA likely plays a structural role in the nucleoskeleton that may be important in nuclear organization whereas in mitosis it appears to be associated with spindle MT organization and chromosome positioning.

INTRODUCTION

NuMA is a high molecular weight nuclear protein that becomes associated with the spindle poles during mitosis (Lydersen and Pettijohn, 1980). It has been proposed that NuMA functions in post-mitotic reorganization of the nucleus by linking the chromosome into the reforming daughter nuclei (Price and Pettijohn, 1986; Compton and Cleveland, 1993). Subsequent studies on the primary structure of NuMA have shown that it is a long coiled-coil protein with two globular end domains separated by a discontinuous α -helix (Yang et al., 1992; Compton et al., 1992). Several other proteins with the similar cell-cycle-dependent redistribution have been reported in recent years, including mitotin, centrophilin,

SPN, SP-H, and proteins individually identified by antibodies fA12, CC-3, H1B2 and Bx63 (Todorov, et al., 1992; Tousson et al., 1991; Kallajoki et al., 1991; Maekawa et al., 1991, He et al., 1991; Thibodeau and Vincent, 1991; Nickerson et al., 1992; and Whitfield et al., 1988). Among these proteins, centrophilin, SPN, and SP-H all have proven to be NuMA or a member of the NuMA family as indicated by analysis of cDNA sequence (Compton et al., 1992; Yang et al., 1992; Kallajoki et al., 1993). Although most reports identify a single band in immunoblots, a recent analysis on different NuMA cDNA clones has suggested the existence of multiple isoforms of NuMA through a diverse splicing process (Tang et al., 1993).

Our previous experiments on the reassembly of spindle MTs following the treatment with MT inhibitors have indicated that centrophilin (NuMA) is localized near the minus end of MTs and may play an important role in spindle MT formation (Tousson et al., 1991). A significant function of NuMA protein in the mitotic process is also supported by several other studies based on the experiments of MT binding, antibody injections and MT inhibition (Kallajoki et al., 1991 and 1992; Maekawa et al., 1991; Yang and Snyder, 1992). Recent experiments involving the expression of truncated NuMA supports a major role in mitotic completion or post-mitotic nuclear reassembly (Compton and Cleveland, 1993). Beyond nuclear assembly, however, little is known of the distribution and function of NuMA in the interphase nucleus.

When the nuclear chromatin is removed by extensive DNase digestion followed by salt extraction, an insoluble network known as the nuclear matrix persists. Although the initial descriptions of this important structure were met with skepticism and controversy (Berezney and Coffey, 1974 and 1977), the presence of a nonchromatin matrix in the eucaryotic nucleus is now well established (reviews: van Driel et al., 1991; Nickerson et al., 1990; Verheijen et al., 1988; Berezney, 1991). Many nuclear activities, such as DNA and RNA synthesis, and RNA splicing, are localized in the discrete nuclear domains rather

than diffusely distributed throughout the nucleoplasm (Carter et al, 1991; Spector, et al., 1983; Nakayasu and Berezney, 1989). Particularly, the localizations of these specific domains persist after the removal of chromatin, indicating that nuclear matrix has a key function in maintaining spatial order within the nucleus. In recent years, matrix associated regions (MARs) have been identified to organize chromatin into topologically constrained loop domains (Gasser et al., 1989; Roberge and Gasser, 1992), suggesting that matrix proteins also play an essential role in chromatin organization and gene expression via the interactions to these conservative DNA elements (Bode et al., 1992; Getzenberg et al., 1991). Moreover, tissue specificity and hormone response were found to associate with nuclear matrix proteins (Getzenberg and Coffey, 1990). Therefore, the nuclear matrix most likely provides the active foci for most significant nuclear functions such as DNA replication, RNA transcription and processing, chromatin organization, and hormone reactions.

A serious obstacle in visualizing nuclear substructure is the immense amount of chromatin which largely conceals the structure of the matrix. Two types of extraction have been used to resolve a DNA-free matrix architecture. Jackson and Cook (1988) successfully electron-eluted DNA fragments in approximately physiological ionic conditions after nuclease digestion on the cells encapsulated on agarose beads. Nuclear filaments around 10 nm in diameter with a 23 nm axial repeat were revealed by these authors and immuno-labeling of DNA synthesis in early S phase was found to be associated with some of these filaments (Hozák et al., 1993).

Alternatively, using a relative low ionic concentration of ammonium sulfate (0.25 M), greater than 95% of chromatin could be removed leaving a RNase sensitive nuclear matrix intact (Fey et al., 1986). This approach revealed structures containing thick, polymorphic fibers associated with the granules of the chromatin remnant and matrix-associated materials. Further fractionation of this complex using higher salt gradients revealed an

intermediate filament–like nucleoskeleton network termed core filaments (He et al., 1990). Such a gradient extraction not only removed additional chromatin residues and scaffold associated components but avoided the harshness of direct 2 M salt treatment. The smooth 9–13 nm filaments are thought to serve as core structures around which other proteins associate to form the complete matrix.

A unique feature of the core filament network is its heterogeneous composition of RNA and proteins (He et al., 1990). Despite the pivotal roles of the matrix in the nuclear functions, relatively little is known about the organization of the nuclear matrix, especially the composition of the nucleoskeleton–core filaments, where thus far, only two proteins fA12 and H1B2 have localized as core filament associated proteins (He et al., 1991; Nickerson et al., 1992).

Despite the original proposal that NuMA is a nuclear matrix protein (Lydersen and Pettijohn, 1980), precise localization of NuMA within the nuclear architecture has not yet been adequately achieved. In this report, we provide biochemical, immuno–cytochemical and ultrastructural evidences that NuMA is a structural component of the core filaments of the interphase nucleus. We also present evidence that NuMA may exist in multiple isoforms. Our results suggest a dual function of NuMA as a cytoskeleton protein in mitosis and a nucleoskeleton in interphase.

MATERIALS AND METHODS

Cell Culture

HeLa cells were grown in DMEM with either 10% FBS or 2.5% FBS and 7.5% calf serum. Human cervical epidermoid carcinoma cells (CaSki; American Type Culture Collection) were cultured in either DMEM containing 10% FBS or RPMI–1640 medium containing 2.5% FBS and 7.5% calf serum. Indian muntjac and PtK1 cells, obtained from American Type Culture Collection, were cultured in F10 medium with 10% FBS.

Extraction of HeLa Cells

HeLa cells were disassociated from culture flasks by disassociation buffer (Sigma). After washing with PBS twice, cells were lysed with 0.5% Triton X-100 in PEM (100 mM PIPES, pH 7.0, 1 mM EGTA and 1 mM MgCl₂) with multiple protease inhibitors (0.1 mM PMSF, 1 ug/ml each of leupeptin, antipain, and pepstatin, PLAP) for 5 min in ice. After centrifuge, the pellet was incubated in 0.5 M NaCl in PBS plus PLAP for 5–15 min. In some preparations, 0.08% SDS was added in 0.5 M NaCl/PBS during the incubation. The extract was collected by micro-centrifuging the sample in eppendorf tube with 14,000 rpm for 10 min at 4°C.

Peptide Mapping

HeLa 0.5 M salt extract was loaded into 7×1.5 mm wells of 5–15% mini-gel at approximately 300 ug/well. After electrophoresis, protein bands around 220, 205, and 160 KD were cut into small bars about 5×2×1.5 mm according to their positions relative to the pre-stained molecular weight markers. The gel bars were frozen at –20°C and then inserted into the wells of a 5% mini-gel. Each well was then overlaid with 25 ul of endoproteinase Glu-C (Boehringer Mannheim Biochemicals) with the concentration of 2–6 ug/ml in a buffer containing 0.125 M Tris, pH 6.8, 0.1% SDS, 1 mM EDTA, and 15% glycerol (Cleveland, et al., 1977). Peptide mapping by limited proteolysis in electrophoresis was performed by turning off the power for 15 min after the prestained markers entered the gel stacker. After digesting, regular electrophoresis and electra-transfer were carried out and the protein bands were reacted with P9 and a monoclonal anti-NuMA antibody 8.22 (Zeng, et al., 1993) following standard blotting procedure.

Core Filament Preparation

CaSki cells were grown on either glass coverslips for fluorescent study or plastic coverslips for EM label. The *in situ* sequential extraction was carried out using a procedure for core filament preparation as described by He et al (1990). After washing in CSK buffer

(10 mM PIPES, pH 7.0, 100 mM NaCl, 300 mM sucrose, 3 mM MgCl₂, 1 mM EGTA, 4 mM vanadyl riboside complex, and protease inhibitors PLAP), cells were lysed with 0.5% Triton X-100 in CSK buffer for 2 min and then digested with 30 units of RNase free DNase I (Boehringer-Mannheim Biochemicals) in 100 ul CSK at 34°C for 40 min. Cells were then extracted with 0.25 M ammonium sulfate in CSK for 5 min on ice. Extraction in 2 M NaCl was applied by adding 4 M salt stock drop by drop into an equal volume of CSK buffer with gentle shaking and placing the sample on ice for 4 min. The volume of CSK buffer should be large enough to avoid too harsh extraction (for 100 mm dish, at least 7 ml CSK buffer was required to make a final extraction volume of 14 ml). For further RNA digestion, cells were incubated with 100 ug/ml RNase A in CSK buffer for 12 min at 32–34°C.

For the Western blots of core filament samples, cells were first detached from the culture flasks by disassociation buffer. Each extraction step was applied to the cell pellet using essentially the same method as described above. Equivalent volumes of the solution were maintained in each fractionation step.

Immunofluorescence Microscopy

Monolayer cells grown on 22×22 mm coverslips were lysed in PEM containing 0.5% Triton X-100 for 2 min, and then fixed in 3.7% formaldehyde in PEM for 30 min at room temperature. The fixed cells were washed with PBS and blocked with 1% bovine albumin in PBS for 5 min. Staining was carried out with the mouse anti-NuMA antibodies followed by rhodamine-conjugated goat anti-mouse IgG at 37°C for 30 min. After washing, cells were counter-stained with H33258 at a concentration of approximately 0.01 ug/ml. Coverslips were mounted onto glass slides in a solution containing 90% glycerol, 10% PBS plus 0.1% phenylene diamine. Images were viewed in a Zeiss Axiophot microscope and analyzed with an Optimus software (Meyer Instruments).

Immuno–Electron Microscopy

Caski cells were grown on plastic coverslips and *in situ* extraction was performed for core filaments as mentioned above. These preparations were fixed in 3% paraformaldehyde and 0.05% glutaraldehyde in CSK buffer and then quenched in NaBH₄ (1 mg/ml) for 10 min. Cells were blocked with 5% normal goat serum (NGS) in TBS1 buffer (10 mM Tris, pH 7.7, 150 mM NaCl, 3 mM KCl, 1.5 mM MgCl₂, 0.05% Tween 20, 0.1% bovine serum albumin and 0.2% glycine) for 30 min and then incubated with 2D3 in TBS1 for 4 hr at room temperature. After washing in TBS1 (3×) and blocking with NGS, a 10 nm gold conjugated goat anti–mouse IgG (Amersham) diluted in TBS2 (20 mM Tris, pH 8.2, 140 mM NaCl and 0.1% bovine serum albumin) was added and the sample was incubated at 4°C overnight. Cells were then washed in TBS2 (3×) and post fixed in 2.5% glutaraldehyde in 0.1 M sodium cacodylate (pH 7.4) for 20 min. After ethanol dehydration, the sample was transferred to n–butanol and then embedded in diethylene glycol distearate (DGD) (Capco et al, 1984).

Samples were sectioned at a thickness of 200–300 nm. The DGD embedding medium was removed by immersing the sections in 100% butanol for 6 hr. The sections were transferred into butanol/ethanol (1:1) followed by three changes of ethanol. After critical point drying, the samples were examined in a JEOL 100C electron microscope.

RESULTS

Previous studies from our laboratory showed that monoclonal antibody 2D3 immuno–reacted with NuMA in both the interphase nucleus and mitotic polar regions (Tousson et al, 1991). Using 2D3, we isolated a 1.9 kb NuMA cDNA fragment from a λgt11 cDNA expression library of the human HT29 cell line. This cDNA clone encompasses a large section of the α–helix region of NuMA (bases 2058–3992 according to the sequence of Compton et al, 1992 and bases 1796–3726 by the sequence of Yang et al., 1992). A β–galactosidase fusion protein was produced in the positive λ–recombinant and used for the

generation of new antibodies. In this report, mouse antiserum (P9) raised against fusion protein, as well as our original 2D3, were selected for further study.

Existence of NuMA Isoforms

As shown by immunoblots on Fig. 1a, 2D3 and P9 recognized the fusion polypeptide of NuMA exclusively from the total protein preparation of the λ -recombinant. In a HeLa preparation extracted with 0.5 M NaCl from the lysed cells, polyclonal antibody P9 resolved NuMA as a double band at apparent 200 and 220 KD. Occasionally this double band was also resolved by 2D3 especially when purified IgG fractions were applied (results not shown). Additionally, a significant 160 KD band was also observed in the blots (Fig. 1b). Moreover, similar blotting patterns could also be resolved by other NuMA antibodies such as A107-7 (Matritech, Inc.) and 1F1 (Compton et al., 1992) (Fig. 1b).

To further identify the relationship of each protein band shown on immunoblots, gel strips containing each band individually were cut and subjected to peptide digesting (Cleveland et al., 1977). Comparison of the peptide patterns on immunoblots using pooled NuMA antibodies indicated that the 220 and 200 KD proteins have relatively high homology as shown in Fig. 2a. Only a slight size difference appeared on the lower bands between the two peptide ladders. Thus, the double band probably represent isoforms of NuMA derived from the post-transcriptional modification. This result is consistent with a recent analysis of various NuMA cDNA clones by Tang et al., which has shown that NuMA gene gives rise to multiple mRNAs and gene products through the alternative splicing mechanism (1993). The apparent molecular mass of 220 and 200 KD shown here may be equivalent to the 230 and 194/195 KD bands resulting from the different RNA processing. On the other hand, the peptide digests of the 160 and 220 KD protein band gave rather different patterns (Fig. 2b). Therefore, the 160 KD band may represent a different protein that is perhaps related to NuMA through a common epitope.

Detection of NuMA in Core Filament Fraction

To learn more about the location and function of NuMA within the nucleus, nuclear core filaments were prepared by *in situ* sequential fractionation (He, 1990). Each stage of nuclear extraction was examined by immunofluorescence with 2D3 antibody (Fig. 3). The human cervical epidermoid carcinoma cell line, CaSki, was chosen for immuno-staining of core filaments since these cells adhered tightly to the coverslip after each of the extraction steps. As shown in Fig. 3a, 2D3 stained the nuclei of CaSki cells diffusely as observed in HeLa cells. When cells were treated with RNase-free DNase I after lysis, DNA staining with H33258 was largely reduced. A 0.25 M ammonium sulfate extraction following DNase I digestion removed most of the residual DNA and almost no interphase DNA staining was observed in the subsequent extraction with 2 M NaCl (Fig. 3h). Regarding antibody reactions, 2D3 decorated the entire nucleus in each sequential step of extraction with an intensity similar to that of the controls.

Immunofluorescent staining of extracted cells indicated that the majority of NuMA protein remained in the nucleus even after extractions in solutions of 0.25–2.0 M ionic strength. Such an extraction released not only the residual DNA fragments but a large number of nuclear proteins. Thus, NuMA appears to be a stable component of the core filament system, the most insoluble component of the nuclear matrix. The immunofluorescent staining pattern observed during the sequential extractions was consistent with the immunoblots (Fig. 4). When each extraction sample was loaded with the amount representing the same number of cells on SDS-PAGE followed with antibody blotting, NuMA was only detected in the pellet of the core filament preparation with 2D3 (Fig. 4a). If polyclonal antibody P9 was used in blotting, only very little NuMA was resolved in each extracting fraction whereas a strong double band was detected in pellet of preparation (Fig. 4b). The doublet ≥ 200 KD revealed by P9 indicated that both isoforms of NuMA existed in core filaments system.

When the core filament preparations were further treated with RNase A after 2 M salt extraction, NuMA was still retained in the nucleus as detected by immunofluorescence (Fig. 5). It should be emphasized, however, the distribution pattern changed dramatically. Instead of diffuse staining in core filament preparation or control cells, 2D3 stained as some dots and several large patches after RNA digestion. Thus, our results support the previous EM work on core filament showing RNA to be a component of core filaments and the destruction of nucleoskeleton following RNase digestion (He et al., 1990). In agreement with earlier results, these experiments indicated that NuMA is also a very stable component of core filament.

Localization of NuMA on Core Filaments

In order to further identify NuMA in core filaments at the ultrastructural level, 10 nm gold conjugated with goat anti-mouse second antibody was used to visualize the localization of 2D3 antibody. The nuclear scaffold is largely masked in thin sections of conventional resin embedded samples. To avoid such masking, we utilized the resinless sections as described by Capco et al. (1984). This technique offers the additional advantage of permitting the visualization of nuclear architecture in sections several times thicker than the conventional ultra-thin sections. Therefore a more three-dimensional-like structure could be dissolved. As shown in Fig. 6a, the nuclear core filament network of CaSki cell was resolved following sequential fractionation as described above. The size of most single fiber was around 9–13 nm although a few thicker fiber about 20 nm also could be seen. The latter might be either overlapping individual fibers on the thick section or bundled fibers produced during extraction. It should be noticed that intermediate filaments were the only cytoskeletal components in the cytoplasm retained after extractions. As pointed out by He et al. (1990), core filaments of the nucleus and intermediate filaments of the cytoplasm shared several common features including size, morphology and solubility properties.

Immuno-gold labeled 2D3 was confined largely to the nucleus where it decorated segments of filaments (Fig. 6a). Actually, two patterns of labeling were observed; in one, gold beads were aligned along some filaments and not others, indicating that NuMA may be confined predominantly to one subset of fibers (Fig. 6, arrows). This localization is consistent with the heterogeneous composition of core filaments (He et al., 1990) and the primary structure of NuMA as a coiled-coil protein with long α -helical region (Yang et al., 1992; Compton et al., 1992). In another pattern, label was confined to dense amorphous regions and a considerable amount linearly aligned gold beads were observed in these areas (Fig. 6, arrowheads). Collectively, these observations suggest that NuMA is on or associated with the core filaments. Most likely, NuMA isoforms appear to be a stable component of some, but not all, core filaments.

DISCUSSION

Our interest in NuMA began with the discovery of a novel centrosome-associated protein localized at the poles of the mitotic spindle of human cells termed centrophilin (Tousson et al., 1991). Recent work in our laboratory on the primary structure of centrophilin (Zeng and Brinkley, unpublished) and on NuMA by other two groups (Compton et al., 1991; Yang et al., 1991) confirmed that the two proteins are in fact one in the same, and very likely the same as the protein SPN and SH-P (Kallajoki et al., 1993). Analysis of centrophilin, SPN, SP-H and NuMA on spindle MT poisoning treatments and microinjection of antibodies suggest that each functions to organize MTs at their minus-ends in mitotic cells (Kallajoki et al, 1991 and 1992; Tousson et al., 1991; Maekawa et al., 1991; Yang and Snyder, 1992). Although the precise function of NuMA in mitosis is still not clear, its unusually long coiled-coil structure predicted from cDNA analysis (Yang et al., 1992; Compton, et al., 1992) suggests a structural rather than a motor or kinetic function.

As stated above, most studies of NuMA have focused on possible functions during the brief period of mitosis and relatively little is known of its localization and function in the interphase nucleus where cells spend approximately >95% of their time during the cell cycle. The present study deals with the nuclear localization of NuMA and its possible function during interphase. Using antibodies raised against a fusion protein, we demonstrate herein, the first evidence that this protein may likely to be a important component of the nucleoskeleton. Moreover, the existence of NuMA isoforms suggests greater complexity of NuMA's function than originally proposed.

The solubility of NuMA has been a serious obstacle to its biochemical characterization. NuMA is highly insoluble by conventional nuclear extraction, i.e., DNA digestion followed by salt extraction up to 2 M (Fig 4). Through various attempts, we found that NuMA is relatively soluble in 0.5 M NaCl prior to DNA digestion but essentially insoluble after DNA has been digested (Figs. 1 and 4). The mechanism for this alternation in solubility is uncertain. Numerous factors have been found to influence the process and degree of the nuclear extraction (Verheijen et al., 1988). Possibly, changes of conformation and surface charge after by DNA digestion are major factors making some scaffold components, including NuMA, more tightly associated. Moreover, we found that the shape and morphology of cells dramatically changed in 0.5 M NaCl, suggesting that cytoskeleton system may be deformed by the extraction (results not shown). Thus, the ionic strength of 0.5 M salt appears to be very effective in differential extraction of proteins.

Several other nuclear proteins share the property of greater solubility in 0.5 M salt. For instance, many RNPs have been detected in the nuclear matrix through DNA digestion and extractions whereas most RNPs could also be extracted from undigested cells with the buffers containing lower concentration of salt as in the Dignam buffer (Dignam et al., 1983). Similarly, the centromere/kinetochore protein, CENP-B, can be selectively solubilized in 0.5 M NaCl in HEPES buffer (Masumoto et al., 1989) but retained in the

interphase core filament fraction (He et al., unpublished results). Thus, our results with NuMA may provide a simple and gentle method in nuclear matrix study for solubilizing certain kinds of proteins, especially the scaffold related components, which were heretofore considered insoluble. Also, this finding implies interesting and poorly understood biochemical and structural interactions among related nuclear proteins.

As a proteinaceous lattice essential for maintaining nuclear compartmentalization and processing, the nuclear matrix likely contains an extensive skeletal frame. Recent studies have shown core filaments to be present throughout the nucleoplasm and are very likely the principle nucleoskeletal filaments of the matrix (He et al., 1990). Unlike the cytoskeletal elements, however, nuclear core filaments are composed of unknown protein components complexed with RNAs. Therefore, our data on NuMA obtained by sequential fractionation and immunogold EM localization, provides initial evidence for a specific protein component in a subset of fibers in this nucleoskeletal system. Indeed, the identification of NuMA as an unusually long coiled-coil macromolecule (Yang et al., 1992; Compton et al., 1992) strongly favors its being a component of nuclear core filaments. Since the double band is also resolved by polyclonal antibody P9 in core filament preparation, a dimeric or polymeric form of NuMA may be the subunit forming those core filaments as we mentioned above.

NuMA was named for its striking property of relocating from the interphase nucleus to the mitotic spindle during each cell cycle (Lydersen and Pettijohn, 1980). Since its initial discovery, other proteins with similar behavior during the cell cycle have been described (Todorov, et al., 1992; He et al., 1991; Thibodeau and Vincent, 1991; Nickerson et al., 1992; and Whitfield et al., 1988). Thus, the term NuMA, originally selected to describe a specific ≥ 200 KD phosphoprotein, may be a more appropriate term for a class of proteins that oscillate between the nucleus and mitotic apparatus.

An intriguing feature of NuMA also suggested by this study is that this protein may have dual functions as well as dual localizations in the cell cycle. It is perhaps worthwhile to note that NuMA can be classified either as a nucleoskeletal or cytoskeletal protein depending on the stage of the cell cycle. During mitosis NuMA may be involved in spindle MT organization as a minus end binding protein. During interphase, NuMA may play important role in maintaining nuclear architecture organization. In our another study, we have identified that a specific state of NuMA protein is colocalized with spliceosomes and NuMA antibodies, including 2D3, precipitate pre-mRNA from the *in vitro* splicing reaction (Zeng, et al., in press). Therefore, NuMA may serve as the structural linkage between the nucleoskeleton and the RNA splicing apparatus. These characterizations imply that other NuMA-like proteins may also play bifunctional roles in the nucleus and spindle. Indeed, proteins such as NuMA that assume multiple roles in cells would seem to have selective advantage in evolution and may be more common than anticipated. It is likely, therefore, that NuMA is one member of a class of structural proteins that resides in both the nucleus and mitotic apparatus forming a molecular fabric to embrace the genome throughout the cell cycle.

We wish to thank Dr. Duane Compton (Johns Hopkins University) and Mr. Dong Pearl (Matritech, Inc) for their kind gifts of NuMA antibodies. We thank Becky Scott for cell culture work and editorial assistance. We also thank Michael Wise for his critical reading of this manuscript.

This work was supported by grants from the National Institutes of Health CA41424 to BRB.

REFERENCES

- Berezney, R. and D. S. Coffey. 1974. Identification of a nuclear protein matrix. *Biochem. Biophys. Res. Commun.* 60:1410–1417.
- Berezney, R. and D. S. Coffey. 1977. Nuclear matrix: isolation and characterization of a framework structure from rat liver nuclei. *J. Cell Biol.* 73:616–637.

- Berezney, R. 1991. The nuclear matrix: a heuristic model for investigating genomic organization and function in the cell nucleus. *J. Cell. Biochem.* 47:109–123.
- Bode, J., Y. Kohwi, L. Dickinson, T. Joh, D. Klehr, C. Mielke, and T. Kohwi-Shigematsu. 1992. Biological significance of unwinding capability of nuclear matrix–associating DNAs. *Sci.* 255:195–197.
- Carter, K. C., K. L. Taneja, and J. B. Lawrence. 1991. Discrete nuclear domains of poly(A) RNA and their relationship to the functional organization of the nucleus. *J. Cell Biol.* 115:1191–1202.
- Capco, D. G., G. Krochmalnic, and S. Penman. 1984. A new method of preparing embedding–free sections for transmission electron microscopy: applications to the cytoskeletal framework and other three–dimensional networks. *J. Cell Biol.* 98:1878–1885.
- Cleveland, D. W., S. G. Fischer, M. W. Kirschner, and U. K. Laemmli. 1977. Peptide mapping by limited proteolysis in sodium dodecyl sulfate and analysis by gel electrophoresis. *J. Biol. Chem.* 252:1102–1106.
- Compton, D. A., I. Szilak, and D. W. Cleveland. 1991. Primary structure of NuMA, an intranuclear protein that defines a novel pathway for segregation of proteins at mitosis. *J. Cell Biol.* 116:1395–1408.
- Compton, D. A., and D. W. Cleveland. 1993. NuMA is required for the proper completion of mitosis. *J. Cell Biol.* 120:947–957.
- Dignam, J. D., R. M. Lebovitz, and R. G. Roeder. 1983. Accurate transcription initiation by RNA polymerase II in a soluble extract from isolated mammalian nuclei. *Nucleic Acids Res.* 11:1475–1489.
- Fey, E. G., G. Krochmalnic, and S. Penman. 1986. The nonchromatin substructures of the nucleus: the ribonucleoprotein (RNP)–containing and RNP–depleted matrices analyzed by sequential fractionation and resinless section microscopy. *J. Cell Biol.* 102:1654–1665.
- Gasser, S. M., B. B. Amati, M. E. Cardenas, and J. F. X. Hofmann. 1989. Studies on scaffold attachment sites and their relation to genome function. *Int. Rev. Cytol.* 119:57–96.
- Getzenberg, R. H., and D. S. Coffey. 1990. Tissue specificity of the hormonal response in sex accessory tissues is associated with nuclear matrix protein patterns. *Mol. Endocrinol.* 4:1336–1342.
- Getzenberg, R. H., K. J. Pienta, W. S. Ward, and D. S. Coffey. 1991. Nuclear structure and the three–dimensional organization of DNA. *J. Cell. Biochem.* 47:289–299.
- He, D., T. Martin, and S. Penman. 1991. Localization of heterogeneous nuclear ribonucleoprotein in the interphase nuclear matrix core filaments and on perichromosomal filaments at mitosis. *Proc. Natl. Acad. Sci. USA.* 88:7469–7473.

- He, D., J. A. Nickerson, and S. Penman. 1990. Core filaments of the nuclear matrix. *J. Cell Biol.* 110:569–580.
- Hozák, P., A. B. Hassan, D. A. Jackson, and P. R. Cook. Visualization of replication factories attached to a nucleoskeleton. *Cell.* 73:361–373.
- Jackson, D. A., and P. R. Cook. 1988. Visualization of a filamentous nucleoskeleton with a 23-nm axial repeat. *EMBO (Eur. Mol. Biol. Organ.) J.* 7:3667–3678.
- Kallajoki, M., K. Weber, and M. Osborn. 1991. A 210 KD nuclear matrix protein is a functional part of the mitotic spindle; a microinjection study using SPN monoclonal antibodies. *EMBO (Eur. Mol. Biol. Organ.) J.* 10:3351–3362.
- Kallajoki, M. J. Harborth, K. Weber, and M. Osborn. 1993. Microinjection of a monoclonal antibody against SPN antigen, now identified by peptide sequences as the NuMA protein, induces micronuclei in PtK2 cells. *J. Cell Sci.* 104:139–150.
- Kallajoki, M., K. Weber, and M. Osborn. 1992. Ability to organize microtubules in taxol-treated mitotic PtK₂ cells goes with the SPN antigen and not with the centrosome. *J. Cell Sci.* 102:91–102.
- Lyderson, B., and D. Pettijohn. 1980. Human-specific nuclear protein that associates with the polar region of the mitotic apparatus: distribution in a human/hamster hybrid cell. *Cell.* 22:489–499.
- Maekawa, T., R. Leslie, and R. Kuriyama. 1991. Identification of a minus end-specific microtubule-associated protein located at the mitotic poles in cultured mammalian cells. *Eur. J. Cell Biol.* 54:255–267.
- Masumoto, H., H. Masukata, Y. Muro, N. Nozaki, and T. Okazaki. 1989. A human centromere antigen (CENP-B) interacts with a short specific sequence in alphoid DNA, a human centromeric satellite. *J. Cell Biol.* 109:1963–1973.
- Nakayasu, H., and R. Berezney. 1989. Mapping replicational sites in the eucaryotic cell nucleus. *J. Cell. Biol.* 108:1–11.
- Nickerson, J. A., D. He, E. G. Fey, and S. Penman. 1990. The nuclear matrix. *In* *The Eukaryotic Nucleus Molecular Biochemistry and Macromolecular Assemblies*. The Telford Press, editors. P. R. Strauss, and S. H. Wilson, New Jersey. 2:763–782.
- Nickerson, J. A., G. Krockmalnic, K. M. Wan, C. D. Turner, and S. Penman. 1992. A normally masked nuclear matrix antigen that appears at mitosis on cytoskeleton filaments adjoining chromosomes, centrioles, and midbodies. *J. Cell Biol.* 116:977–987.
- Price, C. M., and D. E. Pettijohn. 1986. Distribution of the nuclear mitotic apparatus protein (NuMA) during mitosis and nuclear assembly. *Exp. Cell Res.* 166:295–311.
- Roberge, M., and S. M. Gasser. 1992. DNA loops: structural and functional properties of scaffold-attached regions. *Mol. Microbiol.* 6:419–423.

- Spector, D. L., W. H. Schrier, and H. Busch. 1983. Immunoelectron microscopic localization of snRNPs. *Biol. Cell.* 49:1–10.
- Tang, T. K., C. C. Tang, Y. Chen, and C. Wu. 1993. Nuclear proteins of the bovine esophageal epithelium II: the NuMA gene gives rise to multiple mRNAs and gene products reactive with monoclonal antibody W1. *J. Cell Sci.* 104:249–260.
- Thibodeau, A., and M. Vincent. 1991. Monoclonal antibody CC–3 recognizes phosphoproteins in interphase and mitotic cells. *Exp. Cell Res.* 195:145–153.
- Todorov, I. T., R. N. Philidova, G. Joswig, D. Werner, and F. C. S. Ramaekers. 1992. Detection of the 125–kDa nuclear protein mitotin in centrosomes, the poles of the mitotic spindle, and the midbody. *Exp. Cell Res.* 199:398–401.
- Tousson, A., C. Zeng, B. R. Brinkley, and M. M. Valdivia. 1991. Centrophilin: a novel mitotic spindle protein involved in microtubule nucleation. *J. Cell Biol.* 112:427–440.
- van Driel, R., B. Humbel, and L. de Jong. 1991. The nucleus: a black box being opened. *J. Cell. Biochem.* 47:311–316.
- Verheijen, R., W. van Venrooij, and F. Ramaekers. 1988. The nuclear matrix: structure and composition. *J. Cell Sci.* 90:11–36.
- Whitfield, W. G. F., S. E. Millar, H. Saumweber, M. Frasch, and D. M. Glover. 1988. Cloning of a gene encoding an antigen associated with the centrosome in *Drosophila*. *J. Cell Sci.* 89:467–480.
- Yang, C. H., E. J. Lambie, and M. Snyder. 1991. NuMA: an unusually long coiled–coil related protein in the mammalian nucleus. *J. Cell Biol.* 116:1303–1317.
- Yang, C. H., and M. Snyder. 1992. The nuclear–mitotic apparatus protein (NuMA) is important in the establishment and maintenance of the bipolar mitotic spindle apparatus. *Mol. Biol. Cell.* 3:1259–1267.
- Zeitlin, S., A. Parent, S. Silverstein, and A. Efstratiadis. 1987. Pre–mRNA splicing and the nuclear matrix. *Mol. Cell. Biol.* 7:111–120.

Figure 1. Immunoblots of NuMA antibodies. (a) A 180 KD β -galactosidase fusion protein is resolved from the total protein preparation of the positive λ gt-11 recombinant by monoclonal antibody 2D3 (lane 1) and polyclonal antibody P9 (lane 2). (b) When HeLa cells are extracted with 0.5 M NaCl after lysis, 2D3 (lane 1), P9 (lane 2), A107-7 (lane 3), and 1F1 (lane 4) recognize an additional 160 KD band by epitope cross-reactivity (Fig. 2). pAb P9 and mAb A107-7 also probed NuMA as a double band of 220 and 200 KD (lanes 2 and 3).

a



b

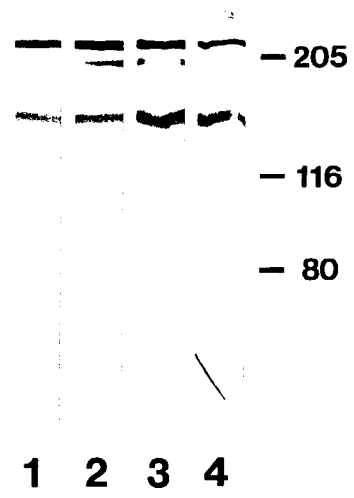
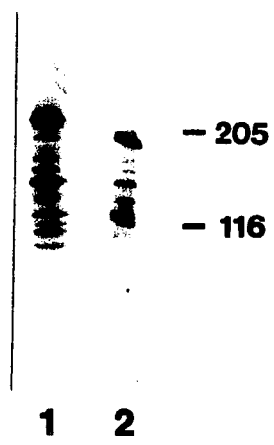


Figure 2. Peptide maps of proteins resolved in immuno-blot by NuMA antibodies. (a) Comparison of each of the two band ≥ 200 KD after incomplete protein digestion with endoproteinase Glu-C and blotted by a pool of NuMA antibodies P9 and a monoclonal antibody 8.22 (Zeng, et al., 1993). The difference between the higher band (lane 1) and the lower one (lane 2) is restricted only in smaller peptide fragments bellow 120 KD, indicating that the doublet revealed by polyclonal anti-NuMA antibody P9 represents isoforms of NuMA. (b) The digesting patterns of the high NuMA band (lane 1) and 160 KD protein (lane 2) are obviously different, suggesting no significant homology between these two proteins.

a



b

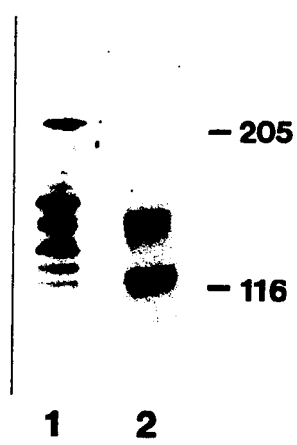
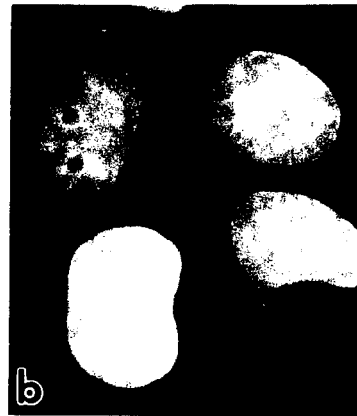
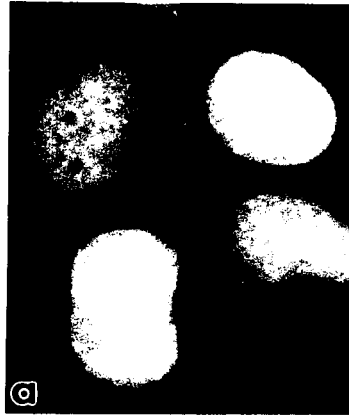


Figure 3. Detection of NuMA in CaSki cells during each step of extraction for core filament preparation. The diffuse pattern of 2D3 staining in control CaSki cell (a) is the same as in HeLa. DNA staining of nuclei (b, d, f, and h) indicate that the chromatin is dramatically removed after digestion of DNA (c, d), extraction with 0.25 M ammonium sulfate (e, f) and 2 M salt (g, h). 2D3 staining shows no obvious difference from the control (a) following each treatment (b, d, and g). Bar, 10 μ m.

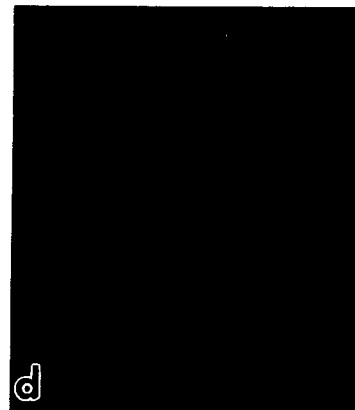
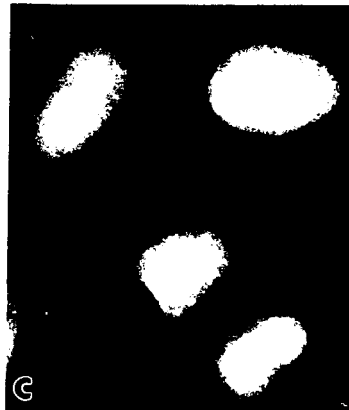
2D3

H33258

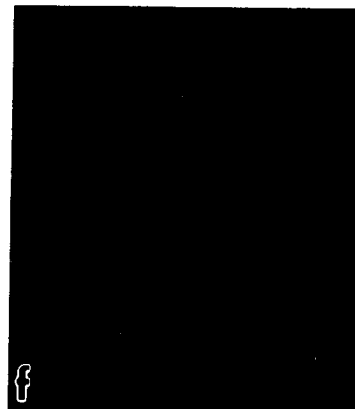
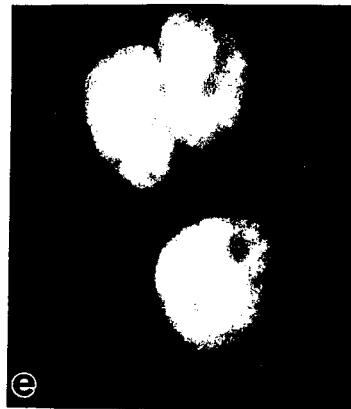
Control



DNase I



0.25 M
 $(\text{NH}_4)_2\text{SO}_4$



2 M
NaCl

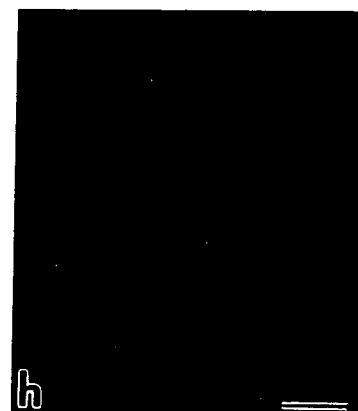
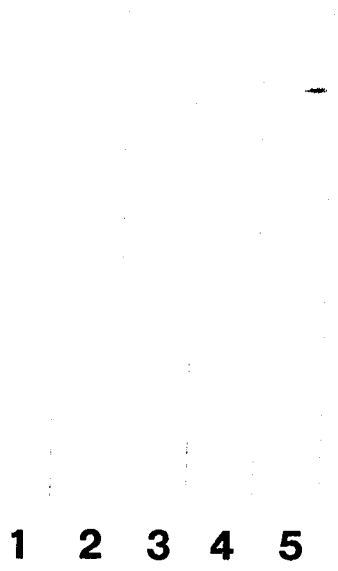


Figure 4. Immunoblotting confirms NuMA as a component of core filaments. Each extracting sample from the same amount of cells is blotted by 2D3 (a) and P9 (b) respectively. Blotted by 2D3, no NuMA was detected in the supernatant of Triton X-100 treatment (lane 1), DNase I digestion (lane 2), 0.25 M ammonium sulfate extraction (lane 3), and 2 M salt extraction (lane 4). NuMA is only resolved in the pellet of core filament preparation (lane 5). Polyclonal antibody P9 (b) resolves only little amount of NuMA protein in extracted fraction (lanes 1-4) while majority of NuMA in core filament pellet as a doublet (lane 5), suggesting that the isoforms of NuMA reside in nucleoskeleton.

a



b

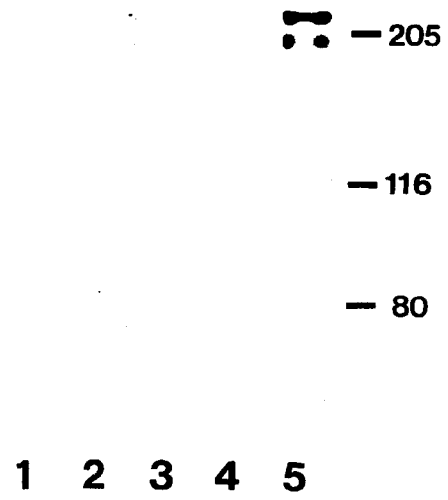


Figure 5. NuMA localization is deformed when core filaments are destructed by RNA digestion. In core filament preparation followed by treatment of RNase A, staining of 2D3 altered into dots and large patches. Bar, 10 μ m.

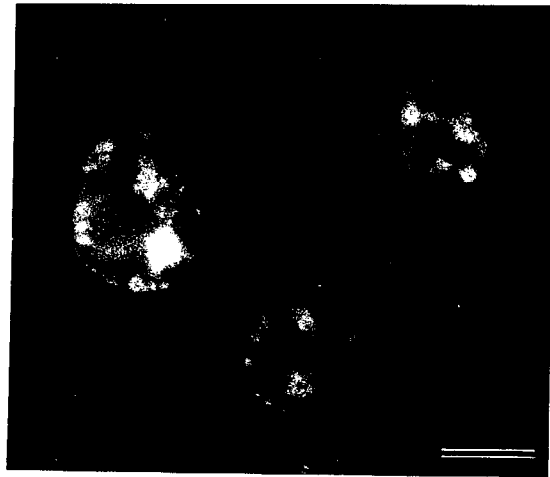
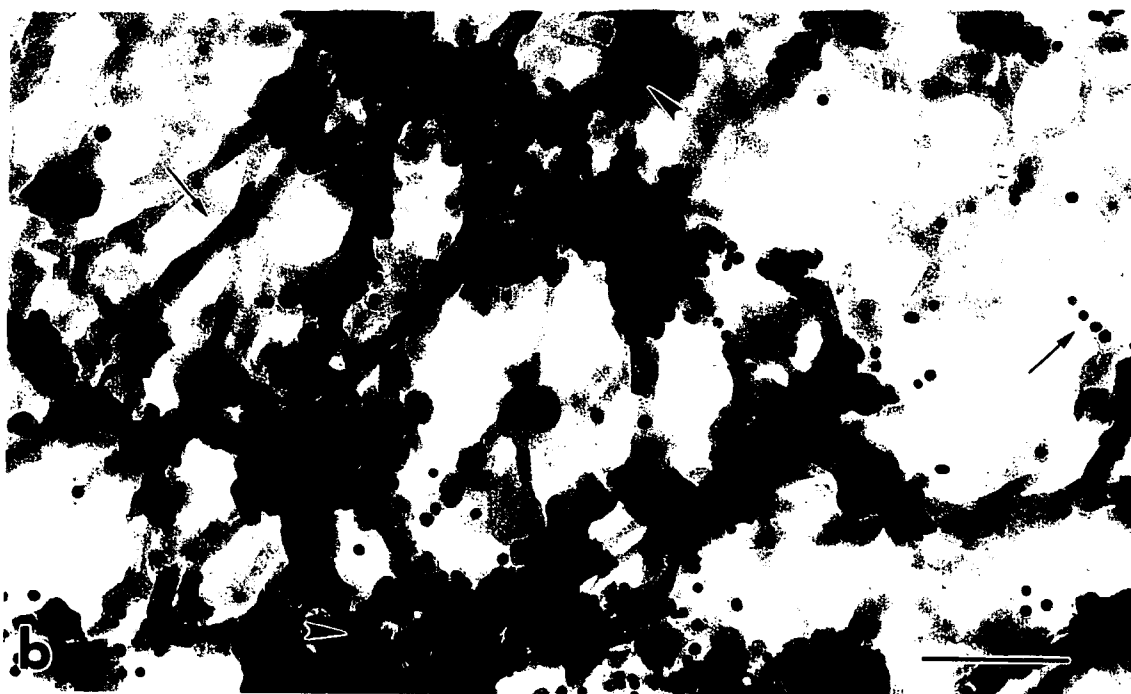
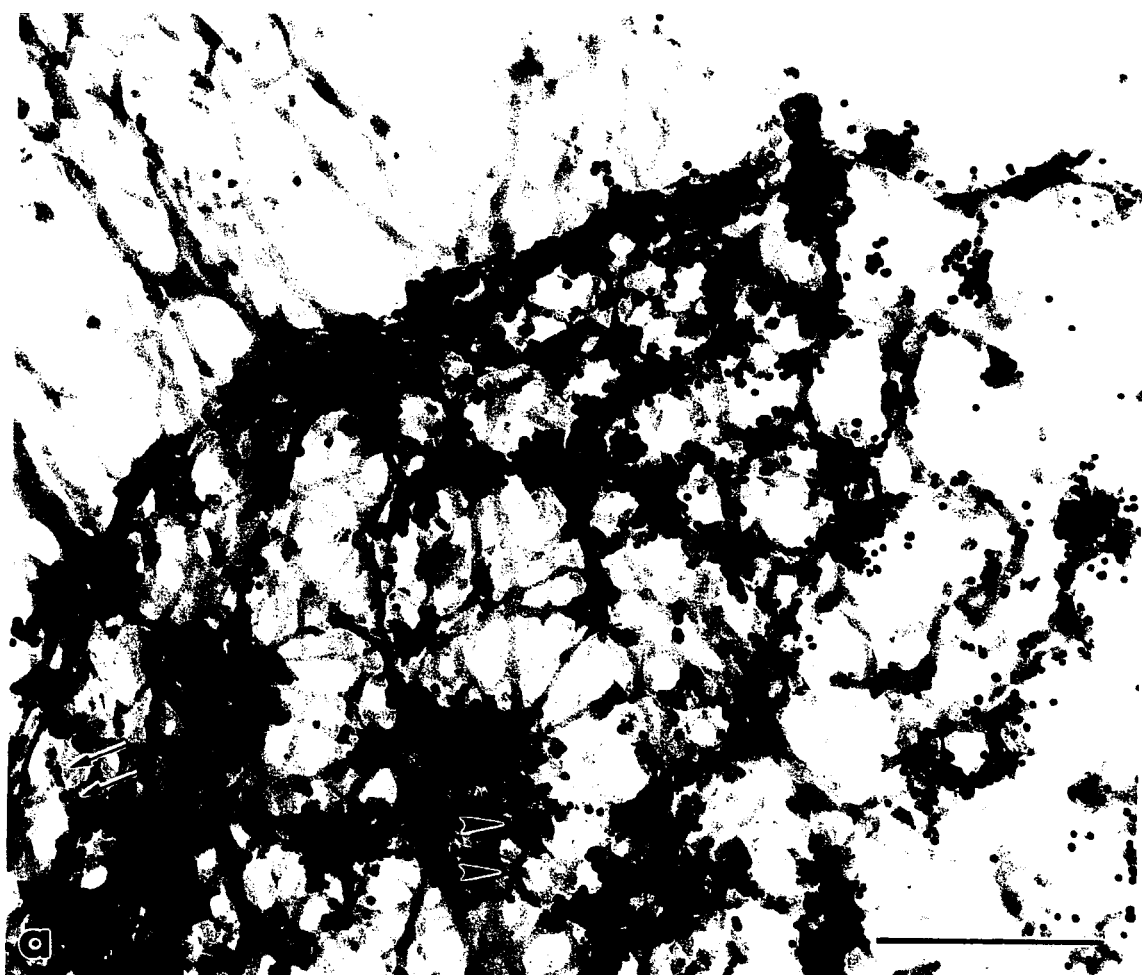


Figure 6. EM immuno-gold labeling of 2D3 on core filaments of CasKi cells. Intermediate filaments were the only components in cytoplasm (a). 2D3 appears to decorate a subset of core filaments (a and b). Arrows: alignment of gold labeling along core filaments, suggesting that the filaments themselves contains NuMA; Arrowheads: aligned gold labeling at amorphous regions, implying where although core filament anastomosed, NuMA appears to contribute to the formation of the filaments. Bars, 0.5 μm (a) and 0.2 μm (b).



**NuMA: A STRUCTURAL PROTEIN INTERFACE BETWEEN
THE NUCLEOSKELETON AND RNA SPLICING**

C. ZENG, D. HE, S. M. BERGET, and B. R. BRINKLEY

Submitted to Proceeding National Academic Science USA

ABSTRACT

Vertebrate splicing factors are localized to discrete domains within the nuclei of somatic cells. The mechanism whereby such nuclear domains, identified as speckles by immunofluorescence microscopy, are generated is unclear. Recent studies suggest that the spatial order within the nucleus is maintained by nuclear matrix factors. Here we show that a protein in the nuclear matrix and mitotic apparatus (NuMA) (Lydersen, B. and Pettijohn, D. [1980] *Cell* **22**, 489–499) co-localizes with splicing factors in interphase nuclei and is associated with small nuclear ribonucleoproteins (snRNPs) in a complex immunoprecipitated from HeLa extract with snRNP antibodies. Moreover, NuMA associates with splicing complexes that are reconstituted *in vitro* using wild type pre-mRNA, but not with nonspecific RNA. Cumulatively, these observations suggest a novel function of NuMA or NuMA-like proteins in interphase cells in providing a bridge between RNA processing and the nucleoskeleton.

INTRODUCTION

The eukaryotic nucleus is a highly organized structure. Electron microscopy has provided excellent morphological evidence for the existence of a complex nucleoskeleton (1, 2). An intermediate filament-like nuclear network termed core filaments has been revealed by a sequential extraction procedure (2, 3). These 9–13 nm filaments may be the core structure to which other proteins associate to form the nuclear matrix. Many nuclear activities, such as DNA and RNA synthesis, and RNA splicing, have been localized in discrete nuclear domains rather than diffusely distributed throughout the nucleoplasm (4–7). Particularly, the localizations of these specific domains persist after the removal of chromatin, indicating that the nuclear matrix has a key function in maintaining spatial order within the nucleus. Recent microscopic studies have suggested that pre-mRNAs are both processed and transported in discrete nuclear "tracks" that might correspond to nuclear filaments (8–11). In addition, earlier experiments revealed a preferential association of

pre-mRNA with the nuclear matrix (12–16). Strong evidence for the relationship of the nucleoskeleton to gene expression, however, has been lacking due to the phenomenological nature of biochemical matrix preparations. No studies have used reagents directed against a well-characterized element of the nucleoskeleton in an attempt to bridge the gap between nuclear architecture and gene expression.

NuMA (17), also known as centrophilin (18), SPN (19), and SP-H (20), is a 230 Kd nuclear protein that resides at the spindle poles during mitosis. Studies on the primary structure of NuMA have shown that it is a long coiled-coil protein with two globular end domains separated by a discontinuous α -helix (21, 22). Analysis of different NuMA cDNA clones has suggested the existence of NuMA isoforms generated by alternative splicing (23), although no correlation has been made between the isoforms and multiple functions for NuMA. In mitotic cells, NuMA appears to play a role in spindle microtubule formation and post-mitotic nuclear assembly as shown by various studies on MT inhibition, antibody injection, and expression of truncated NuMA proteins (18–20, 24–27). Beyond its identity as a nuclear matrix protein (17, 19), however, little is known of the function of NuMA in the interphase nucleus.

Here we investigate the role of NuMA in interphase nuclei via the ability of NuMA-specific antibodies to stain discrete foci and to immunoprecipitate nuclear assemblies. Specifically, we show that NuMA co-localized with the snRNPs required for processing of pre-mRNAs in interphase. Furthermore, we show that NuMA associates *in vitro* with both nuclear snRNPs and reconstituted spliceosomes.

MATERIALS AND METHODS

Cell Culture

HeLa cells were grown in DMEM with 10% fetal bovine serum (FBS). Human cervical epidermoid carcinoma cells (CaSki; American Type Culture Collection) were cultured in RPMI-1640 medium containing 2.5% FBS and 7.5% calf serum.

In situ Sequential Extraction

CaSki cells were chosen for core filament preparation (2) because these cells adhere tightly to coverslips after each of the extraction steps. Cells on coverslips were lysed for 2 min in cytoskeleton (CSK) buffer (10 mM PIPES, pH 7.0; 100 mM NaCl; 300 mM sucrose; 3 mM MgCl₂; 1 mM EGTA; and 4 mM vanadyl riboside complex) containing 0.5% Triton X-100 and multiple protease inhibitors PLAP (0.1 mM PMSF, 1 ug/ml each of leupeptin, antipain, and pepstatin), then digested with 30 units of RNase-free DNase I (Boehringer-Mannheim Biochemicals) in 100 ul CSK buffer at 32°C for 40 min. Subsequently, cells were extracted with 0.25 M ammonium sulfate in CSK in ice for 5 min. The coverslips were then immersed in 7 ml CSK in a 100 mm petri dish and 7 ml of 4 M NaCl stock was added drop by drop with gentle shaking to reach a final concentration of 2M. After incubating on ice for 4 min, core filament preparations were fixed in formaldehyde and subjected to antibody staining. For further RNA digestion, 100 ug/ml of RNase A was added and the cells were incubated at 33°C for 12 min following fixation.

Immunofluorescence

HeLa or CaSki cells were grown on glass coverslips, permeabilized for 2 min in PEM plus 0.5% triton X-100 and then fixed in 3% formaldehyde in PEM for 30 min, except for the samples for core filament preparation. Fixed cells were washed with PBS and stained with primary antibodies for 0.5–3 hr at 37°C. For double label immunofluorescence, cells were stained in turn, with monoclonal antibody 8.22, rhodamine-conjugated goat anti-mouse IgG, α Sm (a snRNP-specific autoantibody) (28), and FITC-conjugated goat anti-human IgG. Optimus software (Meyer's Instruments) was used to analyze images and compute pseudo color.

Immunoprecipitation in HeLa extracts

HeLa cells in one T150 flask were washed twice with Hanks and incubated in 10-ml methionine-free medium and 1 mCi ³⁵S-labeled methionine and leucine (ICN) for 6 hr.

After washing with PBS, cells were lysed with 0.5% Triton X-100 in PEM (100 mM PIPES, pH 7.0, 1 mM EGTA, and 1 mM MgCl₂) with protease inhibitors PLAP for 5 min in ice. The cell pellet was then incubated in 0.5 M NaCl in PBS plus PLAP for 5–15 min or with addition of 0.08% SDS. The extracts were cleared by micro-centrifugation at 4°C and diluted 1:1 with PBS. Before immunoprecipitation, antibodies 2D3 and 8.22 were first conjugated to protein G-agarose (PIERCE) as described by Harlow and Lane (29). For precipitation, 2 ul of Y12 (a snRNP-specific monoclonal antibody) (30), 20 ul of agarose conjugated anti-TMG K121 (31), 20 ul of protein G-agarose conjugated 2D3 or 8.22 antibodies were added to 200 ul of diluted extract respectively. After incubation on ice for 1 hr, 20 ul of agarose protein G was added to the Y12 immunoprecipitation and agitated on a rocker at 4°C for 1 hr. For agarose bead conjugated antibodies, each mixture was gently agitated for 2 hr. Samples were then centrifuged and rinsed three times with 0.25 M PBS and twice with PBS. Pellets were subjected to SDS-PAGE and autoradiography. For samples also used for immunoblots after precipitation, non-labeled HeLa 0.5 M salt extract was prepared. α TMG antibody (30 ul) coupled to agarose, uncoupled protein G agarose, or 2 ul of CREST antibody (32) were used to perform immunoprecipitation as described above and the complexes were analyzed by SDS-PAGE and immunoblotting using P9 or CREST antibodies.

Immunoprecipitation with *in vitro* Reconstituted Spliceosomes

³²P-labeled splicing precursor RNA was transcribed *in vitro* from the MINX adenovirus minigene containing a single intron (16). Precursor RNA was capped during synthesis. HeLa nuclear extract was prepared as described (33) and *in vitro* splicing was performed as reported previously (34). All antibodies were affinity purified from cell culture media, ascites, or serum. Purified antibodies at concentrations of 3–5 ug were added to each reaction and incubated on ice for 15 min. To precipitate the immuno-complexes, we found that the pre-washed streptococcus protein G was much more effective than

agarose conjugated protein G. After incubation with 20 μ l of protein G for 15 min on ice, Pellets were washed with modified NETS (50 mM Tris, pH 7.9, 150 mM NaCl, 0.05% NP-40, 1.5 mM $MgCl_2$, and 0.5 mM DTT). Following ethanol precipitation, RNA was dissolved in 90% formamide, 10 mM EDTA, boiled, and resolved on a 10% acrylamide gel containing 9 M urea.

RESULTS AND DISCUSSIONS

Colocalization of NuMA and snRNPs

To obtain reagents specific for NuMA, a monoclonal antibody (2D3) specific for primate NuMA (18) was used to screen a cDNA library prepared from the human cell line, HT29. A partial cDNA of 1.9 kb was isolated and determined to code for NuMA by sequence analysis (21, 22). A fusion protein fused to β -galactosidase was produced and injected into mice for the generation of antibodies. Resulting antibodies were selected for anti-NuMA activity by detection of mitotic polar staining. One monoclonal antibody, 8.22, and one polyclonal antibody, P9, were chosen for further study. It was noted that P9, 8.22, and 2D3 stained spindle poles during mitosis, consistent with the known specificity of all anti-NuMA antibodies. As shown in Fig. 1, all three antibodies reacted with two or more of a set of three proteins of apparent molecular masses 160, 200 and 220 Kd, upon Western blotting. The largest protein was recognized by all three antibodies and corresponds to previously characterized NuMA (17). The middle band, detected only with the polyclonal antibody, was a known isoform of NuMA produced by alternative splicing (23) as determined by peptide digestion (35) (data not shown). The 160 KD protein recognized by all three antibodies had a different protein digestion pattern than the largest bands and, therefore, probably represents a protein other than NuMA containing a common epitope.

Although all three antibodies exhibited identical staining of spindle poles in metaphase, two distinct patterns of staining were observed for interphase nuclei (Fig. 2).

Both P9 and 2D3 produced a diffuse nuclear staining pattern like that seen with other NuMA antibodies, whereas 8.22 stained discrete foci or speckles. A similar staining pattern has also been seen in two other studies. In their initial report, Lydersen and Pettijohn (17) identified discrete fluorescent spots in the nuclei of HeLa cells stained with anti-NuMA antibody. Another NuMA monoclonal antibody, W1, also produced nuclear speckles in immunofluorescence (23). Since 2D3 and 8.22 resolved the same proteins in immunoblots (Fig. 1), the different fluorescent pattern of the two antibodies is probably due to differential availability of each epitope of NuMA (Fig. 2a and b). This difference in staining suggests that the epitope recognized by 8.22 antibody resides in a particular nuclear domain distinct from those containing the majority of the NuMA protein. The foci produced by 8.22 were reminiscent of the staining patterns of a number of splicing factors. To further investigate this similarity, cells were stained with both 8.22 and an α Sm antibody that reacts with human snRNPs (28) (Fig. 2c-h). In interphase nuclei, the two staining patterns co-localized with the exception that α Sm, but not 8.22, also stained a few distinct spots presumed to be coiled bodies (coilin-containing nuclear foci of unknown function) (36-38) (Fig. 2c-e). During mitosis, however, the staining pattern of the two antibodies differed considerably. As shown in Fig. 2f-h, 8.22 antibody transferred to the polar regions, whereas the α Sm antibody assumed a diffuse localization in the cytoplasm. Both NuMA and α Sm antigens reappeared in the newly formed daughter nuclei at late telophase. The coalescence of snRNP-specific and NuMA-specific antibodies only during interphase indicates that the antibodies are recognizing two distinct epitopes that co-occupy a nuclear domain during only one portion of the cell cycle.

In a separate immuno-electron microscopy study, we found NuMA to be a component of core filaments, the skeleton of the nuclear matrix consisting of heterogeneous proteins and RNAs (2). To further document the co-localization of NuMA and snRNPs, core filaments were prepared by DNA digestion and gradient salt extraction

(Fig. 2i–j). A portion of this material was treated further with RNase A (Figure 2k–l). The two antigens remained co-localized after both treatments, despite the changes each caused to nuclear structure. After DNase I and salt treatment, both antigens retained the same pattern as the control except for more intensive staining. After RNase treatment, which disrupted the core filament system, the speckled pattern was replaced by large patches. These patches were stained equally with NuMA and snRNP antibodies. These results are consistent with the presence of NuMA and snRNPs in the same sub-nuclear regions and suggest that the association of NuMA and snRNPs is relatively stable. In addition, NuMA, but not the 160 KD protein, could be detected in core filament preparation by immunoblots with NuMA antibodies (data not shown). The 160 KD protein therefore, may not exist in core filaments.

NuMA associates with snRNPs

To address further whether NuMA antigens are stably associated with snRNPs, we asked if we could detect NuMA in preparations of snRNPs that had been immunoprecipitated from nuclear extracts with either the α Sm antibody or with an antibody specific for the trimethylguanosine cap associated with snRNAs (α TMG) (31) (Figure 3a–c). The α Sm, α TMG, 2D3, and 8.22 antibodies all immunoprecipitated a doublet of ≥ 200 Kd from nuclear extracts of HeLa cells that had been labeled with ^{35}S -methionine (Figure 3a–b). Immunoblot analysis of the α TMG immunoprecipitate with the polyclonal NuMA antibody P9 indicated that this large doublet was indeed related to NuMA (Figure 3c). As controls, a centromere–kinetochore specific CREST antibody (32) could neither precipitate NuMA (Figure 3c, lane 2), nor detected CREST antigens in α TMG precipitate (Figure 3c, lane 5). Therefore, the association of NuMA with snRNPs is specific and sufficiently strong to survive immunoprecipitation. It should be noted that the 160 KD protein that was observed in Figure 1 to contain NuMA-like epitopes, was not present in any of immunocomplexes as analyzed by either ^{35}S -methionine or immunoblotting. Thus,

the 160 KD appeared not to be associated with snRNP under these experimental conditions.

NuMA Associates with *in vitro* Reconstituted Splicing Complexes

Immunoprecipitation of NuMA by snRNP antibodies suggested that NuMA is associated with snRNPs in interphase nuclei. To address if NuMA might be a part of the actual splicing apparatus, we turned to *in vitro* extracts competent for splicing exogenously provided pre-mRNAs (33). This type of extract is prepared by extracting nuclei in 0.4 M salt and contains both NuMA and multiple snRNPs.

To address the association of NuMA with reconstituted splicing complexes (spliceosomes), we asked if NuMA antibodies could immunoprecipitate radiolabeled pre-mRNA added to a splicing reaction. A wild type, one intron pre-mRNA derived from adenovirus was used as the pre-mRNA (16); a similar length plasmid RNA was used as a negative control RNA. Both RNAs were added to complete splicing reactions and incubated for 10 min at 30°C. This time interval is sufficient to permit assembly of the first ATP-dependent splicing complex, but is not sufficient to permit the appearance of splicing intermediates and products. Both reactions were immunoprecipitated with IgG fractions of NuMA antibodies and with the Y12 monoclonal α Sm antibody. As shown in Figure 4, both 2D3 and 8.22 antibodies immunoprecipitated the pre-mRNA, but not the control RNA, as effectively as the anti-snRNP antibody, suggesting that NuMA protein is associated with *in vitro* reconstituted spliceosomes.

The results shown here demonstrate a correlation between the nucleoskeleton and the pre-mRNA splicing apparatus. Antibody 8.22, which is generated against a portion of NuMA, may represent a specific group of NuMA antibodies, which stain discrete domains in interphase nuclei. Therefore, some epitopes of NuMA appear to be masked in the nucleus and not recognized by all NuMA antibodies. The following points support our conclusion that the speckle pattern of 8.22 is contributed by a specific form of NuMA: a)

if, for example, the nuclear speckles represent the 160 KD protein and not NuMA, 2D3 antibody should stain both a speckle pattern and a diffuse staining pattern since 2D3 and 8.22 resolve the same 160 KD band in immunoblots; b) in core filament preparations, the 160 KD protein disappeared from the immunoblots, whereas the fluorescent speckle pattern of 8.22 remains the same as the control cell; and c) other NuMA antibodies have been reported to produce a speckle staining pattern (17,23). Most likely then, 8.22 antibody, as well as a polyclonal antibody of NuMA and W1 antibody, all recognize a special structural or functional state of NuMA within discrete nuclear domains. Such heterogenous properties of nuclear NuMA protein may be due to post-translational or post-transcriptional modification (21-23) or conformation changes of nuclear NuMA within the nucleus. The regions stained by 8.22 and snRNP antibodies, known as speckles, appear to be actively involved in pre-mRNA processing. Elegant microscopic visualization of cellular RNAs undergoing transcription, processing, and transport indicates that pre-mRNA passes through these snRNP-rich speckles as they mature (8-11). Our results suggest that the processing centers are attached to the nuclear sub-structure through a nuclear core filament protein. Such attachment could poise a pre-mRNA for transport via continued association with nuclear filaments.

Anti-NuMA antibodies also detected a biochemical association between NuMA antigens and both nuclear snRNPs and in vitro reconstituted splicing complexes. Given the filamentous nature of the NuMA protein (21, 22), it seems unlikely that NuMA plays a functional role in the splicing process. More likely, NuMA is a nuclear structural component involved in association of the splicing apparatus with elements of the nucleoskeleton. Electron microscopic visualization of purified in vitro reconstituted splicing complexes has revealed the presence of a fibrous extension from a large globular complex that could represent the NuMA or NuMA-like protein (39). In this light,

alternatively spliced NuMA gene products may represent a subset of nuclear NuMA proteins associated specifically with the splicing apparatus.

We wish to thank Dr. David Spector (Cold Spring Harbor Labs), and Dr. Joan Steitz (Yale University) for their generosity in providing α Sm antibodies.

This work was supported by grants from the National Institutes of Health CA41424 to BRB and GM38526 to SMB.

REFERENCES

1. Jackson, D. A. & Cook, P. R. (1988) *EMBO (Eur. Mol. Biol. Organ.) J.* 7, 3667–3678.
2. He, D., Nickerson, J. A. & Penman, S. (1990) *J. Cell Biol.* 110, 569–580.
3. Nickerson, J. A., He, D., Fey, E. G. & Penman, S. (1990) in *The Eukaryotic Nucleus: Molecular Biochemistry and Macromolecular Assemblies* (The Telford Press, New Jersey), Vol. 2, pp. 763–782.
4. Nakayasu, H. & Berezney, R. (1989) *J. Cell Biol.* 108, 1–11.
5. Spector, D. L., Schrier, W. H. & Busch, H. (1983) *Biol. Cell* 49, 1–10.
6. Verheijen, R., van Venrooij, W. & Ramaekers, F. (1988) *J. Cell Sci.* 90, 11–36.
7. Carter, K. C., Taneja, K. L. & Lawrence, J. B. (1991) *J. Cell Biol.* 115, 1191–1202.
8. Xing, Y., Johnson, C. V., Dobner, P. R. & Lawrence, (1993) *Sci.* 259, 1326–1330.
9. Carter, K. C., Bowman, D., Carrington, W., Fogarty, K., McNeil, J. A., Fay, F. S. & Lawrence J. B. (1993) *Sci.* 259, 1331–1335.
10. Spector, D. L. (1990) *Proc. Natl. Acad. Sci. USA* 87, 147–151.
11. Jiménez-García, I. F. & Spector, D. L. (1993) *Cell* 73, 47–59.
12. Zeitlin, S., Parent, A., Silverstein, S. and Efstratiatis, A. (1987) *Mol. Cell Biol.* 7, 111–120.
13. Fey, E. G., Krochmalnic, G. and Penman, S. (1986) *J. Cell Biol.* 102, 1654–1665.
14. Bouvier, D., Hubert, J., Sève, A. & Bouteille, M. (1985) *Can. J. Biochem Cell Biol.* 63, 631–643.
15. Verheijen, R., Kuijpers, J., Vooijs, P., van Venrooij, W. & Ramaekers, F. (1986) *J. Cell Sci.* 86, 173–190.

16. Smith, H., Harris, S. G., Zillmann, M. & Berget, S. M. (1989) *Exp. Cell Res.* 182, 521–533.
17. Lydersen, B. & Pettijohn, D. (1980) *Cell* 22, 489–499.
18. Tousson, A., Zeng, C., Brinkley, B. R. & Valdivia, M. M. (1991) *J. Cell Biol.* 112, 427–440.
19. Kallajoki, M., Weber, K. & Osborn, M. (1991) *EMBO. J.* 7, 3667–3678.
20. Maekawa, T., Leslie, R. & Kuriyama, R. (1991) *Eur. J. Cell Biol.* 54, 255–267.
21. Yang, C. H., Lambie, E. J. & Snyder, M. (1992) *J. Cell Biol.* 116, 1303–1317.
22. Compton, D. A., Szilak, I. & Cleveland, D. W. (1992) *J. Cell Biol.* 116, 1395–1408.
23. Tang, T. K., Tang, C. C., Chen, Y. & Wu, C. (1993) *J. Cell Sci.* 104, 249–260.
24. Yang, C. H. & Snyder, M. (1992) *Mol. Biol. Cell* 3, 1259–1267.
25. Kallajoki, M., Weber, K. & Osborn, M. (1992) *J. Cell Sci.* 102, 91–102.
26. Compton, D. A. & Cleveland, D. W. (1993) *J. Cell Biol.* 120, 947–957.
27. Kallajoki, M., Harborth, J., Weber, K. & Osborn, M. (1993) *J. Cell Sci.* 104, 139–150.
28. Lerner, R. M. & Steitz, J. A. (1979) *Proc. Natl. Acad. Sci. USA* 76, 5495–5499.
29. Harlow, E. & Lane, D. (1988) in *Antibodies: A Laboratory Manual* (Cold Spring Harbor Laboratory), pp. 521–523.
30. Lerner, E. A., Lerner, M. R., Janeway Jr., C. A. & Steitz, J. A. (1981) *Proc. Natl. Acad. Sci. USA* 78, 2737–2741.
31. Krainer, A. R. (1988) *Nucleic Acids Res.* 16, 9415–9429.
32. Valdivia, M. M. & Brinkley, B. R. (1985) *J. Cell Biol.* 101, 1124–1134.
33. Dignam, J. D., Lebovitz, R. M. & Roeder, R. G. (1983) *Nucleic Acids Res.* 11, 1475–1489.
34. Robberson, B. L., Cote, G. & Berget, S. M. (1990) *Mol. Cell Biol.* 10, 84–94.
35. Cleveland, D. W., Fischer, S. G., Kirschner, M. W., and Laemmli, U. K. (1977) *J. Biol. Chem.* 252, 1102–1106.
36. Raska, I., Ochs, L. E., Andrade, L. E. C., Chan, E. K. L., Burlingame, R., Peebles, C., Fruol, K. & Tan, E. M. (1990) *J. Struct. Biol.* 104, 120–127.
37. Raska, I., Andrade, L. E. C., Ochs, R. L., Chan, E. K. L., Chang, C. –M., Roos, G. & Tan, E. M. (1991) *Exp. Cell Res.* 195, 27–37.

38. Spector, D. L., Lark, G. and Huang, S. (1992) *Mol. Biol. Cell* 3, 555–569.
39. Reed, R., Griffith, J. & Maniatis, T. (1988) *Cell* 53, 949–961.

Figure 1. NuMA antibodies recognize large nuclear proteins. Proteins from a HeLa extract prepared in 0.5 M salt were displayed by SDS-PAGE and immunoblotted with the monoclonal antibodies 2D3 (lane 1) and 8.22 (lane 2), and the polyclonal antibody P9 (lane 3). The largest bands of approximate molecular weight 220 and 200 KD represent known NuMA isoforms of 230 and 195/194 KD (23). The lowest band of 160 KD is an unknown protein that presumably contains NuMA-like epitope (see text).



— 180

— 116

— 84

— 58

— 48

1 2 3

Figure 2. NuMA antibody 8.22 stains nuclear speckles. a–b, staining of interphase (large panel) or mitotic (insert) HeLa cells with 2D3 (a) or 8.22 (b) generated interphase patterns of diffuse nuclear staining or nuclear foci and speckles, respectively; and mitotic patterns of spindle crescents. P9 gave the same staining pattern as 2D3 (data not shown). Nuclear staining of human cervical epidermoid carcinoma cells (CaSki) with 8.22 produced smaller and more numerous nuclear foci and speckles than HeLa cells (c–l). c–h, computerized pseudo color of double immunofluorescence with 8.22 (c and f, green) and human α Sm antibody (d and g, red). The patterns produced by the two antibodies in interphase nuclei are superimposable (e, yellow). The only exception is the specific staining of one to a few round spots presumed to be coiled bodies (36–38) (arrows, and red in e) by α Sm, but not 8.22. f–h show mitotic staining by the same procedure; the majority of 8.22 antibody deposited in the polar regions. Most α Sm assumed a diffuse localization in the cytoplasm. i–j, staining of the nuclear core filament system prepared by DNA digestion and gradient salt extraction (2); the α NuMA (i) and α Sm (j) fluorescence still co-localized, and yielded higher intensity and more foci and speckles, implying more antigens were uncovered by extraction. k–l, staining of the core filaments after the preparations in i–j, respectively, were treated with RNase A. Treatment deformed the speckles to blobs, but co-localization remained.

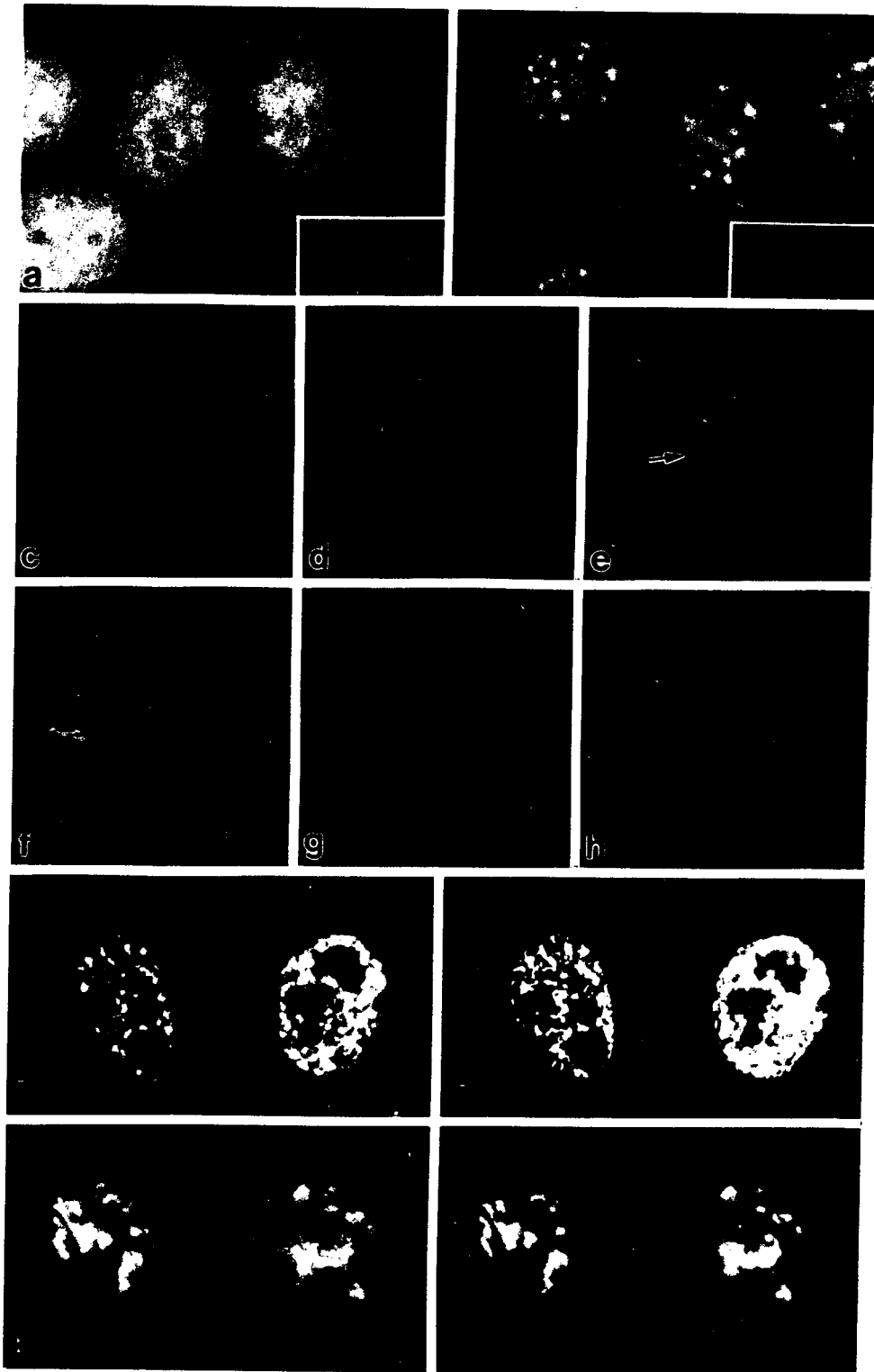


Figure 3. NuMA antigens are associated with snRNPs. (a) Immunoprecipitation of NuMA with anti-snRNP antibodies. An ^{35}S -methionine labeled 0.5 M NaCl HeLa extract was immunoprecipitated with monoclonal αSm antibody Y12 (lane 1) or agarose-conjugated αTMG monoclonal antibody K121 (31) (Oncogene Science, lane 2). (b) Immunoprecipitation of NuMA with anti-NuMA antibodies. An extract prepared with 0.5 M salt and 0.08% SDS was precipitated with protein G agarose-conjugated 2D3 (lane 1) or 8.22 (lane 2). Arrows mark an identical doublet of high molecular weight in all panels. The lower bands in (b) are due to the nonspecific binding of protein G-agarose (data not shown). (c) Immuno-detection of NuMA in anti-TMG immunoprecipitate. Various immunoprecipitates of nuclear extract were immunoblotted with NuMA and control antibodies. Lane 1, protein G-agarose precipitate probed with the P9 NuMA antibody; lane 2, a CREST autoantibody (32) immunoprecipitate probed with P9 NuMA antibody; lane 3, HeLa extract probed with the P9 NuMA antibody; lane 4, αTMG immunoprecipitate probed with the P9 NuMA antibody; and lane 5, the αTMG immunoprecipitate probed with the CREST autoantibody. The bands of approximately 50 and 25 KD in lane 4 are the IgG subunits of the monoclonal antibody used in immunoprecipitation visualized by the utilized anti-mouse secondary antibody.

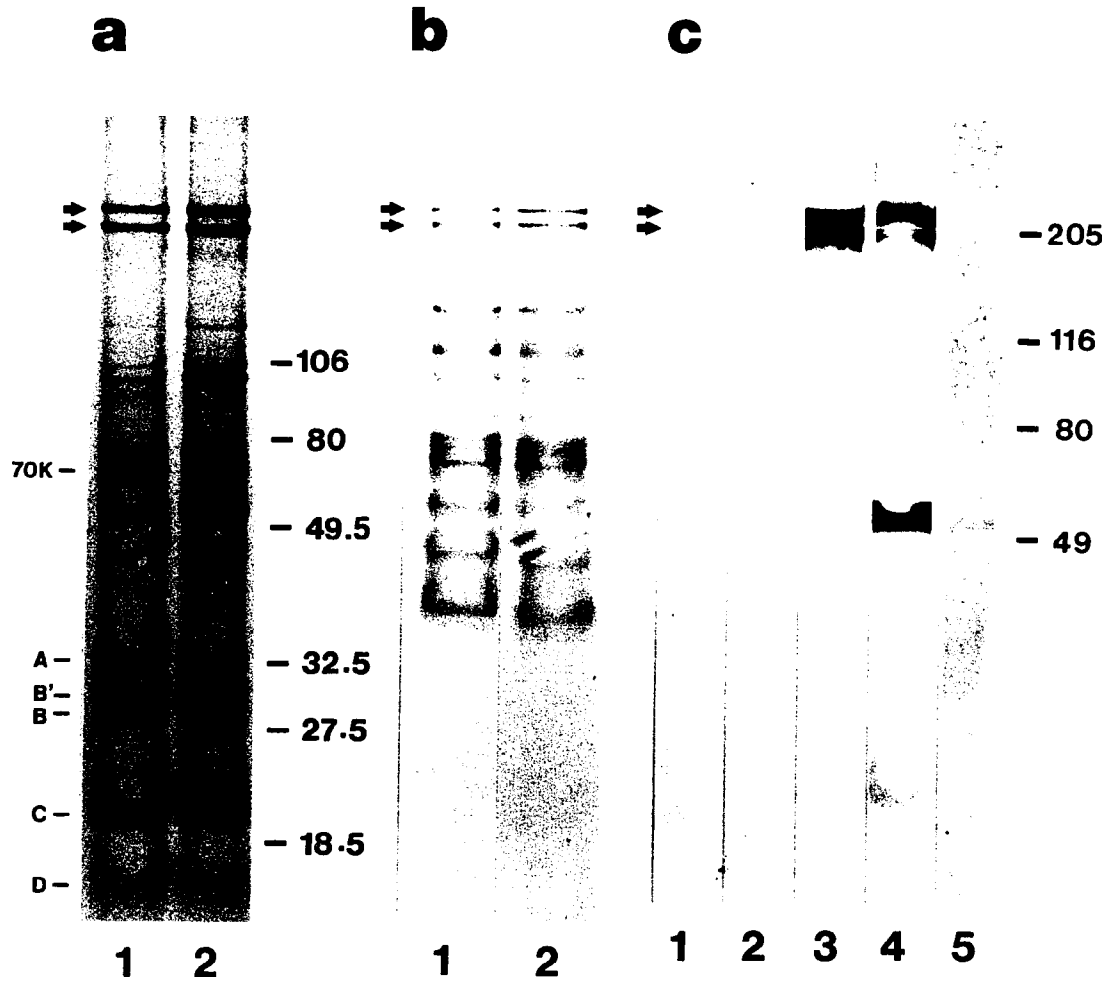
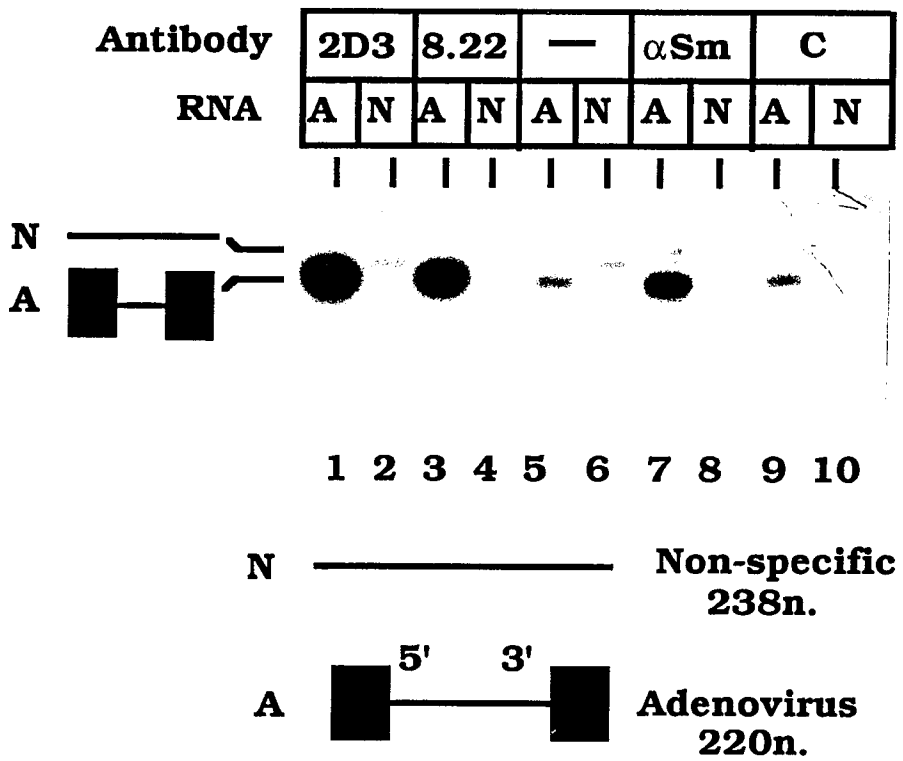


Figure 4. NuMA antibodies immunoprecipitate in vitro reconstituted spliceosomes. In vitro splicing reactions were set up using a radiolabeled 238 nucleotide non-specific plasmid RNA (N) or a 220 nucleotide single-intron pre-mRNA from adenovirus (A). After a 10 min incubation at 30°C, each reaction was split into five parts and immunoprecipitated with IgG fractions of 2D3 (lanes 1–2), 8.22 (lanes 3–4), no antibody (lanes 5–6), Y12 anti-snRNP antibody (lanes 7–8) or a normal human serum as a control (lanes 9–10). Immunoprecipitates were displayed on a denaturing acrylamide gel followed by autoradiography. Marks to the left indicate the bands corresponding to the two RNA substrates employed.



SUMMARY AND GENERAL CONCLUSIONS

The protein described in this dissertation was initially termed centrophilin due to its characteristic localization at the spindle poles of mitotic cells (chapter 1). Comparison of the primary structure of centrophilin with NuMA has confirmed that the two proteins are in fact one in the same (93, 16). NuMA was originally identified in human cells and was proposed to play a role in post mitotic nuclear assembly in the pioneering studies (51, 68). A decade after its initial identification, significant progress has been made in understanding the structure and functions of NuMA protein. cDNA analysis has revealed important structural properties of NuMA (93, 16, 83). More evidence has indicated that NuMA takes part in the organization of the mitotic spindle (chapter 1, 41, 39, 18, 53). From results presented in the present studies, we have begun to understand that it is also involved in the nuclear organization in interphase (chapters 2 and 3). Indeed, this large coiled-coil protein may be a representative of other proteins that play dual roles in maintaining function and structural organization of both the nucleus and mitotic apparatus during the cell cycle.

The investigations described in the chapters of this dissertation address the properties and functions of NuMA as a component of both the cytoskeleton (in mitosis) and the nucleoskeleton (in interphase). Since a detailed discussion has been included in each chapter, a general summary conclusion is presented below.

The results presented in chapter 1 show that redistribution process of NuMA during the cell cycle and the analysis of colocalization of NuMA with the minus ends of mitotic MTs. Using a monoclonal antibody, 2D3, NuMA is localized in the entire nucleus in interphase. It condenses into foci then migrates to the duplicated centrosomes in prophase

as detected by double label immunofluorescence with 2D3 and anti-tubulin antibody. At metaphase, NuMA displays a crescent pattern at the spindle polar regions. During anaphase, NuMA molecules gradually diminish from the spindle poles and subsequently relocate into the daughter nuclei at the end of mitosis. From immunofluorescence studies it appears that all but a small portion of NuMA protein re-enters the nuclei after the completion of mitosis. The residual cytoplasmic NuMA resides at the midbody until it is degraded.

Double-label immunofluorescence studies have shown that NuMA translocates from the nucleus to the minus end of spindle MTs at the onset of mitosis, suggesting that it plays a role in spindle organization. To confirm this possibility, MT inhibitors have been used to induce spindle disassembly. The processes of both disassembly and re-assembly of spindle MTs have clearly revealed an intimate association of NuMA with the minus end of spindle MTs. The disassembly agents lead to the dissolution of both spindle MTs and polar crescents of NuMA into numerous small foci containing both tubulin and NuMA dispersed throughout the cytoplasm. After the removal of MT inhibitors, NuMA constitutes the multiple small MTOCs during the process of the spindle recovery. Nascent MTs emanate from these NuMA positive foci and gradually elongate and converge to form the bipolar spindle. Simultaneously, NuMA appears to undergo consolidation from multiple spots in the cytoplasm to a pair crescents at the spindle poles. Therefore, in both normal and drug treated mitotic cell, NuMA is likely a persistent component and a distinct marker of MTOCs at the minus end of spindle fibers.

The results above are supported by the similar MT inhibition experiments from two other independent studies in which NuMA is also confirmed as mitotic MAP by MT co-sedimentation (53, 41). Since NuMA begins to disassociate from the mitotic poles after the onset of anaphase and the staining is dramatically reduced by late anaphase B, the

function of NuMA appears to be confined largely to the relative early stages of mitosis. As a component of MTOC, it may be involved in the nucleation and stabilization of spindle fibers. The process of spindle elongation, however, seems not to be related to the function of NuMA. Microinjections of NuMA antibodies into primate or marsupial cells also provided evidence that NuMA supports spindle formation and/or maintenance prior anaphase (93, 39).

Chapters 2 and 3 in this dissertation have described the analysis of NuMA in the interphase nucleus. DNA cloning and antibody generation were carried out in an attempt to obtain additional probes for further investigation. Using mAb 2D3 to screen a human cDNA expression library, a 1.9 kb cDNA fragment encoding a α -helical portion of NuMA protein was cloned. Polyclonal antibody P9 and monoclonal antibody 8.22 were produced against a fusion protein induced from the positive DNA recombinant. Immunoblots of HeLa extract with P9 have resolved two protein bands ≥ 200 KD. Peptide mapping followed by immunoblotting has determined that the double band is not due to proteolysis but represents isoforms of NuMA produced by alternative RNA splicing. Moreover, immunofluorescent staining with 8.22 mAb has revealed an unexpected speckle pattern in the interphase nucleus. This pattern of staining is also revealed by two other NuMA antibodies, mAb W1 (83) and pAb in the initial NuMA study (51). Considering that the immunoreactivity of mAb 8.22 is the same as that of mAb 2D3, as indicated by immunoblots and immunoprecipitations, the different interphase staining patterns are most likely due to the differential availability of epitopes for each antibody. The discrete nuclear domains identified by 8.22 appear to represent a structural or functional state of NuMA which colocalized with the RNA splicing complexes (see below).

Collectively, immunoblots and immunofluorescence with the original mAb 2D3 and the newly produced mAb 8.22 and pAb P9 have revealed a heterogeneity of NuMA protein

in the aspects of primary structure, protein conformation, and intranuclear distribution in human cells, suggesting a complex function and regulation mechanism of NuMA during interphase. Such heterogeneous properties are not only generated by the alternative splicing of the RNA transcript but may also be produced by post-translational modification, including phosphorylation/dephosphorylation since NuMA has been identified as a target of numerous cell cycle related kinases (93). Additionally, the associations of NuMA with different nuclear components at discrete nuclear domains may also contribute the differential epitope availability of NuMA molecules.

One obstacle in biochemical studies of NuMA has been its solubility by conventional nuclear extraction procedure. After numerous attempts, extraction with appropriate buffer containing 0.5 M NaCl appears to be the most effective solvent of NuMA from detergent lysed cells. This condition has enabled us to proceed with intact nuclei prior to DNA digestion. Despite the unknown mechanism of this solubilization approach, it has been greatly facilitated biochemical studies of NuMA and may be useful for other nuclear protein with similar solubility problem.

It has been shown that NuMA is a component of the nuclear matrix (51, 40), which is an architectural complex of proteins and RNAs (20, 60). Characterization of the nuclear matrix requires the coordinated usage of microscopic, biochemical, and immunological techniques to reveal its organization. Using a sequential extraction procedure with increasing salt concentration after DNA digestion, a smooth, highly branched 9–13 nm filament system has been revealed by embedding-free electron microscopy. Termed core filaments, this nucleoskeleton serves as the fundamental core around which other proteins associate to form the complete nuclear matrix (28, 59).

For further localization of NuMA, the same procedure of sequential extraction has been performed and NuMA is detected in core filaments by immunofluorescence and

immunoblots with various antibodies. Both the diffuse staining pattern of 2D3 and the speckle pattern of 8.22 remained the same as the controls after each step of digestion and extraction as shown by fluorescent staining. The majority of NuMA protein, including both isoforms, is resolved in core filament preparation but not the extracted fractions as shown by immunoblots. More importantly, immunogold labeled 2D3 was shown to specifically decorate a subclass, but not all, nuclear core filaments as visualized by resinless EM section (10). This observation is consistent with the unique properties of the nucleoskeleton which consists of various types of nuclear proteins and RNAs (28). As the first component of core filaments to be identified, localization of NuMA in this filament network is also a significant advance in our knowledge of nucleoskeletal organization.

The snRNP antibodies also stain nuclear speckles representing the assembled RNA splicing complexes, the spliceosomes. Colocalization of 8.22 and anti-snRNP staining strongly suggests an association between RNA splicing and NuMA protein. Two types of immunoprecipitations have been carried out in order to provide further identification. In the immuno-complex precipitated from the HeLa extract using an antibody against the U-cap of snRNA, a ≥ 200 KD duplicate protein has been revealed along with the common snRNP polypeptides. Furthermore, this double band has been resolved by P9 from the immuno-complex as shown by immunoblotting. This identification suggests that NuMA isoforms may associate with either the spliceosomes, or nonassembled snRNPs or other related factors. If NuMA associates with spliceosomes, immunoprecipitation complex by NuMA antibodies may also contain the active splicing factors including pre-mRNA due to the intimate association of these components in an assembled spliceosome. To test these possibilities, *in vitro* reconstituted splicing reactions has been performed using the nuclear extract with splicing activity and the exogenously provided pre-mRNA. Both NuMA mAbs 2D3 and 8.22 have shown to specifically precipitate the radio-labeled wild type pre-mRNA.

These results strongly suggest that NuMA associated with active spliceosomes or at least complex A (Fig. 1 in introduction), representing the initial stage of RNA processing (55, 49).

What role does NuMA protein play in RNA splicing? Given the structural nature of the protein, it is unlikely that NuMA takes part in the excision or ligation processes, and very possibly as a skeletal component, involved in the 3-D organization of splicing domains. Collectively, the function of NuMA in the interphase nucleus may be in nuclear organization serving as the protein structural interface between RNA splicing complex and the nucleoskeleton.

In summary, these studies have advanced our knowledge of the functions of NuMA in interphase nuclei and in the mitotic apparatus. In addition, these studies have for the first time, revealed a dynamic translocation of NuMA from the nucleoskeleton in interphase to the cytoskeleton of the mitotic apparatus.

Future Directions

The analysis of NuMA in mitotic cells presented in the first chapter has shown that this protein is very likely involved in spindle organization. In addition to the present study, this result has been supported by several other reports (94, 39, 41, 53). On the other hand, NuMA is also thought to function in post-mitotic nuclear assembly although the evidence for this hypothesis is somewhat weaker as mentioned earlier (51, 16, 18). It is possible nevertheless that both functions of NuMA coexist in cells. A detailed biochemical analysis using chromatography purified NuMA protein from mitotic cells may resolve the dispute and the 0.5 M salt extraction procedure described in chapter 2 may afford a better strategy for NuMA purification. It will be of considerable interest to investigate whether microinjected NuMA protein itself will promote assembly of either the mitotic spindle or the post-mitotic nuclei. In addition, biochemical and electron microscopic analysis of tubulin polymerization *in vitro* with or without addition of exogenous NuMA protein may help to

further elucidate the mechanism of NuMA in the control of spindle organization as a mitotic MAP.

The reconstituted *in vitro* splicing reaction followed by immunoprecipitation represented in chapter 3 has provided an excellent system to detect the biochemical relationship between NuMA and splicing factors. Further studies using longer reaction time may answer whether NuMA protein associates with complex B or C of spliceosomes during the processing (55). Introduction of mutant pre-mRNAs as substrate into the splicing reaction may also help to identify whether a motif related to splicing is also required for the *in vitro* association of NuMA with spliceosomes, thereby determining in which step of splicing NuMA may be involved. Equally important are studies utilizing purified NuMA in reconstituted splicing reactions to understand the molecular event of how NuMA takes part in pre-mRNA processing.

EM visualization has revealed a filamentous protein extension from purified globular spliceosomes which could represent NuMA or NuMA-like nucleoskeletal component(s) (69). It will be of great interest to investigate further the possibility, raised for the first time in this study, that NuMA facilitates the attachment and spatial arrangement of spliceosomes with the nuclear matrix.

GENERAL LIST OF REFERENCES

1. Benavente, R. U., and G. Krohne. 1986. Involvement of nuclear lamins in postmitotic reorganization of chromatin as demonstrated by microinjection of lamin antibodies. *J. Cell Biol.* 103:1847–1854.
2. Benavente, R., U. Scheer, and N. Chaly. 1989. Nucleocytoplasmic sorting of macromolecules following mitosis: fate of nuclear constituents after inhibition of pore complex function. *Eru. J. Cell Biol.* 50:209–219.
3. Berezney, R. 1991. The nuclear matrix: a heuristic model for investigating genomic organization and function in the cell nucleus. *J. Cell. Biochem.* 47:109–123.
4. Berkowitz, S. A., J. Katagiri, H. K. Binder and R. C. Williams, Jr. 1977. Separation and characterization of microtubule proteins from calf brain. *Biochem.* 16:5610–5617.
5. Bindereif, A., and M. Green. 1990. Identification and functional analysis of mammalian splicing factors. In *Genetic Engineering*. Plenum Press, editor. J. Setlow, New York. 12, 201–224.
6. Bonifacino, J. S., R. D. Klausner, and I. V. Sandoval. 1985. A widely distributed nuclear protein immunologically related to the microtubule-associated protein MAP1 is associated with the mitotic spindle. *Proc. Natl. Acad. Sci. USA.* 82:1146–1150.
7. Borisy, G. G., J. M. Marcum, J. B. Olmsted, D. B. Murphy, and K. A. Johnson. 1975. Purification of tubulin and associated high molecular weight proteins from porcine brain and characterization of microtubule assembly *in vitro*. *Ann. NY Acad. Sci.* 253:107–132.
8. Brinkley, B. R., E. Stubblefield, and T. C. Tsu. 1967. The effects of colcemid inhibition and reversal on the fine structure of the mitotic apparatus of Chinese hamster cells *in vivo*. *J. Ultrastruct. Res.* 19:1–18.
9. Calarco-Gillam, P. D., M. C. Siebert, R. Hubble, T. Mitchison, and M. Kirschner. 1983. Centrosome development in early mouse embryo as defined by an auto-antibody against pericentriolar material. *Cell* 35:621–629.
10. Capco, D. G., G. Krochmalnic, and S. Penman. 1984. A new method of preparing embedding-free sections for transmission electron microscopy: applications to the cytoskeletal framework and other three-dimensional networks. *J. Cell Biol.* 98:1878–1885.

11. Carter, K. C., K. L. Taneja, and J. B. Lawrence. 1991. Discrete nuclear domains of poly(A) RNA and their relationship to the functional organization of the nucleus. *J. Cell Biol.* 115:1191–1202.
12. Carter, K. C., D. Bowman, W. Carrington, K. Fogarty, J. A. McNeil, F. S. Fay, and J. B. Lawrence. 1993. A three dimensional view of precursor messenger RNA metabolism within the mammalian nucleus. *Sci.* 259:1331–1335.
13. Clayton, L., C. M. Black, and C. W. Lloyd. 1985. Microtubule nucleating sites in higher plant cells identified by an autoantibody against pericentriolar material. *J. Cell Biol.* 101:319–324.
14. Cohen, C., and D. A. D. Parry. 1986. Alpha-helical coiled coils—a widespread motif in proteins. *Trends Biochem. Sci.* 11:245–248.
15. Cohen, C., and D. A. D. Parry. 1990. α -helical coiled coils and bundles: how to design an α -helical protein. *Prot. Struct. Funct. Genet.* 7:1–5.
16. Compton, D. A., I. Szilak, and D. W. Cleveland. 1992. Primary structure of NuMA, an intranuclear protein that defines a novel pathway for segregation of proteins at mitosis. *J. Cell Biol.* 116:1395–1408.
17. Compton, D. A., T. J. Yen, and D. W. Cleveland. 1991. Identification of novel centromere/kinetochore-associated proteins using monoclonal antibodies generated against human mitotic chromosome scaffolds. *J. Cell Biol.* 112:1083–1097.
18. Compton, D. A., and D. W. Cleveland. 1993. NuMA is required for the proper completion of mitosis. *J. Cell Biol.* 120:947–957.
19. Dignam, J. D., R. M. Lebovitz, and R. G. Roeder. 1983. Accurate transcription initiation by RNA polymerase II in a soluble extract from isolated mammalian nuclei. *Nucleic Acids Res.* 11:1475–1489.
20. Fey, E. G., G. Krochmalnic, and S. Penman. 1986. The nonchromatin substructures of the nucleus: the ribonucleoprotein (RNP)-containing and RNP-depleted matrices analyzed by sequential fractionation and resinless section microscopy. *J. Cell Biol.* 102:1654–1665.
21. Finlay, D. R., D. D. Newmeyer, T. M. Price, and D. J. Forbes. 1987. Inhibition of in vitro nuclear transport by a lectin that binds to nuclear pores. *J. Cell Biol.* 104:189–200.
22. Gasser, S. M., B. B. Amati, M. E. Cardenas, and J. F. X. Hofmann. 1989. Studies on scaffold attachment sites and their relation to genome function. *Int. Rev. Cytol.* 119:57–96.
23. Gerace, L. and G. Blobel. 1980. The nuclear envelope lamina is reversibly depolymerized during mitosis. *Cell.* 19:277–287.

24. Getzenberg, R. H., and D. S. Coffey. 1990. Tissue specificity of the hormonal response in sex accessory tissues is associated with nuclear matrix protein patterns. *Mol. Endocrinol.* 4:1336–1342.
25. Getzenberg, R. H., K. J. Pienta, W. S. Ward, and D. S. Coffey. 1991. Nuclear structure and the three-dimensional organization of DNA. *J. Cell. Biochem.* 47:289–299.
26. Goldfarb, D. S., J. Gariépy, G. Schoolnik, and R. D. Kornberg. 1986. Synthetic peptides as nuclear localization signals. *Nature (Lond.)*. 326:641–644.
27. He, D., T. Martin, and S. Penman. 1991. Localization of heterogeneous nuclear ribonucleoprotein in the interphase nuclear matrix core filaments and on perichromosomal filaments at mitosis. *Proc. Natl. Acad. Sci. USA.* 88:7469–7473.
28. He, D., J. A. Nickerson, and S. Penman. 1990. Core filaments of the nuclear matrix. *J. Cell Biol.* 110:569–580.
29. Himmler, A., D. Prechsel, M. W. Kirschner, and D. W. Martin. 1989. Tau consists of a set of proteins with repeated C-terminal microtubule-binding domains and variable N-terminal domains. *Mol. Cell Biol.* 9:1381–1388.
30. Hozák, P., A. B. Hassan, D. A. Jackson, and P. R. Cook. 1993. Visualization of replication factories attached to a nucleoskeleton. *Cell.* 73:361–373.
31. Huang, S., and D. L. Spector. 1991. Nascent pre-mRNA transcripts are associated with nuclear regions enriched in splicing factors. *Genes Devel.* 5:2288–2302.
32. Irminger-Finger, I., R. A. Laymon, and L. S. B. Goldstein. 1990. Analysis of the primary sequence and microtubule-binding region of the *Drosophila* 205 KD MAP. *J. Cell Biol.* 2563–2572.
33. Izant, J. G., J. A. Weatherbee, and J. R. McIntosh. 1982. A microtubule-associated protein found in the mitotic spindle and interphase nucleus. *Nature (Lond.)*. 295:248–250.
34. Jackson, D. A., and P. R. Cook. 1988. Visualization of a filamentous nucleoskeleton with a 23-nm axial repeat. *EMBO (Eur. Mol. Biol. Organ.) J.* 7:3667–3678.
35. Jensen, C. G., E. A. Davison, S. S. Bowser, and C. L. Rieder. 1987. Primary cilia cycle in PtK1 cells: Effects of colcemid and taxol on cilia formation and resorption. *Cell Motil. Cytoskel.* 7, 187–197.
36. Jiménez-García, L. F., and D. L. Spector. 1993. In vivo evidence that transcription and splicing are coordinated by a recruiting mechanism. *Cell* 73:47–59.
37. Kai, R., M. Ohtsubo, T. Sekiguchi, and T. Nishimoto. 1986. Molecular cloning of a human gene that regulates chromosome condensation and is essential for cell proliferation. *Mol. Cell Biol.* 6:2027–2032.

38. Kalderon, D., B. L. Roberts, W. D. Richardson, and A. E. Smith. 1984. A short amino acid sequence able to specify nuclear localization. *Cell* 39:499–509.
39. Kallajoki, M., J. Harborth, K. Weber, and M. Osborn. 1993. Microinjection of a monoclonal antibody against SPN antigen, now identified by peptide sequences as the NuMA protein, induces micronuclei in PtK2 cells. *J. Cell Sci.* 104:139–150.
40. Kallajoki, M., K. Weber, and M. Osborn. 1991. A 210 KD nuclear matrix protein is a functional part of the mitotic spindle; a microinjection study using SPN monoclonal antibodies. *EMBO (Eur. Mol. Biol. Organ.) J.* 10:3351–3362.
41. Kallajoki, M., K. Weber, and M. Osborn. 1992. Ability to organize microtubules in taxol-treated mitotic PtK₂ cells goes with the SPN antigen and not with the centrosome. *J. Cell Sci.* 102:91–102.
42. Kellogg, D. R., C. M. Field, and B. M. Alberts. Identification of microtubule-associated proteins in the centrosome, spindle, and kinetochore of the early *Drosophila* embryo. *J. Cell Biol.* 109:2977–2991.
43. Krainer, A. R., and T. Maniatis. 1988. RNA splicing. In *Frontiers in Molecular Biology: Transcription and Splicing*. IRL Press, editors. B. D. Hames, and D. M. Glover, Washington DC. 131–296.
44. Kung, A. L., S. W. Sherwood, and R. T. Schimke 1990. Cell line-specific differences in the control of cell cycle progression in the absence of mitosis. *Proc. Natl. Acad. Sci. USA.* 87.:9553–9557.
45. Kuriyama, R., and C. Sellitto. 1989. A 225 KD phosphoprotein associated with the mitotic centrosome in sea urchin eggs. *Cell Motil. Cytoskel.* 12:90–103.
46. Lanford, R. E., and J. S. Butel. 1984. Construction and characterization of an SV40 mutant defective in nuclear transport of T antigen. *Cell.* 37:801–813.
47. Lanford, R. E., P. Kanda, and R. C. Kennedy. 1986. Induction of nuclear transport with a synthetic peptide homologous to the SV40 T antigen transport signal. *Mol. Cell Biol.* 8:2722–2729.
48. Lewis, S. A., D. Wang, and N. J. Cowan. 1988. Microtubule associated protein MAP2 shares a microtubule-binding motif with tau protein. *Sci.* 242:936–939.
49. Lührmann, R., B. Kastner, and M. Bach. 1990. Structure of spliceosomal snRNPs and their role in pre-mRNA splicing. *Biochem. Biophys. Acta.* 1087:265–292.
50. Lydersen, B., F. T. Kao, and D. Pettijohn. 1980. Expression of genes coding for non-histone chromosomal proteins in human/Chinese hamster cell hybrids: an electrophoretic analysis. *J. Biol. Chem.* 255:3002–3007.

51. Lydersen, B., and D. Pettijohn. 1980. Human-specific nuclear protein that associates with the polar region of the mitotic apparatus: distribution in a human/hamster hybrid cell. *Cell*. 22:489-499.
52. Maekawa, T., and R. Kuriyama. 1991. Differential pathways of recruitment for centrosomal antigens to the mitotic poles during bipolar spindle formation. *J. Cell Sci.* 100:533-540.
53. Maekawa, T., R. Leslie, and R. Kuriyama. 1991. Identification of a minus end-specific microtubule-associated protein located at the mitotic poles in cultured mammalian cells. *Eur. J. Cell Biol.* 54:255-267.
54. Maniatis, T. and R. Reed. 1987. The role of small nuclear ribonucleoprotein particles in pre-mRNA splicing. *Nature (Lond.)*. 325:673-678.
55. Moore, M. J., C. C. Query, and P. A. Sharp. 1993. Splicing of precursors to messenger RNAs by the spliceosome. In press.
56. Murray, A. W., and M. W. Kirschner. 1989. Dominoes and clocks: The union of two views of the cell cycle. *Sci.* 246:614-621.
57. Nakayasu, H., and R. Berezney. 1989. Mapping replicational sites in the eucaryotic cell nucleus. *J. Cell. Biol.* 108:1-11.
58. Newmeyer, D. D., and D. J. Forbes. 1988. Nuclear import can be separated into distinct steps *in vitro*: nuclear pore binding and translocation. *Cell*. 52:641-653.
59. Nickerson, J. A., D. He, E. G. Fey, and S. Penman. 1990. The nuclear matrix. In: *The Eukaryotic Nucleus Molecular Biochemistry and Macromolecular Assemblies*. The Telford Press, editors. P. R. Strauss, and S. H. Wilson, New Jersey. 2:763-782.
60. Nickerson, J. A., G. Krochmalnic, K. M. Wan, and S. Penman. 1989. Chromatin architecture and nuclear RNA. *Proc. Natl. Acad. Sci. USA*. 86:177-181.
61. Nickerson, J. A., G. Krockmalnic, K. M. Wan, C. D. Turner, and S. Penman. 1992. A normally masked nuclear matrix antigen that appears at mitosis on cytoskeleton filaments adjoining chromosomes, centrioles, and midbodies. *J. Cell Biol.* 116:977-987.
62. Nishimoto, T., E. Ellen, and C. Basilico. 1978. Premature chromosome condensation in a tsDNA mutant of BHK cells. *Cell*. 15:475-483.
63. Nishitani, H., M. Ohtrubo, K. Yamashita, H. Iida, J. Pines, H. Yasudo, Y. Shibata, T. Hunter, and T. Nishimoto. 1991. Loss of RCC1, a nuclear DNA binding protein uncouples the completion of DNA replication from the activation of cdc2 protein kinase and mitosis. *EMBO (Eru. Mol. Biol. Organ.) J.* 10:1555-1564.

64. Noble, M., S. A. Lewis, and N. J. Cowan. 1989. The microtubule binding domain of MAP1B contains a repeated sequence motif unrelated to that of MAP2 and tau. *J. Cell Biol.* 109:3367–3376.
65. Nyman, U., H. Hallman, G. Hadlaczy, I. Pettersson, G. Sharp, and N. R. Ringertz. 1986. Intranuclear localization of snRNP antigens. *J. Cell Biol.* 102:137–144.
66. Pepper, D. A., H. Y. Kim, and M. W. Berns. 1984. Studies of a microtubule-associated protein using a monoclonal antibody elicited against mammalian mitotic spindles. *J. Cell Biol.* 99:503–511.
67. Price, C. M., G. A. McCarty, and Pettijohn. 1986. NuMA protein is a human autoantigen. *Arth. Rheum.* 27:774–779.
68. Price, C. M., and D. E. Pettijohn. 1984. Distribution of the nuclear mitotic apparatus protein (NuMA) during mitosis and nuclear assembly. *Exp. Cell Res.* 166:295–311.
69. Reed, R., Griffith, J. & Maniatis, T. 1988. Purification and visualization of native spliceosomes. *Cell* 53:949–961.
70. Reuter, R., B. Appel, P. Bringmann, J. Rinke, and R. Lührmann. 1984. 5'-Terminal caps of snRNAs are reactive with antibodies specific for 2, 2, 7-trimethylguanosine in whole cells and nuclear matrices. *Exp. Cell Res.* 154:548–560.
71. Rieder, C. L., and R. E. Palazzo. 1992. Colcemid and the mitotic cycle. *J. Cell Sci.* 102:387–392.
72. Roberge, M., and S. M. Gasser. 1992. DNA loops: structural and functional properties of scaffold-attached regions. *Mol. Microbiol.* 6:419–423.
73. Sato, C., K. Tanabe, K. Nishizawa, T. Nakayma, T. Kobayashi, and H. Nakamura. 1985. Localization of 350K molecular weight and related proteins in both the cytoskeleton and nuclear flecks that increase during G1 phase. *Exp. Cell Res.* 160:206–220.
74. Scheele, R. D., and G. G. Borisy. 1979. In vitro assembly of microtubules. In: *Microtubules.* (eds. Roberts K. and Hyams J. S.), pp175–254. Acad. Lond.
75. Smith, H. C., S. G. Harris, M. Zillmann, and S. M. Berget. 1989. Evidence that a nuclear matrix protein participates in pre-messenger RNA splicing. *Exp. Cell Res.* 182:521–533.
76. Smith, H. C. 1992. Organization of RNA splicing in the cell nucleus. *Curr. Topics Cell Regul.* 33:145–166.
77. Sparks, C. A., P. L. Bangs, G. P. McNeil, J. B. Lawrence, and E. Fey. 1993. Assignment of the nuclear mitotic apparatus protein NuMA gene to human chromosome 11q13. *Genomics* 17:222–224.

78. Spector, D. L. 1984. Colocalization of U1 and U2 small nuclear RNPs by immunocytochemistry. *Biol. Cell.* 51:109–112.
79. Spector, D. L. 1990. Higher order nuclear organization: three-dimensional distribution of small nuclear ribonucleoprotein particles. *Proc. Natl. Acad. Sci. USA.* 87:147–151.
80. Spector, D. L., W. H. Schrier, and H. Busch. 1983. Immunoelectron microscopic localization of snRNPs. *Biol. Cell.* 49:1–10.
81. Spector, D. L., and H. C. Smith. 1986. Redistribution of U–snRNPs during mitosis. *Exp. Cell Res.* 163:87–94.
82. Stubblefield, E. 1964. DNA synthesis and chromosomal morphology of Chinese hamster cells cultured in media containing colcemid. In *Cytogenetics of Cells in Culture* (ed. R. J. Harris), pp. 223–248. New York Academic Press.
83. Tang, T. K., C. C. Tang, Y. Chen, and C. Wu. 1993. Nuclear proteins of the bovine esophageal epithelium II: the NuMA gene gives rise to multiple mRNAs and gene products reactive with monoclonal antibody W1. *J. Cell Sci.* 104:249–260.
84. Thibodeau, A., and M. Vincent. 1991. Monoclonal antibody CC–3 recognizes phosphoproteins in interphase and mitotic cells. *Exp. Cell Res.* 195:145–153.
85. Todorov, I. T., R. N. Philipova, G. Joswig, D. Werner, and F. C. S. Ramaekers. 1992. Detection of the 125–kDa nuclear protein mitotin in centrosomes, the poles of the mitotic spindle, and the midbody. *Exp. Cell Res.* 199:398–401.
86. Uchida, S., T. Sekiguchi, H. Nishitani, K. Miyauchi, M. Ohtsubo, and T. Nishimoto. 1990. Premature chromosome condensation is induced by a point mutation in the hamster RCC1 gene. *Mol. Cell Biol.* 10:577–584.
87. Valdivia, M. M. and B. R. Brinkley. 1985. Fractionation and initial characterization of the kinetochore from mammalian metaphase chromosomes. *J. Cell Biol.* 101:1124–1134.
88. van Driel, R., B. Humbel, and L. de Jong. 1991. The nucleus: a black box being opened. *J. Cell. Biochem.* 47:311–316.
89. van Ness, J., and D. E. Pettijohn. 1983. Specific attachment of NuMA protein to metaphase chromosomes: possible function in nuclear reassembly. *J. Mol. Biol.* 171:175–205.
90. Verheijen, R., H. Kuijpers, P. Vooijs, W. van Venrooij, and F. Ramaekers. 1986. Distribution of the 70K U1 RNA-associated protein during interphase and mitosis. *J. Cell Sci.* 86:173–190.
91. Verheijen, R., W. van Venrooij, and F. Ramaekers. 1988. The nuclear matrix: structure and composition. *J. Cell Sci.* 90:11–36.

GRADUATE SCHOOL
UNIVERSITY OF ALABAMA AT BIRMINGHAM
DISSERTATION APPROVAL FORM

Name of Candidate Changqing Zeng

Major Subject Cell Biology

Title of Dissertation Characterization of Nuclear-Mitotic Apparatus

Protein During the Cell Cycle

Dissertation Committee:

Bill R. Brinkley , Chairman

Gerald M. Fuller

Lester I. Binder

Thomas A. Rado

Thomas H. Howard

Bill R. Brinkley

Gerald M. Fuller

Lester I. Binder

Thomas A. Rado

Thomas H. Howard

Director of Graduate Program John B. Couchman

Dean, UAB Graduate School Jan F. Loden

Date 10/14/93